

Aggregation and Redispersion of Switchable Latexes

By

Catherine O'Neill

A thesis submitted to the Graduate Program in Chemistry

in conformity with the requirements for the

Degree of Master of Science

Queen's University

Kingston, Ontario, Canada

September 2011

Copyright © Catherine O'Neill, 2011

Abstract

Amidine-based switchable surfactants can be used as stabilizers during emulsion polymerization and the resulting latexes can then be destabilized by the removal of CO₂. High T_g polymers have been successfully redispersed, as shown by recovery of primary particle size (measured by light scattering methods), but an input of energy was required. Sonication was the first method used, but lower-energy methods such as rotor-stators and a blender have also been successful in redispersing aggregated latexes. Colloidal stability was found to be reversible for at least three aggregation/redispersion cycles, and redispersibility was retained after the removal of water and addition of fresh water. Stimuli-responsive polymer colloids with reversible colloidal stability may have many uses. The shipping of high T_g latexes, for example, would be easier and less energy intensive if the latex particles could be aggregated and the bulk of the water removed. The latexes would then have to be redispersed prior to use.

Switchable surfactants have also been used for the semi-continuous copolymerization of butyl acrylate and methyl methacrylate to form a high solids content (42 wt%), low- T_g latex. The latex can be destabilized with air and heat but cannot undergo redispersion because the low T_g polymer particles fuse upon aggregation. The copolymer, when dried at room temperature, formed a continuous film. Latexes with high solids content and low T_g 's are representative of latex paint formulations. Because the switchable surfactants have been shown to be successful in preparing these latexes, it is possible that they may be useful in the latex paint industry, for example as fast setting paints.

Acknowledgements

As I finish writing up this thesis all I can think is “thank goodness this degree is over”, but after giving it a second thought, it was a pretty great two years. I met great friends and got to experience a lot of new things. And it was all pretty awesome.

I need to first thank my supervisors Dr. Michael Cunningham and Dr. Philip Jessop. They helped me and guided me throughout this project and gave me many opportunities to travel and learn during my time at Queen’s.

Thank-you to the past and present Jessop and Cunningham group members. You guys have been great friends and colleagues and I don’t think I could have done it without you all. I had some great times, and hopefully there will be more in the future! A special thank-you also to Darrell Dean, who helped me with *many* technical issues.

A very special shout-out to my polymer twin, Candace Fowler. I know I couldn’t have gotten through the past two years without you, both personally and academically. Thanks for listening to all my life stories (multiple times) and helping me make new ones (broken foot). And thanks for bringing me back to the ground and reminding me that it’s not so bad when I start losing my cool. I’m glad Philip told you to befriend me those two long years ago. You are a great friend.

Patrick, you know what you mean to me. Thanks for all the Skype dates.

Thank-you mom and dad for your support and for wasting your precious retirement hours talking on the phone with me. Your visits were always appreciated, I’ve never eaten quite as good when you aren’t around.

Thank-you to Dawn Free who helped with all the administration stuff, you made my life a lot easier!

Thank-you to the people who provided me with training on instruments over the past two years and to those who ran measurements for me. A special thank-you also to Mohsen Soleimani Kheibari from Dr. Winnik's group at the University of Toronto for the help with semi-batch polymerizations.

Thanks to NSERC and the Government of Ontario for financial support who made it possible for me to work on this project and not go hungry for two years. And thank-you to Xerox Research Centre of Canada for helpful conversations and the use of their equipment.

One last word: Finally.

Table of Contents

| | |
|--|-------------|
| Abstract..... | i |
| Acknowledgements | ii |
| Table of Contents | iv |
| List of Tables | vii |
| List of Figures..... | viii |
| List of Symbols and Abbreviations | xi |
| 1. Introduction..... | 1 |
| 1.1 General background | 1 |
| 1.2 Surfactants..... | 2 |
| 1.3 Switchable surfactants | 4 |
| 1.4 Environmental impact of switchable surfactants | 7 |
| 1.5 Emulsions..... | 9 |
| 1.6 Emulsion polymerization | 11 |
| 1.7 Colloidal stability | 14 |
| 1.8 Redispersible latexes..... | 19 |
| 1.9 Film formation | 22 |
| 1.10 Goals | 23 |
| 2. Experimental Methods | 24 |
| 2.1 Materials | 24 |
| 2.2 Emulsion stability test..... | 24 |
| 2.3 Emulsion polymerization | 25 |
| 2.3.1 Batch emulsion polymerization | 25 |
| 2.3.2 Emulsion polymerization of a latex containing no switchable groups | 26 |
| 2.3.3 Surfactant mixtures during polymerization | 26 |
| 2.3.4 Semi-continuous emulsion polymerization..... | 26 |
| 2.4 Characterization | 28 |
| 2.5 Destabilization | 28 |

| | |
|--|-----------|
| 2.6 Redispersion..... | 29 |
| 2.6.1 Redispersion methods | 29 |
| 2.6.2 Dewatering latexes for redispersion..... | 31 |
| 2.6.3 Addition of extra surfactant after polymerization..... | 32 |
| 2.7 Latex films | 33 |
| 3. Characterization Method Development..... | 34 |
| 3.1 Introduction..... | 34 |
| 3.2 Light scattering | 35 |
| 3.2.1 Dynamic light scattering | 36 |
| 3.2.2 Static light scattering..... | 38 |
| 3.3 Comparison of dynamic and static light scattering..... | 39 |
| 3.4 Sample stability during measurements | 43 |
| 3.5 Light scattering background | 46 |
| 3.6 Non-spherical particles | 48 |
| 3.7 Conclusions..... | 49 |
| 4. Results and Discussion: Redispersion | 50 |
| 4.1 Redispersion of a latex containing no switchable groups..... | 50 |
| 4.2 Destabilization | 51 |
| 4.2.1 Factors affecting destabilization | 51 |
| 4.2.2 Scanning electron microscope images | 53 |
| 4.3 Particle size distributions | 54 |
| 4.4 Redispersion..... | 56 |
| 4.4.1 Varying amount of “dryness” | 56 |
| 4.4.2 Different methods of redispersion | 57 |
| 4.4.3 Redispersion with different sized rotor-stators | 64 |
| 4.4.4 Redispersion of polystyrene particles | 68 |
| 4.4.5 Redispersion with extra surfactant added after aggregation | 70 |
| 4.4.6 Redispersion of an aggregated latex polymerized with a switchable-nonswitchable surfactant mixture | 71 |
| 4.4.7 Reversibility | 73 |

| | |
|--|------------|
| 4.4.8 Dewatering..... | 75 |
| 4.5 DLVO theory | 76 |
| 4.6 Conclusions..... | 79 |
| 5. Results and Discussion: Low T_g polymer for film formation..... | 82 |
| 5.1 Glass transition temperature | 82 |
| 5.2 Copolymerization..... | 83 |
| 5.3 Semi-continuous polymerization | 84 |
| 5.4 Chain transfer agent | 85 |
| 5.5 Emulsion stability | 86 |
| 5.6 Latex synthesis..... | 88 |
| 5.7 Latex characterization..... | 89 |
| 5.8 Destabilization | 91 |
| 5.9 Film formation | 93 |
| 5.10 Conclusions..... | 95 |
| 6. Conclusions and Future Work..... | 97 |
| 6.1 Conclusions..... | 97 |
| 6.2 Future Work | 99 |
| References..... | 102 |
| Appendix A : Important spectra and data sheets | 106 |

List of Tables

| | |
|---|----|
| Table 1.1. The 96 h LC ₅₀ 's in rainbow trout of switchable surfactants 1a , 1b , and 1c as well as SDS and CTAB..... | 9 |
| Table 4.1. Redispersion by sonication ^a of a PMMA latex that was aggregated by the addition of aluminum sulfate. ^b | 51 |
| Table 4.2. Redispersion of rehydrated aggregated latexes in the presence of CO ₂ . Redispersion was carried out in the presence and absence of additional surfactant and with and without sonication. | 57 |
| Table 4.3. The redispersion of a 5 wt% aggregated PMMA latex with different methods of agitation in the presence and absence of CO ₂ . ^a | 61 |
| Table 4.4. The redispersion of a 15 wt% aggregated PMMA latex with different methods of agitation in the presence and absence of CO ₂ . ^a | 63 |
| Table 4.5. Long-term colloidal stability of a 15 wt% aggregated PMMA latex after redispersion with 10 % sonication (probe) and CO ₂ | 64 |
| Table 4.6. The redispersion of a 5 wt% aggregated polystyrene ^a latex redispersed by 10 % sonication with a sonicator probe in the presence and absence of CO ₂ | 69 |
| Table 4.7. Redispersion of aggregated PMMA latexes ^a with additional surfactant added after aggregation. | 71 |
| Table 4.8. Polymerization of MMA with C12 (0.12 mol%) and varying amounts of non-switchable surfactant (CTAB). ^a | 72 |
| Table 4.9. Multiple cycles of aggregation and redispersion of a 5 wt% PMMA latex. ^a .. | 75 |
| Table 4.10. Redispersion of a rehydrated 4.9 wt% aggregated PMMA latex with 10 % sonication (probe) for 1 min in the presence and absence of CO ₂ . ^a | 76 |
| Table 5.1. Glass transition temperatures from the copolymerization of BA and MMA in different weight ratios. ^a | 83 |
| Table 5.2. The characterization of two latexes prepared by semi-continuous copolymerization under the same conditions to determine reproducibility. ^a | 91 |

List of Figures

| | |
|--|----|
| Figure 1.1. Examples of a) anionic, b) cationic, and c) nonionic surfactants. | 3 |
| Figure 1.2. Examples of a) ferrocene, b) pyrazinium, c) viologen, and d) azobenzene based switchable surfactants, where the active surfactant structure is on the left side of the equilibrium arrows. | 6 |
| Figure 1.3. The reversible reaction between an amidine and CO ₂ or air and heat where the charged species is the active surfactant. | 7 |
| Figure 1.4. Examples of oil-in-water (o/w) and water-in-oil (w/o) emulsions where blue is the water and yellow is the oil. | 10 |
| Figure 1.5. The steps involved in emulsion polymerization, where particle nucleation occurs via micellar nucleation. | 14 |
| Figure 1.6. The electrical double layer of a positively charged surface, where the red line represents the decay in the electrical potential from a charged surface. | 18 |
| Figure 1.7. The reversible reaction between the switchable initiator, VA-061, and CO ₂ or air and heat. | 22 |
| Figure 1.8. The steps involved during film formation: 1) evaporation of water; 2) deformation of particles; and 3) interdiffusion of particles. | 23 |
| Figure 3.1. Particle sizes of different latexes (polystyrene (•) and PMMA(◆)) measured on the Mastersizer 2000 (d _v) and the Zetasizer Nano ZS (d _z). The line represents the ideal relationship when the particle sizes measured are the same from both instruments. | 42 |
| Figure 3.2. Particle size distributions (volume distributions) of a 5 wt% polystyrene latex measured on both the Zetasizer Nano ZS and Mastersizer 2000. | 42 |
| Figure 3.3. Trend graphs of a) a stable sample and b) unstable sample in the Mastersizer 2000. | 45 |
| Figure 3.4. Different Mastersizer 2000 backgrounds: a) good; b) contaminated dispersant or containing bubbles; c) bubbles stuck on the cell window. | 47 |
| Figure 4.1. Destabilization over time at different temperatures of a 5 wt% latex with 0.12 mol% and 0.07 mol% switchable surfactant, C12, and initiator, VA-061, respectively. The arrows indicate the appropriate axes for the curves. Reprinted with permission from Fowler, C. I.; Muchemu, C. M.; Miller, R. E.; Phan, L.; O'Neill, C.; Jessop, P. G.; Cunningham, M. F. <i>Macromolecules</i> , 2011 , <i>44</i> , 2501-2509. Copyright 2011 American Chemical Society. ⁴⁶ | 52 |
| Figure 4.2. SEM images of a PMMA latex made with 0.12 mol% C12 and 0.07 mol% VA-061 before and after destabilization by heating the 5 wt% latex at 65 °C and sparging with air. Reprinted with permission from Fowler, C. I.; Muchemu, C. M.; Miller, R. E.; Phan, L.; O'Neill, C.; Jessop, P. G.; Cunningham, M. F. <i>Macromolecules</i> , 2011 , <i>44</i> , 2501-2509. Copyright 2011 American Chemical Society. ⁴⁶ | 54 |

| | |
|--|----|
| Figure 4.3. Particle size distributions of a latex after preparation, after aggregation (with air at 80 °C) and after redispersion (10 % sonication with a probe sonicator for 1 min). The 5 wt% original latex contained 0.12 mol% C12 surfactant and 0.07 mol% VA-061. Distributions were measured using static light scattering. The peak at 110 μm is due to bubbles. | 55 |
| Figure 4.4. Redispersion of a 5 wt% aggregated PMMA latex with 1 cm, 1.9 cm and 2.5 cm rotor-stators at 6000 rpm. The latex was made with 0.12 mol% C12 and 0.07 mol% VA-061 and produced a particle size of 135±2 nm with a zeta potential of 36±1 mV. The latex was aggregated to 10.2 μm with air at 80 °C. | 65 |
| Figure 4.5. Redispersion of a 5 wt% aggregated PMMA latex with a 1 cm rotor-stator at various rotational speeds. The latex was made with 0.12 mol% C12 and 0.07 mol% VA-061 and produced a particle size of 135±2 nm with a zeta potential of 36±1 mV. The latex was aggregated to 10.2 μm with air at 80 °C. | 66 |
| Figure 4.6. Redispersion of a 5 wt% aggregated PMMA latex with a 1.9 cm rotor-stator at various rotational speeds. The latex was made with 0.12 mol% C12 and 0.07 mol% VA-061 and produced a particle size of 135±2 nm with a zeta potential of 36±1 mV. The latex was aggregated to 10.2 μm with air at 80 °C. | 67 |
| Figure 4.7. Redispersion of a 5 wt% aggregated PMMA latex with a 2.5 cm rotor-stator at various rotational speeds. Original particle size was 135±2 nm with a zeta potential of 36±1 mV and aggregated to 10.2 μm. | 68 |
| Figure 4.8. The reaggregation of a reconstituted PMMA latex by three different methods. Original latex was made with 0.12 mol% C12 and 0.07 mol% VA-061 to give an initial particle size of 132±1 nm and a zeta potential of 43±1 mV. The latex was initially aggregated with air at 80 °C to a particle size of 8 μm and a zeta potential of 20±1 mV. | 74 |
| Figure 4.9. The interaction energies between two spherical PMMA particles with diameters of 150 nm in the presence of charged (“on”) and neutral (“off”) switchable surfactant, as a function of distance between the surfaces. | 79 |
| Figure 5.1. Emulsion stability tests of a BA/MMA/H ₂ O emulsion with a monomer content of 58.6 wt% with different concentrations of C12 relative to the total monomers. | 88 |
| Figure 5.2. Photograph of the coagulated BA/MMA copolymer. The sample was destabilized with air and heat (80 °C). | 92 |
| Figure 5.3. An SEM image of the coagulated BA/MMA copolymer. The sample was destabilized with air and heat (80 °C). | 93 |
| Figure 5.4. Optical microscope images of the films from a) a BA/MMA copolymer and b) a PMMA polymer latexes at 10x magnification. | 94 |
| Figure 5.5. An SEM image of the film produced by a BA/MMA copolymer. | 95 |
| Figure A.1. The datasheet from the Zetasizer Nano ZS after the particle size measurement | |

| | |
|---|-----|
| of a polystyrene latex. | 106 |
| Figure A.2. The datasheet from the Zetasizer Nano ZS after the zeta potential measurement of a redispersed PMMA latex. | 107 |
| Figure A.3. The datasheet from the Mastersizer 2000 after the particle size measurement of a polystyrene latex. | 108 |
| Figure A.4. The datasheet from the Mastersizer 2000 after the particle size measurement of an aggregated PMMA latex. | 109 |
| Figure A.5. The datasheet from the Mastersizer 2000 after the particle size measurement of a redispersed PMMA latex. | 110 |
| Figure A.6. The proton NMR of the BA-MMA copolymer made by a semi-continuous process with peak assignments. ⁶¹ | 111 |
| Figure A.7. Photographs of the a) sonicator probe, b) the 5.5 cm rotor-stator, c) the blender and d) the stirrer propeller..... | 111 |

List of Symbols and Abbreviations

| | |
|-----------------|---|
| $t_{1/2}$ | aggregation half-life |
| N_A | Avogadro's number |
| VA-061 | 2,2'-azobis[2-(2-imidazolin-2-yl)propane] |
| VA-044 | 2,2'-azobis[2-(2-imidazolin-2-yl)propane] dihydrochloride |
| k | Boltzmann constant |
| BA | butyl acrylate |
| CTAB | cetyl trimethylammonium bromide |
| CTA | chain transfer agent |
| c_i | concentration |
| l_0 | contact distance |
| cmc | critical micelle concentration |
| κ^{-1} | Debye length |
| DLVO | Derjaguin-Landau-Verwey-Overbeek |
| ε | dielectric constant of a medium |
| ε_0 | dielectric constant of a vacuum |
| D | diffusion constant |
| r_0 | distance between molecules |
| a | distance between particle surface and shear plane |

| | |
|------------------|---|
| l | distance between surfaces |
| x | distance from a surface |
| C12 | N'-dodecyl-N,N-dimethylacetamidinium bicarbonate |
| ψ | electrical potential |
| ψ_0 | electrical potential of a surface |
| U_E | electrophoretic mobility |
| e | elemental charge |
| XDLVO | extended-Debye-Hückel-Landau-Verwey-Overbeek |
| ΔS | change in entropy |
| FRET | fluorescence resonance energy transfer |
| GPC | gel permeation chromatography |
| ΔG | change in Gibb's free energy |
| T_g | glass transition temperature |
| $f(\kappa a)$ | Henry's function |
| C16 | N'-hexadecyl-N,N-dimethylacetamidinium bicarbonate |
| LC ₅₀ | lethal concentration to kill 50 % of the population |
| d(0.5) | mass median diameter |
| M2000 | Mastersizer 2000 |

| | |
|----------|---|
| MMA | methyl methacrylate |
| MFFT | minimum film formation temperature |
| $[M]_p$ | monomer concentration |
| NMR | nuclear magnetic resonance |
| N_p | number of particles |
| n | number of radicals per particle (average) |
| o/w | oil-in-water emulsion |
| γ | oil-water interfacial tension |
| d | particle diameter |
| d_z | particle diameter based on intensity distribution |
| d_v | particle diameter based on volume distribution |
| R | particle radius |
| PdI | particle size polydispersity index |
| PMMA | poly(methyl methacrylate) |
| PVA | Polyvinyl alcohol |
| k_{ij} | rate constants |
| k_p | rate constant of propagation |
| R_p | rate of polymerization |
| r | reactivity ratio |

| | |
|------------------------|----------------------------------|
| SEM | scanning electron microscope |
| SDS | sodium dodecyl sulfate |
| ϕ | solids content |
| ΔA | change in surface area |
| γ_3^{LW} | surface energy of a medium |
| γ_1^{LW} | surface energy of a surface |
| T | temperature |
| TEM | transmission electron microscope |
| z_i | valency |
| η | viscosity |
| D[4,3] | volume mean diameter |
| w/o | water-in-oil emulsion |
| ζ | zeta potential |

1. Introduction

1.1 General background

There are many different industrial uses of latexes. A latex is defined as “a stable colloidal dispersion of a polymeric substance in an aqueous medium”.¹ In the year 2000, 8.5 million metric tons of polymer dispersion (dry), with a solids content of 50 %, was produced of a total 189 million metric tons of plastic industrially.² The break down of the world demand in 1998 for polymer dispersions in different industries was as follows: 26 % paints and coatings, 23 % paper, 22 % adhesives, 11 % carpet backing and 18 % in other markets. In the paints and coatings industry, polymer dispersions could be used in anything from paint for walls and cars, to coatings for optical fibers and electronic components. The paper industry uses polymer dispersions to make paper hydrophobic and to bind pigments. Polymer dispersions are even used in the printing inks used to print on paper. They are also used in the adhesives industry. Adhesives are used instead of welding or riveting to attach two things together. Polymer dispersions are used in packaging, automobiles and even in aircraft construction. Polymer dispersions are also used for the leather industry, asphalt modification and plastic modification.²

Emulsion polymerization is used to produce many different types of polymer colloids, and it is an environmentally desirable process because of the aqueous continuous phase. Aqueous-based latexes have much less volatile organic compounds than the solvent-based latexes. Volatile organic compounds can accumulate and degrade in the atmosphere to contribute to climate change and ozone depletion. Emulsion polymerization is used to produce 90 % of the polymer dispersions industrially.²

However, in industries where a polymer resin is the desired product (and not the dispersion), large amounts of salts or acids are used to destabilize latexes. The increase in ionic strength causes a collapse of the electrical double layer, which causes aggregation of the polymer particles.³ The large amounts of chemicals used in destabilization then need to be cleaned from the product. The large amounts of water and acid or salt waste reduces the environmental friendliness of the process.

1.2 Surfactants

Surfactants are molecules that contain a hydrophobic tail and a hydrophilic head. The tail is generally a long alkyl chain that will orient itself towards an organic phase, while the head is usually a polar or ionic group that will orient itself towards the water phase. The tail can either be a branched or linear chain. This structure leads to an amphiphilic molecule that will orient itself perpendicular to all the interfaces in a system. Ionic surfactants can be split into cationic and anionic surfactants where the head group contains either a positive or a negative charge, respectively. There are also nonionic surfactants, which contain no charge but contain polar head groups. Examples of the different types of surfactants are shown in Figure 1.1. Some surfactant types are more desirable than others depending on the application. Cationic surfactants are best for adsorbing onto negatively charged surfaces while anionic surfactants are best for adsorbing onto positively charged surfaces. They both provide electrostatic stabilization. A nonionic surfactant is not charged and therefore cannot provide stabilization by electrostatic means, but it does provide steric stabilization. Nonionic and anionic

surfactants are the most widely used surfactants and cationic surfactant production only accounts for about 10 % of total surfactant production.⁴

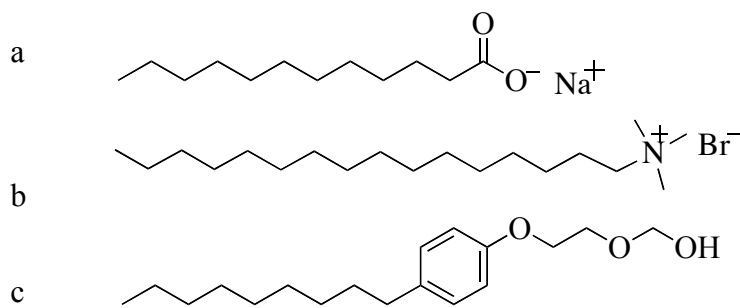


Figure 1.1. Examples of a) anionic, b) cationic, and c) nonionic surfactants.

Surfactants are useful molecules in a vast variety of different applications. One of the most common uses of surfactants by the common consumer is for cleaning. Soaps and detergents are used to solubilize oil and remove dirt from clothing, skin, dishes and other items. Soaps were first synthesized from animal fats 2300 years ago with the use of a campfire.⁵ Nowadays, synthetic detergents are manufactured to have pleasant smells and superior cleaning abilities. Regardless of how a detergent is made, whether it is in an industrial plant or over a fire, it contains the basic hydrophilic/hydrophobic structure. Surfactants are also widely used in the petroleum industry, pharmaceuticals industry, food industry, and coatings industry as well as many others.⁵

Surfactants in solution will orient themselves perpendicular to the air/water interface and any other surface/water interfaces. The surfactant will lower the interfacial tension. Once these surfaces become saturated, the excess surfactant will begin to exist as

individual solubilized surfactant molecules. At a certain concentration it will no longer be thermodynamically favourable to individually solubilize the surfactant molecules, and they will form aggregates called micelles. This concentration is called the critical micelle concentration (cmc). Micelles will have different geometries depending on their critical packing parameter, which will depend on the geometry of the surfactant itself (e.g. tail length, head group area). Surfactants with single tails and large head groups will orient themselves into spherical micelles. There are also cylindrical or rod-like micelles, or surfactants can also form bilayer structures like vesicles or extended planes.⁵ The number of surfactant molecules in a micelle is called the aggregation number. At the cmc, there will be a drastic change in several of the solution properties such as conductivity and surface tension among others.⁴

1.3 Switchable surfactants

Switchable surfactants are molecules whose surface activity can be reversibly switched between active and inactive or less active states by means of a trigger. Most switchable surfactants that have been studied rely on a change in oxidation state, or a conformational change. The change in the oxidation state of ferrocenes and viologens for the use of switchable surfactants was reported by Anton et al.⁶ and Saji et al.⁷ Molecules with ferrocenyl headgroups form micelles when ferrocene has an oxidation state of zero, but once oxidized to +1 the micelles break apart due to electrostatic repulsion (Figure 1.2a). The electrochemical switching was monitored by cyclic voltammetry and is reversible. Viologen based surfactants act as surfactants when both nitrogens are charged (Figure 1.2c). After a two-step reduction the neutral viologen group no longer acts like a surfactant. Pyrazinium salts were also described as switchable surfactants based on an

oxidative switch.⁸ The oxidized molecule contains a charged head group which is characteristic of a surfactant and after a two-step reduction the head is left neutral resulting in an inactive surfactant (Figure 1.2b). Then there are the switchable surfactants whose trigger is light as in azobenzenes (Figure 1.2d).⁹ In the trans conformation, the surfactant molecules orient themselves into vesicles which have several applications including drug delivery. Upon UV irradiation, the molecule switches to the cis conformation and the vesicles break up (potentially releasing whatever the vesicle contained). It has already been said that the number of molecules in a micelle will depend on the geometry of the surfactant. Surfactants with long and less voluminous hydrophobic tails have a lower cmc because less surfactant is needed to form one micelle. The trans conformation has a long hydrophobic group so it will form vesicles. However, the cis conformation increases the volume of the hydrophobic portion at the same time as making it shorter causing vesicles to break up. The vesicles are recovered after irradiating with visible light again. The problem with the above surfactants is that oxidants or reductants need to be added to induce the switching, which may cause product contamination. Opacity of a product may be an issue for photochemical switching because light will have difficulties penetrating an opaque product. Some of these surfactants are also expensive to make as in the case of ferrocene containing molecules, or may be toxic such as the viologen containing molecules.¹⁰

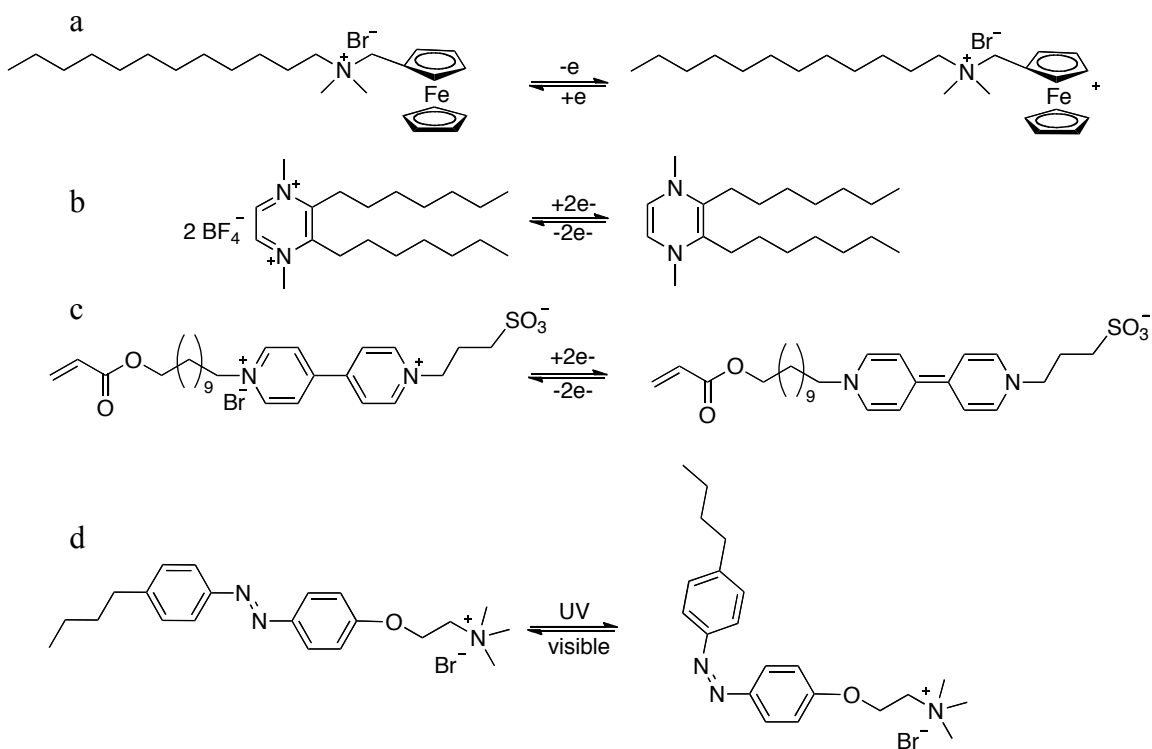


Figure 1.2. Examples of a) ferrocene, b) pyrazinium, c) viologen, and d) azobenzene based switchable surfactants, where the active surfactant structure is on the left side of the equilibrium arrows.

The switchable surfactants that have been developed in the Jessop group are based on a switch from an amidine to an amidinium bicarbonate salt due to a change in pH by the addition of carbon dioxide (Figure 1.3).¹¹ The CO_2 dissolves in water to form carbonic acid which can then protonate the dissolved amidine to form an amidinium bicarbonate salt. The reaction is reversed by removing the CO_2 from solution by bubbling with an inert gas, such as argon, nitrogen or air, and heating. The switchability of the surfactant in solution has been proven by conductivity measurements.¹¹ The amidinium bicarbonate salt can be isolated and is stable if stored in a sealed vial. The CO_2 is lost at a faster rate at higher temperatures and so, typically, the surfactant is stored in a refrigerator.

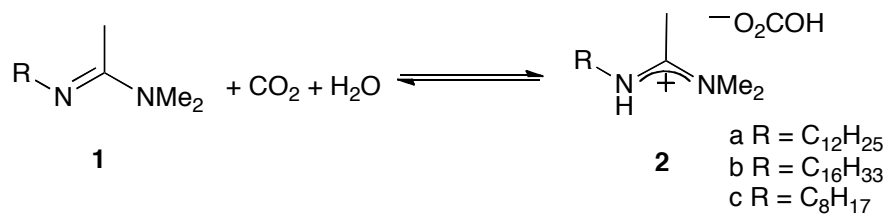


Figure 1.3. The reversible reaction between an amidine and CO₂ or air and heat where the charged species is the active surfactant.

A surfactant that can stabilize an emulsion at one point in a process and then switch to provide no stabilization can be very useful for many applications. Pipeline transport of viscous crude oils is much easier as an oil-in-water emulsion, but the oil must then be separated from the water for use. If a switchable surfactant were used to stabilize the emulsion, the oil could be separated by simply switching the surfactant to its inactive form.¹² Also relevant to the oil industry would be the washing of oil sands for oil recovery.¹³ But switchable surfactants are not only useful for the oil industry, they can be used for cosmetics, the preparation of nanoparticles and the preparation of latexes by emulsion polymerization (which is implemented in this project).^{11,14}

1.4 Environmental impact of switchable surfactants

The branched-tail surfactants used as detergents prior to 1970 had low biodegradability and therefore accumulated in the environment.⁵ The build-up of surfactant in rivers downstream from run-offs caused significant foaming in the water, especially at the bottom of waterfalls. Linear-tailed surfactants, which showed higher biodegradability, replaced the old branched-tail surfactants so that there would be less environmental impact. An increase in biodegradability is seen with certain structural groups such as linear hydrophobic groups, terminal phenyl groups, or the presence of

ethylene oxide groups.⁴ The amidine switchable surfactants are said to be “green” chemicals because of the benign trigger, CO₂, and the many potential energy and materials saving applications. But their biodegradability and their persistence in the environment need to be studied to determine whether they are really “green”. The amidine switchable surfactants discussed in this project may not have ethylene oxide or phenyl groups, but they do have a linear alkyl chain to help with biodegradability. Also, the surfactant does not contain any metals or halogens that could escape into the environment. The hydrolysis of amidines to less toxic products also helps to reduce the environmental impact. Under acidic conditions amidines are stable but above pH 7 there is significant decomposition to amines and amides.¹⁵

Surfactants are used for cleaning and will eventually end up in the water system. If these chemicals end up in rivers and lakes it is necessary to know if they will be harmful to any living thing. Toxicity measurements were carried out on rainbow trout to measure LC₅₀'s of the switchable surfactants.¹⁶ LC₅₀ is the concentration of chemical that kills 50 % of the test animals in a designated time. In this case, the LC₅₀'s reported were for a 96 h period. Table 1.1 shows the LC₅₀'s for switchable amidine surfactants with 16-, 12- and 8-carbon tails and sodium dodecyl sulfate (SDS) and cetyl trimethylammonium bromide (CTAB), two commonly used surfactants. With longer carbon tails the toxicity increases, so it would be best to use the shorter chains if possible. Although the switchable surfactants are not less toxic than already existing surfactants, they are not any more toxic, especially when compared to CTAB. However, with all the potential applications of switchable surfactants that involve saving energy and materials, it is still valid to call them “greener” surfactants.

Table 1.1. The 96 h LC₅₀'s in rainbow trout of switchable surfactants **1a**, **1b**, and **1c** as well as SDS and CTAB.

| Surfactant | 96 h LC ₅₀ (mg/L) |
|------------|---------------------------------|
| 1b | 0.08 |
| 1a | 0.43 |
| 1c | 8.94 |
| CTAB | 0.14 |
| SDS | 15.48 |

1.5 Emulsions

An emulsion is a heterogeneous mixture of two immiscible liquids. Typically, one phase will be aqueous and the other organic. One phase, the dispersed phase, is dispersed in another, called the continuous phase. When water is dispersed in an organic continuous phase it is called a water-in-oil (w/o) emulsion. Conversely, when the opposite is true it is called an oil-in-water (o/w) emulsion (Figure 1.4). It is also possible to get double emulsions such as water-in-oil-in-water.¹⁷ The type of emulsion that is produced will not only depend on the weight ratio of the phases but also the geometry of the surfactant.^{3,5} The geometry of the surfactant will affect the packing ability. If the tails are wider than the heads, then the tails will point towards the outside of the droplets, producing a w/o emulsion. The hydrophilicity of the surfactant will also have an affect on the type of emulsion produced. A general rule is that the phase the surfactant is more soluble in will be the continuous phase.³

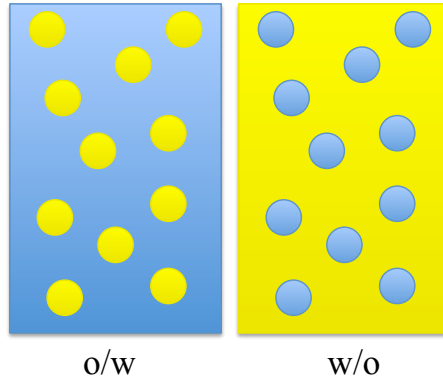


Figure 1.4. Examples of oil-in-water (o/w) and water-in-oil (w/o) emulsions where blue is the water and yellow is the oil.

In an emulsion, the oil-water interfacial area is greatly increased which is not thermodynamically favourable. Equation 1.1 shows the Gibbs free energy change (ΔG) in relation to the change in surface area of the droplets (ΔA) during the emulsification process:

$$\Delta G = \gamma\Delta A - T\Delta S \quad (1.1)$$

where γ is the oil-water interfacial tension, T is the temperature and ΔS is the entropy.¹⁸ The initial state is a biphasic mixture of two immiscible liquids and the final state is an emulsion. Disorder is greatly increased when creating an emulsion and so the process is entropically favoured. However, the surface area is increased greatly and so the process is enthalpically disfavoured. Because the surface area after emulsification will be so large, ΔA is effectively A_{final} and the first term of the equation will dominate. ΔG will always be positive which is why the emulsification process is never thermodynamically favourable.³ The use of a surfactant decreases the oil-water interfacial tension by orienting itself at the interface, which in turn will decrease the free energy change. Emulsions are not

thermodynamically stable also because the free energy will always be positive. Emulsions, however, are kinetically stable. Long-term stability of an emulsion is increased when surfactant is added because the activation energy of coalescence is altered. The activation energy is increased when the free energy change of the system is decreased (because G_{final} is decreased).

1.6 Emulsion polymerization

Emulsion polymerization is a type of heterogeneous free-radical polymerization. The polymerization reaction takes place in a different phase than the continuous phase. This process has been widely used to produce latex products since the 1930's¹⁸ and is considered environmentally friendly because the continuous phase is water instead of an organic solvent.

Surfactant is added to stabilize the large monomer droplets in the continuous phase to form an emulsion. Surfactant will be found at the air/water interface, the monomer/water interface and some will be dissolved in the aqueous phase. If the concentration of surfactant is above the critical micelle concentration (cmc) then the surfactant will begin to form micelles. Some monomer will migrate into the hydrophobic centers of the micelles. The monomer droplets act as giant reservoirs during polymerization to feed the monomer-swollen micelles. There is also a small amount of monomer dissolved in the aqueous phase, which is necessary to begin the polymerization reaction.¹⁸

Free-radical polymerization involves three steps: initiation, propagation and termination. There are 3 different types of particle nucleation that can occur during the

initiation step: micellar, homogeneous or coagulative nucleation. Homogeneous and coagulative nucleation will occur when the concentration of surfactant is below the cmc. Micellar nucleation will be discussed here, because the polymerizations carried out in this project contained surfactant concentrations above the cmc (0.5 mM for switchable amidine surfactant **2a** in water).¹⁹ First, to initiate the polymerization, an initiator must be added. A water-soluble initiator decomposes at a certain temperature to produce radicals and begin the reaction. The radicals will react with monomer dissolved in the aqueous phase adding a few monomer units together to form oligoradicals, which become increasingly hydrophobic. The oligoradicals become so hydrophobic that they can no longer exist in the aqueous phase; they can either move into a monomer droplet or a monomer-swollen micelle. Since the micelles have a much larger total surface area than the monomer droplets it is more likely that the oligoradical will enter a micelle. Once inside the micelle the oligoradical will continue to grow until the monomer in the micelle is consumed. Once the monomer is consumed, monomer from other micelles, that were not nucleated, will diffuse into the particle nuclei to continue growth. Particle nucleation ends when all the monomer-swollen micelles are consumed. It may be intuitive, but the length of the nucleation period will depend on the amount of surfactant and initiator. With more surfactant, there will be more micelles to nucleate leading to a longer nucleation time. With less initiator, it will take longer to nucleate all of the micelles. Micelles that were not nucleated will break apart so more surfactant can adsorb onto the growing particle surface to help maintain colloidal stability. Surfactant will also desorb from the monomer droplet surface and diffuse to the particle surface.¹⁸

During interval II, propagation, monomer from the monomer droplets diffuses

into the particle nuclei to continue the growth of the polymer. Smith-Ewart theory shows that the rate of polymerization (R_p) is:

$$R_p = k_p[M]_p \left(\frac{nN_p}{N_A} \right) \quad (1.2)$$

where k_p is the rate constant of propagation, $[M]_p$ is the concentration of monomer in the particle, n is the average number of radicals per particle, N_p is the number of particles and N_A is Avogadro's number. This equation is valid for interval II if the number of particles remains constant (no new particle nucleation), the latex is monodispersed, desorption of radicals from the particles does not occur and the bimolecular termination of radicals is instantaneous. If these assumptions are valid, there can only ever be one or zero radicals in a particle at any time. Once a radical enters a particle it will remain there, but if another enters they will terminate each other immediately. The average number of radicals in a particle is therefore 0.5. It is said to be "Case 2 kinetics" when n is 0.5 and this case is most easily applied. If radicals can desorb from a particle, then Case 1 is observed where $n < 0.5$. If bimolecular termination is not instantaneous, then Case 3 is observed where $n > 0.5$. The rate of polymerization during interval II will be constant (with Case 2 kinetics) because the number of particles should not change after the nucleation interval and the concentration of monomer is held constant due to the thermodynamic balance between polymer/monomer mixing and the growth of the polymer. Gibbs energy is decreased when the monomer in the water phase moves into the polymer particle. However, as the particle size grows the energy of the particle surface will increase because of the reduction in surfactant surface coverage.²⁰ It is this

balance that keeps the monomer concentration constant. Interval II ends when monomer diffusion is no longer thermodynamically favourable.¹⁸

In interval III, the rate of polymerization decreases as the remaining monomer in the particles reacts. Figure 1.5 is a schematic of emulsion polymerization depicting micellar nucleation and particle growth within a micelle.¹⁸

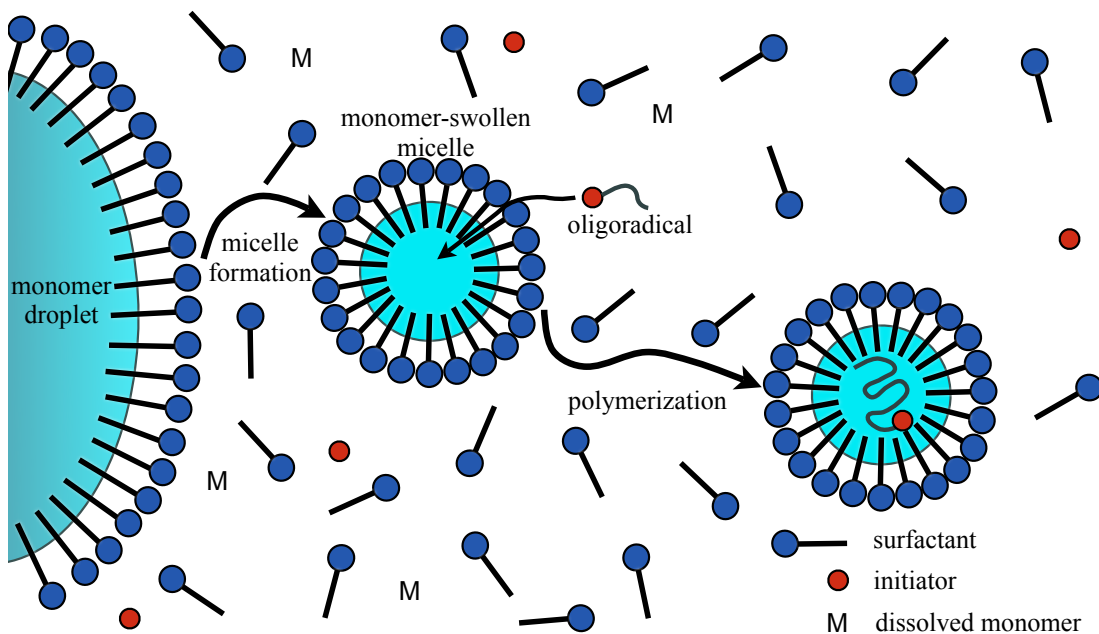


Figure 1.5. The steps involved in emulsion polymerization, where particle nucleation occurs via micellar nucleation.

1.7 Colloidal stability

Colloidal stability originates from the balance of non-covalent intermolecular forces. The first type of intermolecular force which is present is van der Waals, which can

be further split into three forces: Keesom (dipole-dipole), Debye (dipole-induced dipole) and London (instantaneous dipole-induced dipole). Keesom and Debye will only be present when molecules have permanent dipoles, whereas London forces are always present. The interaction energy between two dipoles will depend on their relative angles, but because molecules have the freedom to rotate it is possible to take an average of the angles. The Keesom interaction energy ends up being inversely proportional to the distance between the molecules to the sixth power. The Debye interaction energy will also have an average angle value and results again in an inverse proportionality to the distance between molecules to the sixth power. Both the Keesom and Debye interaction energies are very weak between macroscopic bodies in liquid media, and do not contribute significantly to the overall van der Waals forces. London, or dispersion, forces contribute the most to van der Waals forces between macroscopic bodies. Dispersion forces have a few simple characteristics: 1) they are always present; 2) they are long-range forces (10 nm or more); 3) they can be attractive or repulsive (but between two of the same molecule they will always be attractive); and 4) they are nonadditive (the interaction between two bodies will be affected by other nearby bodies). On average a non-polar molecule will contain no dipole, but for an instantaneous moment there will be a dipole due to the position of the electrons and protons. This instantaneous dipole creates an electric field and causes an induced dipole in a neighbouring molecule. Averaging over time, this creates the dispersion interaction energy. Dispersion forces also contain an inverse proportionality to the distance between the molecules to the sixth power. The total van der Waals forces is the summation of the Keesom, Debye and London forces which contain the r_0^{-6} proportionality (where r_0 is the distance between the molecules).^{3,21}

Hamaker was the first to apply van der Waals forces to large macroscopic bodies. The interaction energy between the larger bodies will decay longer, because van der Waals energies will no longer have an r_0^{-6} relationship. Surface (or bulk) properties are used to calculate the interaction energies instead of molecular properties. Since Hamaker, there have been many approximations to simplify the calculation intensive equations.²¹

The next type of non-covalent interactions are coulombic interactions, or electrostatic interactions. Surface charge can arise from preferential adsorption of ions on a surface or ionization of surface groups. Once there is charge on the surface, counter ions in solution move closer to the surface. This structured arrangement of charge near the surface is the electrical double layer seen in Figure 1.6.^{3,21,22} The layer of counter-ions associated with the charge on the surface of a particle is called the Stern layer, and the diffuse layer is the thick layer of counter-ions whose concentration decays exponentially with distance from the Stern layer. The plane between the Stern layer and diffuse layer is called the shear plane (or the slipping plane). This model of the electrical double layer is the Gouy-Chapman-Stern-Grahame model. The electrical potential (ψ) at a distance x from the surface can be approximated using the Debye-Huckel approximation:

$$\psi = \psi_0 e^{-\kappa x} \quad (1.3)$$

where ψ_0 is the electrical potential at the surface, and κ is the reciprocal of the Debye length.³ Equation 1.3 describes the electrical potential decay after the Stern layer to be exponential, but between the surface and the Stern layer the decay will be linear.²³ The Debye length, (κ^{-1}) is calculated by the following:

$$\frac{1}{\kappa} = \left(\frac{\varepsilon_0 \varepsilon k T}{e_i^2 \sum c_i z_i^2} \right)^{1/2} \quad (1.4)$$

where ε_0 is the dielectric constant in a vacuum, ε is the dielectric constant of the medium, k is the Boltzmann constant, T is the temperature, e_i is the elementary charge, c_i is the concentration of i , and z_i is the valency of i .^{3,22} From this equation it can be seen that as the electrolyte concentration increases (increasing the $\sum c_i z_i^2$ term), the Debye length, which is effectively the thickness of the double layer, shrinks. When the electrical double layer shrinks, the particles can physically come closer together because there is less electrostatic repulsion. This is why adding salts, acids or bases can cause destabilization. The electrical potential at the shear plane is called the zeta potential. The surface potential, which is needed to calculate the electrostatic interactions between surfaces, can be calculated from the zeta potential. The zeta potential can be measured experimentally. The following is the equation for surface potential (ψ_0):

$$\psi_0 = \zeta \left(1 + \frac{a}{R} \right) e^{\kappa a} \quad (1.5)$$

where ζ is the zeta potential, a is the distance between the particle surface and the shear plane, and R is the particle radius. The interaction energy due to electrostatic interactions can be calculated as a function of distance between the particle surfaces.²¹

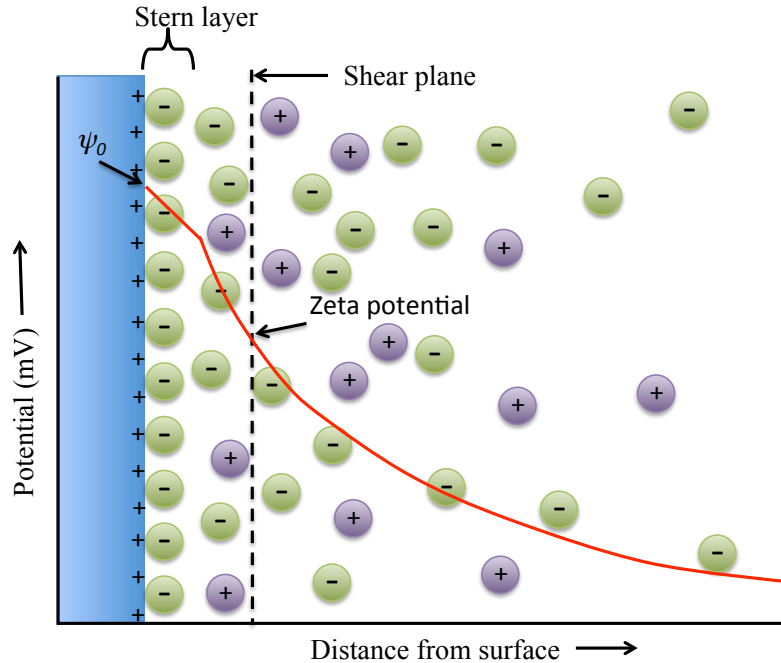


Figure 1.6. The electrical double layer of a positively charged surface, where the red line represents the decay in the electrical potential from a charged surface.

Derjaguin-Landau-Verwey-Overbeek (DLVO) theory allows us to calculate the total interaction energy between two surfaces in a medium. The interaction energies will be affected by the surface geometries. The interaction between a flat plane and a sphere will be different from that of two spheres. If the two spheres are of very different sizes, one could approximate the larger sphere to be a flat plane when compared to the small sphere. The electrostatic interaction energy (ΔG^{EL}) between two spheres of radii R_1 and R_2 is:

$$\Delta G^{EL} = \left(\frac{R_1 R_2}{R_1 + R_2} \right) \psi_0^2 \epsilon \ln[1 + e^{-kl}] \quad (1.6)$$

where l is the distance between the surfaces.²¹ The interaction energy between two spheres of the same material due to van der Waals (ΔG^{LW}) is:

$$\Delta G^{LW} = 2\pi \left(\frac{R_1 R_2}{R_1 + R_2} \right) \left(-2 \left[(\gamma_1^{LW})^{1/2} - (\gamma_3^{LW})^{1/2} \right]^2 \right) \frac{l_0^2}{l} \quad (1.7)$$

where γ_1^{LW} and γ_3^{LW} are the surface energies of the surface and medium, respectively, and l_0 is the contact distance. These two equations can be plotted versus the distance between the surfaces to give DLVO plots. The sum of the two gives the total interaction energy. There is also an extended-DLVO (XDLVO) theory that takes into account acid-base interactions and provides a more accurate result for the interaction energies, but for simplicity this will not be discussed.²¹

DLVO theory describes colloidal stability, and allows us to predict the stability of a system. If the total interaction energy is positive there will be repulsion between the particles, meaning a stable dispersion is obtained. If the particles overcome a potential energy barrier they will fall into the primary minimum and aggregate, and in most cases, this will be irreversible. If the total interaction energy is always negative then there is no possibility of a stable dispersion.^{3,21}

1.8 Redispersible latexes

Redispersible powders are heavily used in the building and construction industry. Protective colloids are added to latex dispersions before the spray drying process to prevent the formation of a film. The dry particles can then be redispersed when water is reintroduced to the system. Redispersible powders modified with polymers have allowed

for on-site mixing of mortars to be used in construction. This also allows for cheaper transportation costs of building materials.²

Redispersible latexes also have the potential to be useful in reducing shipping costs of latexes over long distances. Currently latexes are shipped with a significant amount of water that makes long-distance transportation expensive and less environmentally friendly. It would be ideal if the majority of the water could be removed before shipping. If minimal water containing latexes were sold in this form, this would also result in fewer materials for packaging. If all of the water could be removed it would not be necessary to provide protection against freezing and bacteria. Redispersible latexes have been reported, but in most cases require the addition of acids or bases to induce redispersion.^{24,25,26}

Guziak et al.²⁴ reported preparing a latex with at least 10 wt% of a monomer containing a carboxylic acid group (methacrylic acid). The latex was dried to a granular free-flowing solid, which when added to water produced no latex, but once base was added, a reconstituted latex was obtained. The base was required to deprotonate the carboxylic acid groups creating a significant amount of charge on the particle surface leading to colloidal stability. The reconstituted latex, once dried again, was not redispersible for a second time.

Saija et al.²⁵ also report the use of acidic groups to produce a redispersible polymer. A low glass transition temperature (less than room temperature), T_g , polymer could be made redispersible by doing a sequential copolymerization to add a higher T_g polymer shell. The higher T_g layer prevented the soft cores from fusing during the spray-

drying process to give a dry powder. Water was reintroduced along with a strong base to redisperse. By using stronger acid groups during polymerization, they reported that redispersion was possible at lower pH.

Greene et al.²⁷ also made use of acidic surface groups for redispersion. When they dried their latex, it formed a film with poor strength and integrity. No base was required to redisperse the dried latex, but instead 2 min of blending with a Waring blender was needed.

Also in the literature is the use of a polyvinyl alcohol (PVA) membrane as a protective colloid to produce a redispersible film.²⁸ The PVA shields the particles from each other and keeps them separated during film drying making it possible to redisperse when water is reintroduced. Redispersion was possible by simply adding water with a minimal amount of shear (when surfactant was not present in the system). However, it was found that association between the membrane and the surfactant (SDS) degraded the membrane and led to non-redispersible film.

Another pH sensitive example is the use of macroazoinitiators to form “hairy” latex particles.²⁶ The particles were prepared by dispersion polymerization and the azoinitiator was used as both the initiator and stabilizer. Base was added to deprotonate and cause the collapse of the “hairs” to induce aggregation. The reconstituted latex was obtained when the pH was lowered again. Reversibility was only possible for 3 cycles before salt induced aggregation occurred.

Discussed in a publication from our group is the redispersion of aggregated latexes prepared with amidine based switchable surfactants.²⁹ The amidine switchable

surfactants as well as a switchable initiator were used to prepare the latexes. 2,2'-Azobis[2-(2-imidazolin-2-yl)propane] (VA-061) is an azo-based initiator that contains two imidazoline groups which when in carbonated water become protonated and form a bicarbonate salt (Figure 1.7). The initiator group, which becomes chemically bound to the particle surface, also helps with switching along with the surfactant. It was found that latexes were only switchable if both switchable surfactant and switchable initiator were used. If a switchable molecule (surfactant or initiator) was used in conjunction with a nonswitchable molecule, switchability was lost. The redispersions were carried out on polystyrene latexes prepared with large amounts of switchable groups. The amount of switchable initiator ranged between 1 and 10 mol% and 1.5 mol% of switchable surfactant was used. Redispersion was carried out with sonication for 15 min, in a sonicator bath, with and without 15 min of CO₂ exposure. It was found that redispersion was successful with and without CO₂.

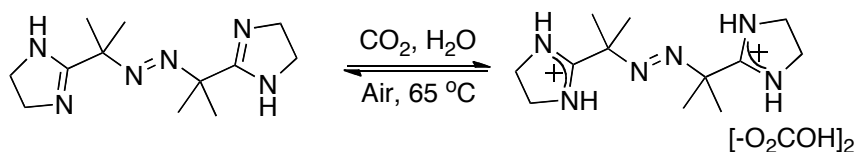


Figure 1.7. The reversible reaction between the switchable initiator, VA-061, and CO₂ or air and heat.

1.9 Film formation

There are three main steps to film formation: 1) water loss; 2) deformation of particles; and 3) particle interdiffusion (Figure 1.8).^{30,31,32} During the first step water evaporates from the continuous phase and the particles pack closer together. Then, if the particles are soft enough they will begin to deform, filling the voids between the spherical

particles. When the voids between the particles are filled this will lead to a clear film because there will no longer be any holes to scatter light, this will occur at the minimum film formation temperature (MFFT). The last step can only occur when the film is dried above the polymer's glass transition temperature (T_g). The molecular chains from particles will diffuse into each other until there are no longer any particle boundaries leading to a continuous film.^{18,30}

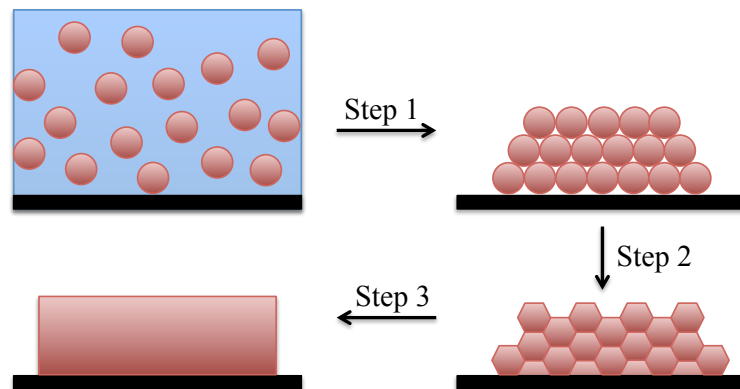


Figure 1.8. The steps involved during film formation: 1) evaporation of water; 2) deformation of particles; and 3) interdiffusion of particles.

1.10 Goals

The goal of this project was to make redispersible polymer colloids using the amidine switchable surfactants. The destabilization and redispersion of polymers prepared with the switchable surfactant have already been shown to be successful but with very little optimization of the redispersion. Another goal was to use the surfactants to make a latex containing a low T_g polymer with high solids content. This would represent a more realistic latex used industrially. The film produced by this latex was also examined.

2. Experimental Methods

2.1 Materials

2,2'-Azobis[2-(2-imidazolin-2-yl)propane] (VA-061), and 2,2'-azobis[2-(2-imidazolin-2-yl)propane] dihydrochloride (VA-044) from Wako Pure Chemical Industries Ltd. (Osaka, Japan) and cetyl trimethylammonium bromide (CTAB, 98 %), from Aldrich were used without further purification. Methyl methacrylate (MMA, 99 %) and butyl acrylate (BA, 99 %), from Aldrich, contained monomethyl ether hydroquinone (MEHQ, 10-100 ppm in MMA and 10-60 ppm in BA) as an inhibitor and styrene (99 %), from Aldrich, contained 4-*tert*-butylcatechol (TBC, 10-15 ppm) as an inhibitor. All monomers were purified by passing them through inhibitor removal columns (Aldrich). N'-Dodecyl-N,N-dimethylacetamidinium bicarbonate (**2a**, hereafter referred to as C12) and N'-hexadecyl-N,N-dimethylacetamidinium bicarbonate (**2b**, hereafter referred to as C16) were prepared according to our previously reported procedure.¹¹ Medical grade CO₂ from Praxair and distilled deionized water were used throughout the project. Disponil A 3065®, a 30 wt% mixture of non-ionic surfactants from Cognis, was used after dilution to 1 wt% and 1-dodecanethiol (98 %), from Aldrich, served as a chain transfer agent.

2.2 Emulsion stability test

Emulsions with 58.6 wt% monomer consisted of 60 wt% BA (3 g) and 40 wt% MMA (2 g). Varying amounts of C12 (0.24, 0.48, 1.0, 2.0 mol% based on total monomers) were dissolved in the monomers before adding the water (3.5 mL) to create an emulsion. The emulsions were stirred magnetically for 1 h in 20 mL scintillation vials after exposure to CO₂ by bubbling with a needle for 15 min. The vials were then capped

and sealed with Parafilm[®] after CO₂ exposure. Stirring was stopped after 1 h and the emulsions were left to sit on the benchtop. A photo was taken at 1, 5, 15, 30 and 60 min to visually determine emulsion stability.

2.3 Emulsion polymerization

2.3.1 Batch emulsion polymerization

Carbon dioxide was sparged through distilled water (60 mL) in a round bottom flask with a needle for 30 min to carbonate the water. Meanwhile, C12 (0.12 mol% with respect to monomer, 11.9 mg) was dissolved in methyl methacrylate (31.3 mmol) with the help of sonication from a 100 W sonicator bath for approximately 1 min. The monomer-surfactant mixture was added to the carbonated water and allowed to stir for 30 min to create an emulsion. During that time a portion (~5 mL) of the previously carbonated water was added to VA-061 (0.07 mol%, with respect to monomer, 5.5 mg) to create a solution of the bicarbonate salt of the initiator. The round bottom flask was then equipped with a condenser and the initiator solution was added. The polymerization was performed at 65 °C while maintaining bubbling with CO₂ and stirring. The reaction proceeded for 5 h before removing from heat. The latex produced had a solids content of 5 wt% that was measured gravimetrically. Monomer conversion was typically between 80-95 % which was determined gravimetrically. The T_g of the polymers produced was not measured.

2.3.2 Emulsion polymerization of a latex containing no switchable groups

For a control sample, a latex was prepared with no switchable groups. In order to achieve this, the same procedure was followed as above, however the surfactant and initiator used were CTAB and VA-044, respectively, and argon, rather than CO₂, was sparged through the system.

2.3.3 Surfactant mixtures during polymerization

Varying amounts of CTAB were added before the polymerization of MMA so that there was a mixture of C12 and CTAB during the polymerization. The latex produced had a solids content of 5 wt%. The same experimental procedure for polymerization was followed as in Section 2.3. The CTAB (0.06, 0.03, 0.015 and 0.0075 mol% based on monomer) and C12 (0.12 mol% based on monomer) were dissolved in the MMA before making the emulsion.

2.3.4 Semi-continuous emulsion polymerization

The latex of a copolymer was prepared by the general procedure modified from literature.³³ A 10 g mixture of comonomers was prepared, containing 52 wt% butyl acrylate (40.5 mmol, 5.2 g) and 48 wt% methyl methacrylate (47.9 mmol, 4.8 g). This should result in a copolymer with a glass transition temperature between 7 and 11 °C. A preemulsion was first prepared with the monomers, chain transfer agent (1-dodecanethiol, 0.14 mol% based on total monomers, 25 mg), C12 surfactant (2 mol% based on total monomers, 560 mg) and carbonated water (5 g) in a 25 mL round bottom flask. The surfactant and chain transfer agent were dissolved in the monomer with the help of

sonication (sonicator bath for 1 min). The preemulsion was stirred for 30 min. To create the seeded particles by batch polymerization, 0.44 g of the preemulsion was added to a 100 mL round bottom flask with an additional 4 g of carbonated water, C12 (0.09 mol% based on total monomer, 25 mg) and VA-061 initiator (0.25 mol% based on total monomer, 55.3 mg, in 1 g of water). CO₂ was first sparged through the VA-061 and water mixture with a needle to convert to the bicarbonate salt. The batch reaction proceeded for 20 min at 80 °C with continuous stirring with a magnetic stir bar. Additionally, the reaction flask was equipped with a condenser and CO₂ was bubbled through the reaction with a needle at all times. Concurrently, the remaining preemulsion was stirred while the batch reaction was taking place.

VA-061 (0.04 mol% based on total monomer, 8.8 mg) was dissolved in 2 g of carbonated water and added to the preemulsion. After the batch reaction, a model A99-E syringe pump from Razel Scientific Instruments was used to feed the preemulsion and additional initiator over time. A 5 mL syringe was loaded with 3 mL of the preemulsion/initiator mixture and set to feed at 0.1 mL/min. The syringe was refilled every 30 min with more preemulsion until it was all added to the reaction flask. There was some separation of the emulsion in the syringe, however this effect was reduced if CO₂ was bubbled through the preemulsion for 1 min prior to loading the syringe. After all the preemulsion was added, the system was allowed to react for an additional 30 min at 80 °C. A 42 wt% latex was produced with 7.5 to 10.4 % coagulum. ¹H-NMR spectroscopy (400 MHz) was used to determine the relative amounts of BA and MMA in the copolymer, the spectrum is shown in Appendix A. The *T_g* of the polymer produced was not measured.

2.4 Characterization

The particle sizes and zeta potentials of latexes produced by emulsion polymerization were measured using dynamic light scattering with a Zetasizer Nano ZS (Malvern). The particle sizes of aggregated latexes and the redispersed latexes were measured using static light scattering with a Malvern Mastersizer 2000 (Malvern) equipped with a Hydro2000S optical unit. During Mastersizer 2000 measurements there is extreme dilution of the sample; because of this, a nonionic surfactant, Disponil A 3065® (0.5 wt% with respect to mass of aggregated latex), was added to the sample before a measurement to prevent any further aggregation within the instrument. The conversion of methyl methacrylate was determined gravimetrically. Molecular weights were measured using gel permeation chromatography (GPC) using a Viscotek GPCmax VE 2001 containing a PAS-106M mixed bed column coupled with a differential refractive index detector. Tetrahydrofuran (THF) was used as the eluent at a flow rate of 1.0 mL/min. SEM images were obtained using a Hitachi TM-1000 or Hitachi S-2300 scanning electron microscope. Samples were sputter coated with gold and the SEM was operated at 20 kV. Optical microscope images were taken with a bright field Micromaster® optical microscope (Fisher Scientific) at 10x magnification.

2.5 Destabilization

Aggregation of the control sample was accomplished by adding salt (0.1 g of $\text{Al}_2(\text{SO}_4)_3$) to increase the ionic strength and cause destabilization. The aggregated latex was centrifuged for 10 min at 3500 rpm to decant the supernatant. Fresh water was added (~20 mL) and centrifuged again at the same conditions. This supernatant was decanted to

remove the salt. Finally, fresh water (~20 mL) was added to yield a solids content of 3.4 wt%.

Aggregation of latexes prepared with the switchable surfactant and initiator was done by sparging with air while heating between 65 and 80 °C until the particle size increased (this was generally determined visually by an increase in viscosity, before the particle size was measured). The aggregation time ranged between 2.5 and 24 h, depending on both the temperature and the volume of latex that was being destabilized.

Aggregation of a BA/MMA copolymer latex was accomplished with a 0.1 M solution of KOH in water. A 0.5 mL aliquot of KOH solution was added to 1 g of latex to cause destabilization.

2.6 Redispersion

2.6.1 Redispersion methods

Redispersion was attempted using four different methods. For all redispersion methods, some samples were exposed to CO₂ by bubbling with a needle for 10 min and some were not. All redispersions were carried out at room temperature. After the particle sizes and zeta potentials of the redispersed samples were measured, all vials were capped and sealed with Parafilm[®].

a) Bath sonicator: A Fisher Scientific Model FS30 sonicator bath was used to redisperse approximately 10 mL of aggregated latex in a 20 mL scintillation vial for 1 min.

b) Probe sonicator: An Omni Sonic Ruptor 250 W Ultrasonic Homogenizer, equipped with a 3/8" titanium processing tip (Omni International) was placed approximately

1.5 cm into 20 mL of an aggregated latex in a 35 mL vial. The probe power was set to 10 % and the sample was sonicated for 1 min. See Appendix A for a photograph of the probe (Figure A.7).

c) Rotor-stator: Rotor-stators of various sizes were used for redispersion. i) An aggregated latex (500 mL) was redispersed in a vessel, with a condenser jacket, using a VMI Rayneri TURBOTEST rotor-stator, with a diameter of 5.5 cm, at 2500 rpm for 1 min. See Appendix A for a photograph of the rotor-stator (Figure A.7). ii) A 40 mL sample was redispersed in a 60 mL wide-mouth glass bottle for 15 min (without cooling) using a 1 cm diameter rotor-stator with a Ultra Turrax IKA T18 basic motor (IKA). Redispersion was carried out at rotational speeds between 6000 and 18000 rpm and the particle sizes were measured at 1, 5, 10, 15 min. The temperature increased after 15 min. iii) A 1.9 cm rotor-stator was used with the same method as the 1 cm rotor-stator. iv) A 2.5 cm rotor-stator was also used with the same method as the previous two rotor-stators with the exception of the motor. An Ultra Turrax IKA T25 digital motor was used.

d) A hand-held blender: Approximately 200 mL of aggregated latex was placed in a tall (30 cm) plastic vessel. A Lancaster 1-Speed Hand Blender (purchased from Canadian Tire) was immersed into the aggregated latex so that the blade was approximately 3 cm from the bottom of the vessel and was turned on for 1 min of blending. The samples were not cooled during redispersion and the temperature increased only slightly after agitation. See Appendix A for a photograph of the blender (Figure A.7).

e) An overhead stirrer: Approximately 80 mL of aggregated latex was put in a 150 mL tall-form Berzelius beaker and an IKA Power Control-Visc overhead stirrer (130 W)

equipped with an IKA R2305 four-blade propeller was used for redispersion. The four-blade stirring probe was placed approximately 1 cm above the bottom of the beaker and the aggregated latex was stirred at 900 rpm for 1 min. See Appendix A for a photograph of the stirring probe (Figure A.7).

2.6.2 Dewatering latexes for redispersion

A 5 wt% polystyrene latex prepared with 0.12 mol% C16 and 0.07 mol% VA-061 (particle size of 80 nm) was first aggregated by sparging with air and heating to 65 °C for approximately 5 h to yield a particle size of 40 µm. This sample was then divided into three portions (~20 mL) and water was removed by different methods. The first aggregated latex was washed with approximately 20 mL of water while collecting by suction filtration using a glass frit. The polymer was then transferred to a watch glass and dried in an oven overnight at 80 °C. The next portion was collected with suction filtration using a glass frit to remove as much water as possible and the polymer was then stored in a capped vial to prevent any further drying. The last portion was centrifuged in a Sorvall Legend RT centrifuge at 4 °C for 10 min at 3500 rpm and the supernatant was poured off. Similarly to the second portion, the polymer was then stored in a capped vial to prevent further drying.

Fresh water (5 g) was added to the samples prior to redispersion. All samples were exposed to CO₂ by bubbling with a needle for 30 min. Each sample was exposed to four different scenarios for redispersion; 1) only CO₂, 2) CO₂ and additional surfactant, 3) CO₂ and sonication, and 4) CO₂, additional surfactant and sonication (where sonication was provided by a sonicator bath in all cases). Additional surfactant added to aid

redispersion was C16 (14 wt% based on the weight of polymer or wet polymer). Samples were then centrifuged for 10 min at 3500 rpm to examine, qualitatively, the effectiveness of redispersion.

Water was also removed from an aggregated 5 wt% PMMA latex prepared with 0.12 mol% C12 and 0.07 mol% VA-061. The original latex had a particle size of 124 ± 2 nm and a zeta potential of 49 ± 3 mV. The latex was aggregated with air at 80 °C for approximately 5 h resulting in a particle size of 9 μ m. Water was removed from 40 mL of aggregated latex by centrifuging for 20 min at 3500 rpm and decanting the supernatant (30 mL) to yield a wet polymer with a solids content of 18 wt%. The sample was rehydrated with fresh water (28 mL) and redispersed by the sonication method (probe) from Section 2.6.

2.6.3 Addition of extra surfactant after polymerization

Additional surfactant (0.06 mol% based on monomer) was added to a 5 wt% PMMA latex (11 mL) after the aggregation step to assist with redispersion. The original latex was prepared with 0.12 mol% C12 and 0.07 mol% VA-061 resulting in a particle size of 128 ± 1 nm and a zeta potential of 51 ± 1 mV. The latex was aggregated with air at 80 °C for approximately 5 h resulting in a particle size of 22 μ m. Then either nonswitchable CTAB or switchable C12 (charged form) were added and redispersion was accomplished with a sonicator bath for 1 min in the presence or absence of CO₂. Samples were exposed to CO₂ by bubbling with a needle 10 min prior to the sonication treatment.

2.7 Latex films

Films were cast on glass microscope slides by dropping 3-4 drops of a latex (prepared as described in Sections 2.3 and 2.3.4) with a disposable glass pipette onto a slide. The glass slides were then placed under a flow of air to allow the films to dry overnight. Films were examined by optical and scanning electron microscope.

3. Characterization Method Development

3.1 Introduction

Particle size and particle size distributions are important characteristics of latexes that affect the final product. Properties such as film formation, opacity and colloidal stability, among others, are affected by the particle size and particle size distribution.³⁴ There are different methods to measure particle size such as microscopy, separative and light scattering techniques. SEM and TEM (transmission electron microscopy) can be used, but these techniques are expensive.³⁵ Particle size was a major method of characterization in this project, so the use of microscopy techniques would not have been realistic for the number of samples that were measured. Separative techniques are two-step techniques where there is first the physical separation of different sized particles by centrifugation or some flow method, and second, the particle sizes are measured. The particle sizes are typically measured by dynamic light scattering.³⁵ Light scattering techniques can be used to measure the particles size distributions and particles sizes without any separation. This technique is fast and therefore very useful when measuring a large number of samples.

The difficulty with using light scattering techniques in this project is the range of particle sizes that were obtained. Latexes generally had particle sizes of approximately 140 nm, which were then aggregated to approximately 6 μm . After redispersion there was a possibility that there would be populations of both these sizes present. Dynamic light scattering is generally suitable for measuring smaller particle sizes (submicron), whereas static light scattering is more suitable for measuring larger particle sizes (micron). Neither

instrument used in this project was designed to measure the redispersed samples with the two very different particles sizes. This chapter discusses the challenges of using light scattering techniques during this project and the instrumental complications encountered during the project.

3.2 Light scattering

A Mastersizer 2000 (M2000) was used to measure particle size distributions using static light scattering. Particle sizes on the order of microns were obtained when aggregating latexes made with the switchable surfactant. A Zetasizer Nano ZS has a particle size measurement range of 0.6 nm to 6 μm , according to the user manual, and was therefore not suitable for measuring aggregates because they would have been at the upper limits of the instrument. However, the Zetasizer can measure the zeta potential of particles up to 30 μm .³⁶ The M2000 has a particle size range of 0.05 to 1000 μm according to the user manual.⁴⁰ Because it was possible that, after redispersion, there could be populations of both small and large particles, it was decided that the M2000 would be best suited to measure the particle sizes of redispersed samples.

Diffraction patterns are dependent on the size of the particle. When light interacts with a particle it will reflect, refract, absorb and diffract the photons all at the same time. However, there will be more than a single particle in the light path during measurements, so the following assumptions are made to extend light diffraction from one particle to multiple particles: a photon will only scatter once (no multiple scattering), there is no optical interference between scattered beams of light; and the diffraction pattern of

multiple particles is the sum of the all the individual diffraction patterns. Below are further discussions of dynamic and static light scattering.

3.2.1 Dynamic light scattering

The Zetasizer Nano ZS uses dynamic light scattering to measure particle size distributions. A detector is placed at 173° from the light beam to collect backscattering, reducing the effects of multiple scattering.³⁶ Smaller particles will move more due to Brownian motion than large particles, and so it is not valid to average the diffraction patterns (as in static light scattering) because they will become too different, even over a short time. The velocity at which the particles move can be related to their size by the diffusion constant, D . The diffusion constant can be related to the particle size by the Stokes-Einstein equation:

$$D = \frac{kT}{3\pi\eta d} \quad (3.1)$$

where k is Boltzmann constant, T is temperature, η is the viscosity of the dispersant phase and d is the diameter of the particle.²² The correlation between successive diffraction patterns is calculated in the software. The correlation over time of larger particles would decay slower than that of small particles, because they will move slower and therefore it will take longer for the diffraction patterns to differ.^{22,36} Algorithms in the software calculate a particle size from the correlation function. The radius that is measured is the hydrodynamic radius, which is the radius of a hypothetical sphere that has the same diffusion constant. This radius will depend on the thickness of the solvated layer around the particle and the speed at which it moves through solution. This radius is the most

accurately measured by dynamic light scattering. Typically, diameters are reported as the particle size. The diameter that refers to the measured radius in dynamic light scattering is the z-average diameter (d_z) that is calculated from an intensity distribution.

Zeta potential is also measured on the Zetasizer Nano ZS, by a phenomenon called electrophoresis. As mentioned previously in Section 1.7, zeta potential is the electrical potential at the slipping plane and is a means of measuring the amount of surface charge on a particle. When an external electric field is applied, colloidal particles that have surface charge will move toward the oppositely charged plate. The velocity with which they move per unit of applied electric field gives the electrophoretic mobility. The electrophoretic mobility (U_E) can then be related to the zeta potential (ζ) by using the Henry equation and the Smoluchowski approximation.

$$U_E = \frac{2\varepsilon\zeta f(\kappa a)}{3\eta} \quad (3.2)$$

Where ε is the dielectric constant of the medium, η is the viscosity of the medium and $f(\kappa a)$ is the Henry's function which is approximated to be 1.5 by the Smoluchowski approximation. When the particles are moving in the electric field the light will undergo Doppler shifting which can allow for the measurement of the particle velocity. By measuring the velocity, the electrophoretic mobility can be calculated which can then be used to calculate the zeta potential.²²

3.2.2 Static light scattering

The M2000 measures particle size by static light scattering. Static light scattering measures the radius of gyration but a diameter based on the volume distribution is generally reported (d_v). Mie theory³⁷ is the analytical solution of Maxwell's equations for light diffraction and takes into account all the different types of light interaction. The difficulty with Mie theory is the need for optical constants such as refractive index and absorption. Because it takes into account the different types of light interaction it is necessary to know the refractive index and absorption constants for the material in question and dispersant phase, however sometimes these properties are not known. Mie theory also assumes spherical particles, which can lead to inaccurate measurements if the particles are not spherical. Mie theory should be used when the particle size is on the order of the wavelength of light, but when the particles become much larger it is possible to obtain an approximation of the particle size using the Fraunhofer model. The Fraunhofer model assumes opaque particles and so does not require any optical constants.³⁸ It also assumes disk-shaped 2D particles and that there will only be diffraction from the contours of the disks. The M2000 uses a He-Ne laser that has a wavelength of 633 nm.⁴⁰ This is on the order of the particle sizes being measured, and so Mie theory is applied.

There are 52 detectors placed at different angles in the M2000 to measure scattering in all directions. Detectors at higher angles will measure light scattered from smaller particles. Particles in the path of light create diffraction patterns and several of these patterns are collected and averaged to one diffraction pattern. Each diffraction pattern is called a snap, and there will be over 2000 snaps collected in one millisecond.

Larger particles take much longer to move due to Brownian motion, so the diffraction patterns will not change significantly over a short period of time and it is valid to average the diffraction patterns (unlike in dynamic light scattering). The software then calculates particle size distributions based on these averaged diffraction patterns.²² Mie theory assumes perfect spheres and uses the method of equivalent spheres to determine a diameter, so the M2000 will give one number as the particle size result. There are different methods of equivalent spheres, one example is equivalent surface area. The surface area of a particle is measured and the diameter of a spherical particle that would have the same surface area is calculated. This is very accurate if the particles are spherical and non-porous. It is also possible to measure the maximum or minimum length of irregular particles to determine diameter, but this would result in an overestimation or underestimation, respectively. The M2000 determines the particle size by equivalent volumes.⁴⁰ The volume of the particle is measured and the diameter is that of a sphere with the same volume. SEM images shown later (in Section 4.2.2) will prove that the particles prepared during this project were spherical, so the use of Mie theory and, thus, the M2000 is valid.

3.3 Comparison of dynamic and static light scattering

It is generally poor practice to change the method of characterization within a single experiment. The latexes in this project were measured with dynamic light scattering using a Zetasizer Nano ZS. Dynamic light scattering measures the hydrodynamic radius. The apparent size of the particle will depend on the solvation of the particle surface and its diffusion through the medium.³⁹ The radius of gyration, which is measured in static light scattering, is smaller than the hydrodynamic radius. Aggregated

and redispersed samples were measured with static light scattering on a M2000. The need to use the different techniques and compare the results is forced upon us by the limitations of each instrument. The particles made were initially of one size and then aggregate to a size that was no longer in the range of measureable particles in the Zetasizer. After redispersion it was most likely that a population of these two particle sizes existed, and neither machine is particularly adequate at measuring both. It will be discussed which instrument was used for each condition and why.

Schneider and McKenna³⁵ compared the particle sizes and particle size distributions of different methods of particle characterization, including static and dynamic light scattering. They found that the particle sizes of monomodal latexes measured by dynamic light scattering were larger than the true values, most likely because of the hydrodynamic radius. In a bimodal latex they report that dynamic light scattering (with a single angle detector) greatly overestimated the volume % of larger particles (20-40 %) whereas static light scattering only overestimated 5-10 %. They conclude that static light scattering in some cases did not accurately measure the particle size of one of the populations present in a bimodal latex, based on the true value measured by SEM. However, the two particle sizes of their bimodal latex were in the measurable range of the dynamic light scattering machine, whereas this is not the case in this project. Also, although the M2000 may not have provided an accurate measure of the particle size, it did provide a more accurate measure of the *amount* of small or large particles present, in terms of volume ratio. In this project the measurement of the volume of small particles after redispersion is the approach taken to compare different redispersion methods.

The particle sizes of a series of latexes (polystyrene and PMMA latexes) were measured on both the M2000 and the Zetasizer Nano ZS. The results are shown in Figure 3.1, where the line represents the ideal relationship when the particle sizes measured on the two instruments are the same. The z-average, or cumulants average, from the Zetasizer is always reported in this project and is based on the intensity distribution. The Zetasizer user manual claims that this is the most stable value of particle size from dynamic light scattering.³⁶ The mass median diameter, $d(0.5)$, from the volume distribution is always reported in this project (M2000). This diameter is always very similar to the volume mean diameter, $D[4,3]$, for monomodal distributions, only in bimodal distributions do these two values differ significantly. The deviation between d_z (particle size based on an intensity distribution) and d_v (particle size based on a volume distribution) from the Zetasizer is very small at smaller particle sizes and only increases at larger particle sizes (3 % difference at ~165 nm versus 11 % difference at ~250 nm). In almost all cases, the particle size measured by the Zetasizer was larger than the particle size measured by the M2000. This is expected because the Zetasizer measures the hydrodynamic radius. It was found that the two instruments agreed most at lower particle sizes. Once the particles reached approximately 200 nm (measured by the Zetasizer) the M2000 measured a particle size 75 nm less. However, the latexes measured in this project were generally 120-150 nm, and in this range the two instruments agreed with an average difference of 14 % (4.5-22.6 % range), compared to an average difference of 41 % (37-45 % range) at higher particle sizes. The polymer composition did not seem to have an effect on the differences between the instruments. The particle size distribution from the M2000 is also broader than that from the Zetasizer, as shown in Figure 3.2 (both are

volume distributions). This is likely due to the fact that the small particles measured are well within the valid range for the Zetasizer but M2000 distribution is approaching the limit of the instrument.

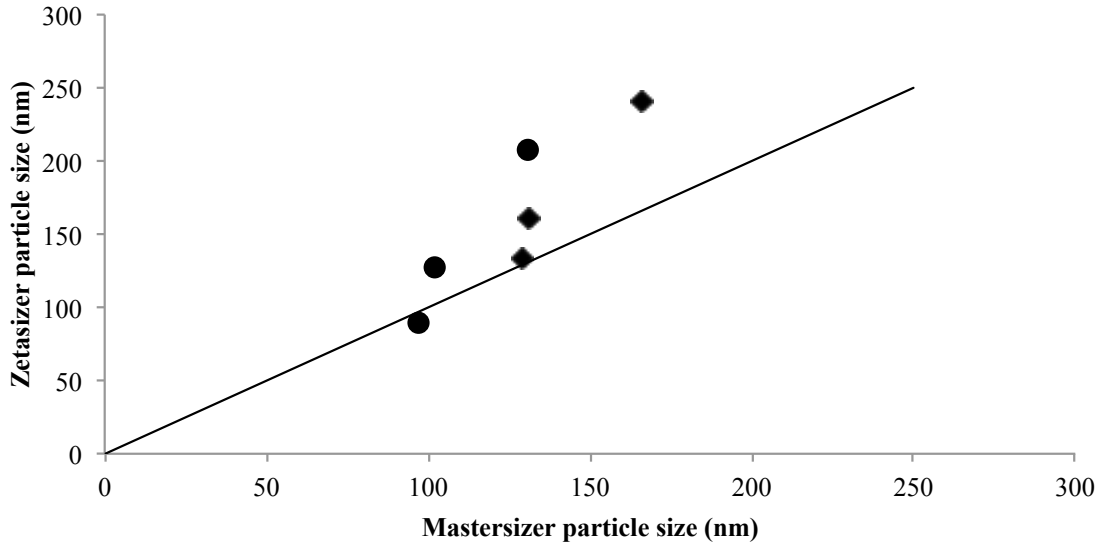


Figure 3.1. Particle sizes of different latexes (polystyrene (•) and PMMA(◆)) measured on the Mastersizer 2000 (d_v) and the Zetasizer Nano ZS (d_z). The line represents the ideal relationship when the particle sizes measured are the same from both instruments.

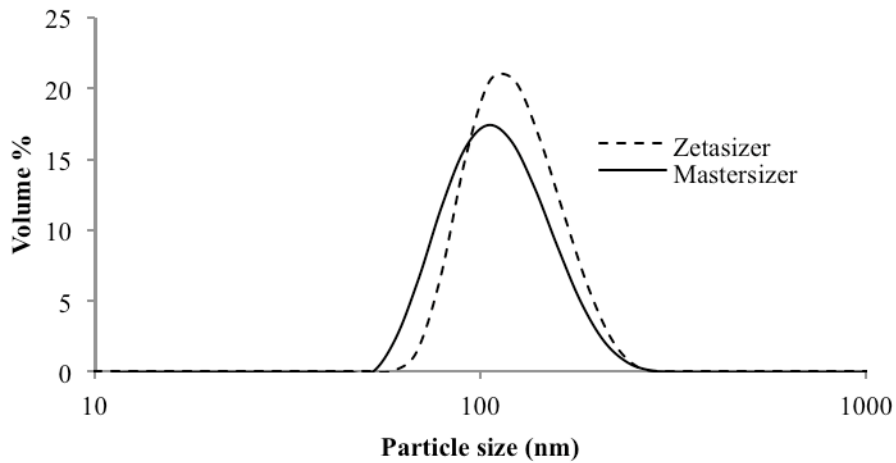


Figure 3.2. Particle size distributions (volume distributions) of a 5 wt% polystyrene latex measured on both the Zetasizer Nano ZS and Mastersizer 2000.

The M2000 was not used for all three stages (latex, aggregation and redispersion) because the Zetasizer has a better measurable range for latex particle sizes. Even though the M2000 can theoretically measure the latex particle sizes (~140 nm), this size is approaching the limit of the instrument when you consider the scale of particle sizes it measures. However, it was necessary to measure the redispersed samples with the M2000 so that any large particles present could be measured as well. The M2000 coped better at measuring particles at its lower measurement limit, than the Zetasizer did at its higher measurement limit. However, as shown above, the particle sizes measured from the instruments are not so different that they cannot be compared.

3.4 Sample stability during measurements

Before turning off the M2000, Cole-Parmer[®] Micro-90[®] cleaning solution is added to the reservoir to keep bacteria from growing in the machine or tubing. It is necessary to clean this surfactant mixture out of the instrument before use. When the M2000 is turned on for the first time on any given day, it is necessary to perform cleaning cycles before using the instrument. At least three wash cycles were found to be required to ensure all of the surfactant solution was flushed out. If not enough cleaning cycles were done, the first three measurements of the day would be stable, but a sample measured a second time after these three measurements would be unstable. A stable sample maintains the same particle size during the course of the measurement, whereas an unstable sample aggregates within the instrument during a measurement. It is believed that cleaning solution helped stabilize samples in the instrument. This was the desired

effect, but as it was not a controlled amount of surfactant added for every measurement it was best to make sure Micro90[®] is not present in the system.

Samples are diluted >1000x during the measurement procedure which can cause colloidal stability problems. Ensuring stability is critical during measurements and the use of additional surfactants or stabilizers is suggested.⁴⁰ After discovering the effect the Micro90[®] had on measurements, a nonionic surfactant, Disponil A 3065[®], was added to samples immediately before a measurement to help with stabilization in the instrument.

Figure 3.3 shows examples of (a) good and (b) bad trend graphs that were acquired during the project. A trend graph is simply the particle size over the course of a single measurement. A single measurement of a sample actually consists of several individual measurements that are averaged to give a final result. A sample must be adequately dispersed to ensure good measurements. Figure 3.3a shows that over the five measurements of the sample the particle size remained constant, while Figure 3.3b shows an increase in particle size. The increase in particle size during the experiment means that the particles aggregated in the instrument and results were meaningless.⁴¹ If aggregation occurs during a measurement, the addition of nonionic surfactant to help stabilize particles may alleviate the problem.

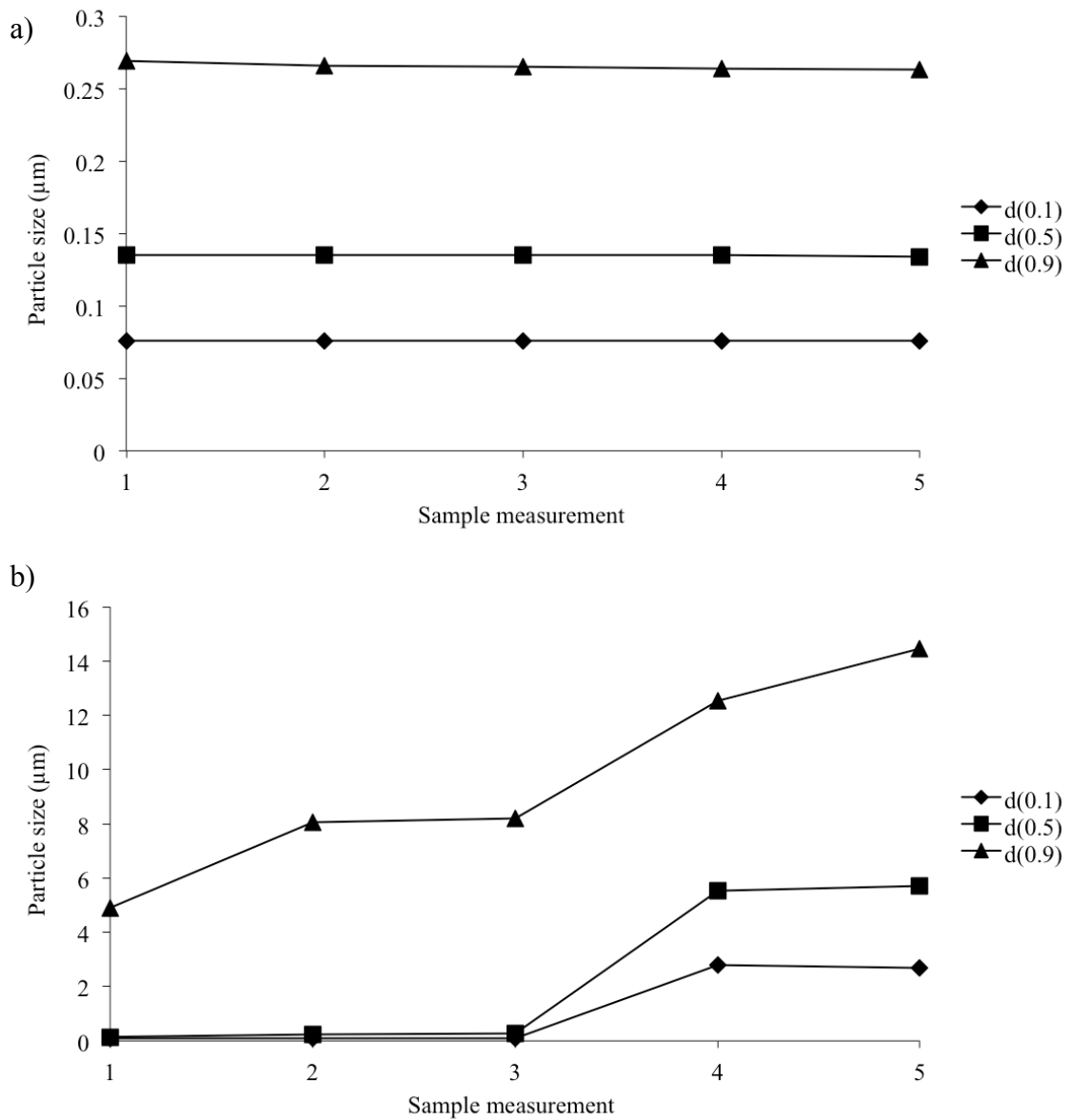


Figure 3.3. Trend graphs of a) a stable sample and b) unstable sample in the Mastersizer 2000.

After adding sample to the M2000 reservoir, it was important to allow the dispersion time to stabilize. It was found that if the measurement was started immediately after sample addition, the initial particle size measured was large, but it subsequently decreased during the measurement. The stirrer in the reservoir does not provide enough

energy to cause redispersion of the particles if they are aggregated. So because the particles at the end of the measurement were small, this was their correct size and we believe they were not properly dispersed at the beginning of the measurement.

3.5 Light scattering background

Obtaining a good light scattering background is crucial to obtaining good particle size measurements. The M2000 measures the background before every measurement, and the background can be viewed with the M2000 software. There are a couple of general rules for a good background: 1) the background should look like a decreasing exponential curve; and 2) the light energy should be less than 20 units at detector number 20 (light intensity decreases as the detector number increases). If these criteria were met, then a good background was obtained. Figure 3.4 shows examples of different backgrounds that were encountered during the project. Figure 3.4a is an example of a good background that met both criteria. Figure 3.4b is an example of a background where the dispersant was contaminated or contained bubbles, and Figure 3.4c is the resulting background when there were bubbles stuck on the cell window. If the dispersant phase was contaminated, the M2000 reservoir needed to be manually cleaned with a scrub brush, followed by a cleaning cycle using the software. When bubbles caused an issue, it was sometimes from bubbles in the water line in the building. Generally, running the water 30 min prior to measurements helped to eliminate this problem. Bubbles were more likely to occur on days after maintenance on the water line. If a peak appears in the background at approximately detector number 35 this is an indication that there is material stuck to the

cell window. Although this was not encountered during the project, one would simply need to dismantle the cell to physically clean the glass with lens wipes.⁴²

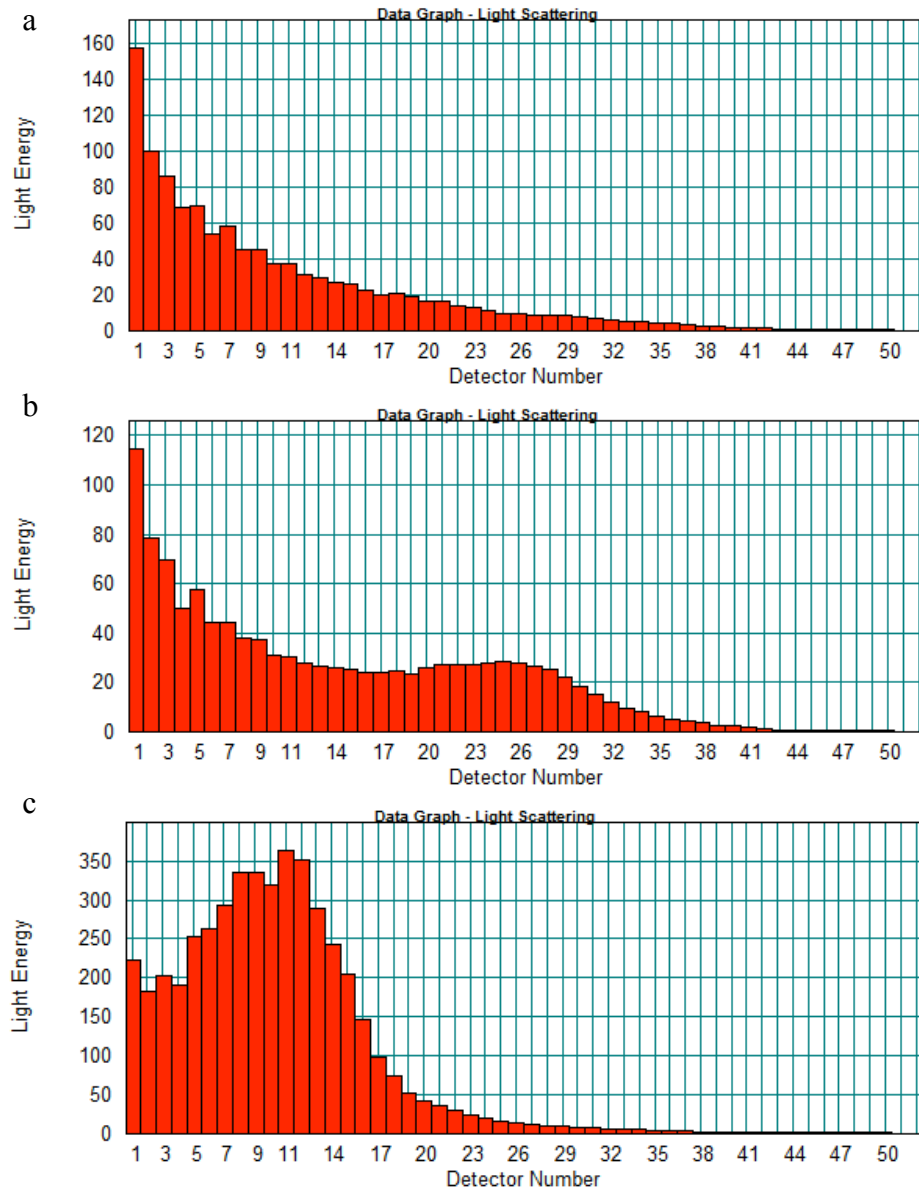


Figure 3.4. Different Mastersizer 2000 backgrounds: a) good; b) contaminated dispersant or containing bubbles; c) bubbles stuck on the cell window.

It is important to first have a good background before starting measurements. A poor background may lead to negative data. The difference is taken between the

background and measurement intensity and if the background is higher in intensity, then negative data will be obtained. The signal-to-noise ratio will be very small and results may not be reliable. To avoid this problem, the signal-to-noise ratio was increased by adding more sample to increase the amount of scattering (i.e. increase obscuration). Obscuration is a measure of light intensity loss due to sample in the light path. It allows the user to set an appropriate concentration of sample for a measurement. If too much sample is added the obscuration will be too high, and this can lead to multiple scattering.³⁸ Multiple scattering occurs when one photon scatters off multiple particles, leading to scattering at higher angles. Detectors at higher angles are intended to detect light scattering from smaller particles, so if multiple scattering occurs the instrument will incorrectly report the presence of smaller particles.

3.6 Non-spherical particles

Mie theory assumes perfect spheres when calculating particle diameter. So, if a sphere is not representative of the particle being measured, this could create a problem. If a rod-shaped particle is in the path of light, its orientation could be end-on, side-on or any other angle. During a measurement it is likely that all of these orientations will be present and therefore the M2000 will calculate a multimodal distribution.⁴³ To distinguish whether the distribution is actually multimodal or if it is the particle shape that is causing the appearance of multiple modes, it is good practice to do a visual observation under a light microscope before measuring with light diffraction.⁴⁴ Generally, this practice can only be done on particles of at least 300 nm in diameter, but it will depend on the magnification power of the light microscope.³⁸ This was not done in this project

because the redispersed particles were below the limit of an optical microscope. However, the particles will be shown to be spherical in a later section (Section 4.2.2).

3.7 Conclusions

The M2000 is an instrument that can provide reliable data about particle size and particle size distribution. Although the instrument, at first sight, is very simple to use, a sound understanding of how to use the instrument is necessary. There are many factors that can lead to poor particle size measurements and they need to be recognized by the operator. It was also determined that measurements from the Zetasizer and M2000 can be reliably compared to each other because the difference in particle size is so great between primary particles and aggregates that there would need to be a significant amount of error to not be able to distinguish between the two sizes.

4. Results and Discussion: Redispersion

Poly(methyl methacrylate), PMMA, latex samples were prepared by emulsion polymerization using the switchable surfactant, C12, and the switchable initiator, VA-061. Polystyrene and PMMA are glassy polymers with T_g 's of 100 °C and 105 °C, respectively. These latexes were then aggregated with air and heat (65-80 °C). Introducing CO₂ to switch the surfactant back to its active form was not sufficient to redisperse the aggregated latexes, a form of energy was needed to induce redispersion. Sonication was initially used, but as it is not viable on an industrial scale, other methods were explored for low-energy redispersion. Rotor-stators, an immersion blender and an overhead stirrer were also tested for redispersion.

4.1 Redispersion of a latex containing no switchable groups

A control sample of 5 wt% PMMA, prepared by emulsion polymerization with a non-switchable surfactant (0.12 mol% CTAB) and a non-switchable initiator (0.07 mol% VA-044), had a particle size of 80 nm and a zeta potential of 45 mV. The latex (6 g) was aggregated by addition of salt (0.1 g aluminum sulfate), producing a particle size of 7 µm. The redispersion of this aggregated latex was then attempted using a sonicator probe with and without prior washing of the sample. In the washing procedure, the sample was centrifuged at 3500 rpm for 10 min, the aqueous layer was poured off, and fresh water was added. Table 4.1 shows the results of the redispersion attempts, including the volume % below 1 µm and the zeta potential of the redispersed control samples immediately after redispersion and 7 days later. The unwashed aggregated control sample was redispersed after 1 min of sonication, resulting in 133 nm particles. After 7 days

these particles reaggregated. This was likely due to the presence of the salt, which was still depressing the electrical double layer. The washed control sample showed complete redispersion immediately after sonication and had a slightly higher zeta potential. Some surfactant was probably lost during the washing treatment, which is why the original zeta potential of the latex, 45 mV, was not recovered. After 7 days the washed control sample showed only slightly degraded colloidal stability. From these results, it seems that while redispersion of a sample aggregated with salt is possible, it does not have long-term colloidal stability unless the aggregated sample is washed sufficiently to remove the salt.

Table 4.1. Redispersion by sonication^a of a PMMA latex that was aggregated by the addition of aluminum sulfate.^b

| | No washing | | Washed | |
|--------------------------------|-----------------------|-----------------------------|-----------------------|-----------------------------|
| | Vol.%<1 μm | Zeta pot. (mV) ^c | Vol.%<1 μm | Zeta pot. (mV) ^c |
| Immediately after redispersion | 92.1 | 26 \pm 1 | 100 | 30 \pm 1 |
| 7 days later | 0 | 25 \pm 3 | 97.9 | 28 \pm 1 |

^aRedispersion by sonicator probe for 1 min at a setting of 10 %.

^bOriginal sample was a 5 wt% latex prepared with 0.12 mol% CTAB and 0.07 mol% VA-044 with an initial particle size of 80.2 \pm 0.6 nm and zeta potential of 45 \pm 1 mV which was aggregated, by addition of aluminum sulfate, to 10.5 μm and 7.2 μm .

^cThe error in zeta potential is the standard deviation from the five measurements that are taken for one sample.

4.2 Destabilization

4.2.1 Factors affecting destabilization

The destabilization of a PMMA latex prepared with switchable surfactant, C12, and initiator, VA-061, by emulsion polymerization was accomplished by bubbling air through the latex while heating. This resulted in a clear water layer and polymer particles

if given enough time to settle. Different factors were found to affect the destabilization time. Air was bubbled through a 5 wt% latex with 0.12 mol% and 0.07 mol% switchable surfactant, C12, and initiator, VA-061, respectively, and heated to various temperatures while monitoring the volume % below 1 μm over time. With increasing temperature, destabilization time was reduced (Figure 4.1).⁴⁶ The zeta potential of the sample heated at 80 °C is also shown as a function of time. The zeta potential first decreased to approximately 20 mV before aggregation began to occur and then remained constant. This surface charge seems to be a threshold for all PMMA samples. A surface charge threshold for aggregation is a common occurrence when using electrolytes to cause destabilization. Everette reported a critical value of approximately 30 mV.⁴⁵

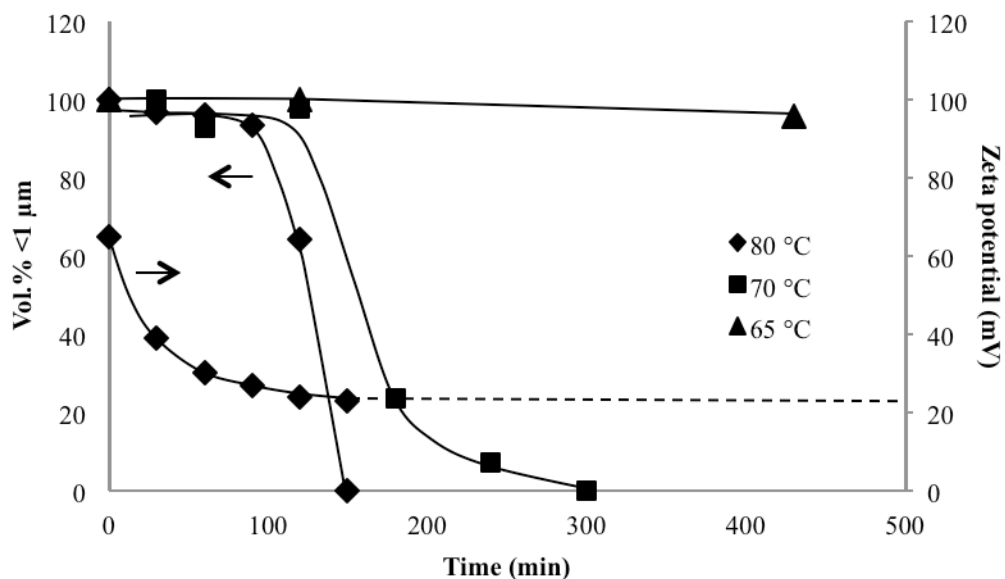


Figure 4.1. Destabilization over time at different temperatures of a 5 wt% latex with 0.12 mol% and 0.07 mol% switchable surfactant, C12, and initiator, VA-061, respectively. The arrows indicate the appropriate axes for the curves. Reprinted with permission from Fowler, C. I.; Muchemu, C. M.; Miller, R. E.; Phan, L.; O'Neill, C.; Jessop, P. G.; Cunningham, M. F. *Macromolecules*, **2011**, *44*, 2501-2509. Copyright 2011 American Chemical Society.⁴⁶

The effects of polymer and switchable group concentrations were examined by another member of the Jessop group.⁴⁶ It was found that with increasing amounts of switchable groups (from both the surfactant and initiator) the destabilization time was decreased, and when increasing the solids content the destabilization time was again decreased.

In this project it was found that at higher solids content, ~15 wt%, viscosity increased drastically if the latexes were destabilized for too long a time. If destabilization was continued for longer than an optimal time, then the aggregated latex became very viscous, as if the particles were self-associating and forming a structured network similar to a gel. The optimal destabilization time depends on the amount of latex being aggregated, the solids content of the latex and the temperature at which it is being destabilized. Although 85 % of the sample was water, to the eye there appeared to be very little dispersant phase. Redispersion of such samples was very difficult. The particle size must be monitored, visually, while destabilizing a high solids content latex to ensure optimal destabilization time and avoid increasing the viscosity.

4.2.2 Scanning electron microscope images

In order to determine whether the latex particles were coming together and fusing into a large coagulated particle, or whether the small particles were merely flocculating and clumping together, scanning electron microscopy images were taken of a latex and a destabilized latex after bubbling with air and heating (Figure 4.2).⁴⁶ Figure 4.2a shows the solitary particles of the latex, although there are some aggregates in the image probably due to the sample preparation prior to imaging. Figure 4.2b confirms that

primary particle sizes are retained after aggregation and that the large aggregated particles measured are clumps of these primary particles. If the particles had fused together this would have been problematic for redispersion because sonication would probably not have been strong enough to break the particles apart.

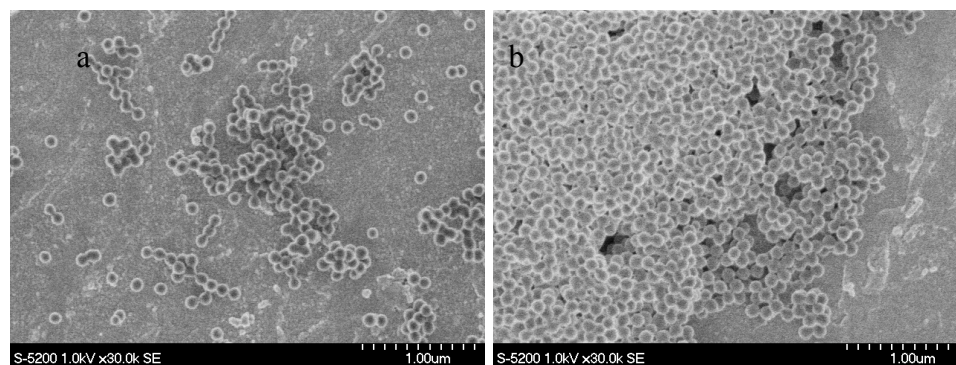


Figure 4.2. SEM images of a PMMA latex made with 0.12 mol% C12 and 0.07 mol% VA-061 before and after destabilization by heating the 5 wt% latex at 65 °C and sparging with air. Reprinted with permission from Fowler, C. I.; Muchemu, C. M.; Miller, R. E.; Phan, L.; O'Neill, C.; Jessop, P. G.; Cunningham, M. F. *Macromolecules*, **2011**, *44*, 2501-2509. Copyright 2011 American Chemical Society.⁴⁶

4.3 Particle size distributions

Typical particle size distributions from the Mastersizer 2000 are shown in Figure 4.3. The plot is based on volume distribution, which means that the large particles will be emphasized in plots of samples containing both large and small particles. Latex samples show a monomodal distribution and after heating and bubbling with air, aggregates also show a monomodal distribution. The peak at approximately 110 μm in the aggregated latex distribution is not due to particles, but is due to bubbles in the instrument. Disponil A 3065® was added to an aggregated sample to ensure that it did not help with redispersion. The aggregated sample still consisted of large particles even with the

nonionic surfactant present, demonstrating that the extra surfactant only helped with maintaining stability during measurements and did not trigger redispersion. The extra surfactant sometimes caused bubbles during measurements, which appeared as peaks at higher particle sizes ($\sim 100 \mu\text{m}$). To examine the effectiveness of different redispersion methods the volume percent below $1 \mu\text{m}$ is reported in the sections below. In all cases, redispersion regenerated the primary particle size suggesting that the large aggregates are clumps of primary particles. This was shown to be true from the SEM images in Figure 4.2. It has also been shown that during aggregation the particle size distribution peak did not shift to higher particle sizes; rather, a new peak emerges at higher particle sizes while the original peak decreases.⁴⁶ It is likely that this will also be the case in the reverse direction for redispersion. However, because redispersion happens on such a fast time scale (1 min), the trend of the peaks increasing and decreasing over time was not observed.

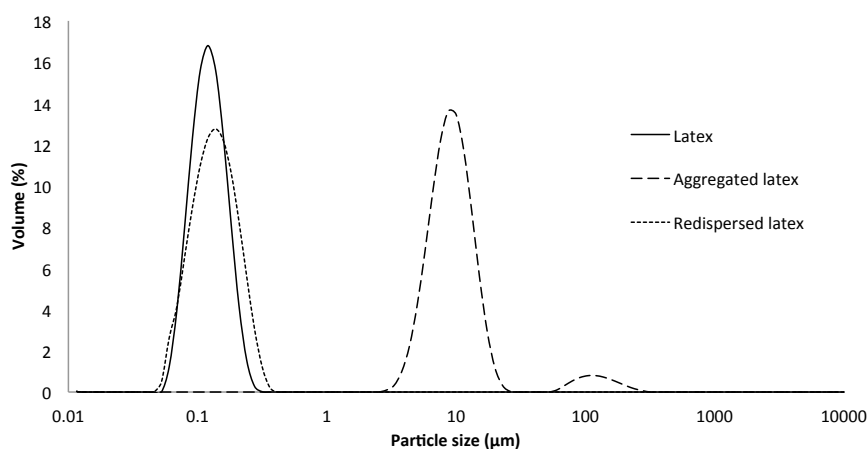


Figure 4.3. Particle size distributions of a latex after preparation, after aggregation (with air at $80 \text{ }^\circ\text{C}$) and after redispersion (10 % sonication with a probe sonicator for 1 min). The 5 wt% original latex contained 0.12 mol% C12 surfactant and 0.07 mol% VA-061. Distributions were measured using static light scattering. The peak at $110 \mu\text{m}$ is due to bubbles.

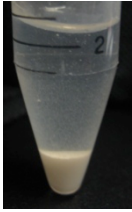
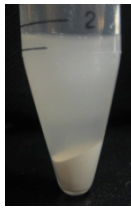
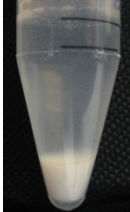
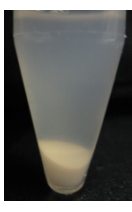
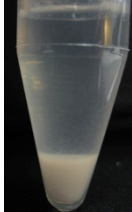
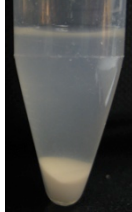

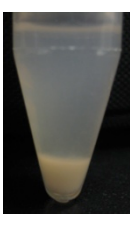



4.4 Redispersion

4.4.1 Varying amount of “dryness”

Polystyrene samples were prepared by emulsion polymerization with the switchable surfactant C16 and switchable initiator VA-061. A 5 wt% 80 nm latex made with 0.12 mol% C12 and 0.07 mol% VA-061 was aggregated with air and heat (65 °C) to give 40 μm particles. The particles settled and left a clear water layer. The aggregated latex was then split into three portions, which were subjected to three different methods of removing water before redispersion. One portion was filtered, washed and dried before redispersion, another was only filtered and the last was decanted. The filtered and decanted samples had solid contents of 14 and 13 wt%, respectively. 5 mL of fresh deionized water was added and redispersion was attempted by bubbling CO₂ for 30 min on all three samples with and without extra C16 (in its charged form), and with and without sonication. Sonication was provided by a sonicator bath. Samples were centrifuged for 10 min at 3500 rpm and the clarity of the supernatant layer was assessed as a qualitative method of determining the effectiveness of redispersion. Table 4.2 contains photos of the samples after centrifugation. The most clear supernatant layers were those that had no extra surfactant and were not sonicated, indicating that redispersion was not successful. After the addition of extra surfactant the supernatant became cloudy, even without sonication, which suggests that there was redispersion of some particles. Sonication appeared to help with redispersion in most of the cases (although the filtered sample with no extra surfactant still had a clear supernatant layer)

and samples with both sonication and extra surfactant had the most opaque supernatant layers indicating the most successful redispersion.

Table 4.2. Redispersion of rehydrated aggregated latexes in the presence of CO₂. Redispersion was carried out in the presence and absence of additional surfactant and with and without sonication.

| | Filtered, washed and dried | | Filtered | | Decanted | |
|---------------|---|--|--|---|--|--|
| | No extra surfactant | Extra surfactant | No extra surfactant | Extra surfactant | No extra surfactant | Extra surfactant |
| No Sonication |  |  |  |  |  |  |
| Sonication | n/a |  |  |  |  |  |

4.4.2 Different methods of redispersion

Earlier in this project, a sonicator bath was used for redispersions, which was extremely unreliable. This was due to inconsistent sonication power delivered from the sonicator because of the standing wave patterns in the bath.⁴⁷ The results from this bath were very irreproducible, where sometimes the percentage of particles below 1 μm after sonication ranged from 60 % to 94 % for the same sample. A sonicator probe was obtained to provide consistent energy during redispersion. Table 4.3 and 4.4 compare the effectiveness of different redispersion methods with and without the presence of CO₂ at different solid contents. Table 4.3 shows the results of the redispersion of 5 wt% latexes

that were aggregated with air at 80 °C. During redispersion attempts in the absence of CO₂, the switchable surfactant should still be in its neutral (“off”) form, which means that there should be no active surfactant in the system. However, the non-zero zeta potential shows that there was still some surface charge, suggesting that there were still some surfactant or initiator end groups in their “on” form. The sonicator (probe), 5.5 cm rotor-stator and blender were all immediately successful in redispersing the 5 wt% aggregated latex. Redispersion was complete after 1 min so no shifting of the peak in the particle size distribution was observed. The stirrer, however, did not provide enough shear to induce redispersion. Even after 7 days, the sonicator- and blender-redispersed samples were still stable. The failure of the rotor-stator sample was probably due to the low zeta potential and the incomplete redispersion. The remaining population of larger particles would have promoted aggregation of the smaller particles because the total interaction energy between a small and big particle is larger than that between two small particles. The stability of the sonicator and blender samples was unexpected because of the absence of active surfactant (the zeta potential was still low after 7 days), but can be explained by Brownian motion. The low solids content meant that particle collisions were very infrequent, and if there were no collisions then aggregation would not occur. The following equation shows the relationship between aggregation half-life, $t_{1/2}$, and solids content, ϕ :

$$t_{1/2} = \frac{\pi\eta d^3}{8kT\phi} \quad (4.1)$$

where η is the viscosity of the medium, d is the particle diameter, k is Boltzmann’s constant and T is the temperature.⁴⁸ This inverse relationship shows that with lower solids

content the time for half of the particles to aggregate will increase. Samples that were exposed to CO₂ also resulted in successful redispersion, although the stirrer was still not able to redisperse the sample. Upon exposure to CO₂, the surfactant should switch back to its charged form and correspondingly the surface charge should increase resulting in a high zeta potential. However, the zeta potentials of the CO₂ exposed samples immediately after redispersion were still low, implying that the surfactant did not immediately switch back on. After 7 days the zeta potentials did increase and the samples still showed colloidal stability. The fact that the rise in zeta potential is slow suggests that the reaction with CO₂ is slow, even though it is known from past experience that the reaction of acetamidines with CO₂ in water normally takes only minutes. It is possible that the slow step is not the reaction in water but rather the dissociation of the amidine head group from the surface. If the amidine head group of the “off” surfactant lies flush with the surface of the particle, then the local environment around that headgroup should be fairly low in polarity; not a situation that favours the conversion of the amidine to the bicarbonate salt. If however, the amidine head-group were to pull away from the surface, then the salt formation could take place readily. The movement of the amidine group from the surface may be the slow step. It is also possible that absorption of neutral amidine into the PMMA particle is affecting the rate at which the zeta potential can increase. Tributylamine has a solubility parameter of 15.8 MPa^{1/2} and dodecane has a solubility parameter of 16.2 MPa^{1/2}, which should place the solubility parameter of the surfactant within this range.⁴⁹ This places the surfactant between ether and THF on a solubility scale. PMMA is soluble in THF but not in ether, so it is probable that the

surfactant is soluble in PMMA, but its solubility is limited. After being absorbed, there would be less surfactant in contact with the water phase to be protonated by CO₂ resulting in less surface charge (lower zeta potential). However, more surfactant could gradually be protonated (resulting in the slow increase in zeta potential) because some of the absorbed surfactant would come back to the surface over time. So, absorption and adsorption of the surfactant could both be contributors to the slow increase in zeta potential.

Table 4.3. The redispersion of a 5 wt% aggregated PMMA latex with different methods of agitation in the presence and absence of CO₂.^a

| | | | Method | | | |
|-----------------------------|--------------------------------|---------------------|-------------------------|---------------------------|----------------------|----------------------|
| | | | Sonication ^b | Rotor-stator ^c | Blender ^d | Stirrer ^d |
| No CO ₂ exposure | Immediately after redispersion | Vol.%<1μm | 99.7 | 60.4 | 98.6 | 0 |
| | | Zeta potential (mV) | 19±1 | 13±6 | 19±2 | 21±2 |
| | 7 days after redispersion | Vol.%<1μm | 98.8 | 0 | 99.7 | 0 |
| | | Zeta potential (mV) | 20±1 | 5±1 ^e | 19±1 | 19±2 |
| CO ₂ exposure | Immediately after redispersion | Vol.%<1μm | 99.8 | 64.9 | 98.4 | 0 |
| | | Zeta potential (mV) | 22±1 | 14±1 | 23±2 | 23±1 |
| | 7 days after redispersion | Vol.%<1μm | 99.8 | 65.8 | 98.2 | 0 |
| | | Zeta potential (mV) | 27±2 | 22±2 | 29±2 | 27±1 |

^aAll latexes were made with 0.12 mol% C12 and 0.07 mol% VA-061 and destabilized with air at 80 °C.

^bOriginal latex with primary particle size of 132±1 nm and zeta potential of 43±1 mV was aggregated to 8.0 μm with a zeta potential of 20±1 mV.

^cOriginal latex with primary particle size of 128±1 nm and zeta potential of 38±1 mV was aggregated to 7.2 μm with a zeta potential of 18±2 mV.

^dOriginal latex with primary particle size of 124±2 nm and zeta potential of 46±3 mV was aggregated to 8.9 μm with a zeta potential of 20±1 mV.

^eSample separation in the capillary cuvette during measurement.

Sonicated samples with and without CO₂ exposure were found to be stable even after 28 days, suggesting that CO₂ exposure is unnecessary. However, these samples only contained 5 % solids, which means, as mentioned above, that the frequency of particle collisions must be very low. The samples not exposed to CO₂ would likely reaggregate, but only after a very long time. Low solids content latexes can undergo initial aggregation because the stirring and air bubbles cause agitation, which increases the number of particle collisions.

Redispersion of latexes having a greater solids content was a more challenging task. With a higher concentration of particles, aggregation due to Brownian motion should happen much faster. When redispersion was attempted with latexes having 15 wt% solids content, redispersion was not possible in the absence of CO₂ (Table 4.4). With all four methods, primary particle sizes were not obtained even immediately after the redispersion method. Even in the presence of CO₂, redispersion was unsuccessful with the rotor-stator, blender, and stirrer although the zeta potential of the sample treated with the blender did increase. Particle sizes of the sample treated with the rotor-stator could not be measured because the sample was turned into a foam by the high shear. Redispersion was found to be successful only with sonication (probe) in combination with CO₂. The order of the redispersion method was important. If CO₂ exposure was performed after sonication, the sample was still very frothy and foamy which indicated that the particle size was still large. However, if the sample was exposed to CO₂ for 5 min and then sonicated for 1 min, followed by CO₂ bubbling for another 10 min, then the zeta potential immediately after the treatment increased from 24 mV to 31 mV. With the surfactant in its active form, it stabilized the newly redispersed particles, whereas with no

CO₂ the particles simply reaggregated. This sample was monitored over 3 weeks and it maintained its stability and high zeta potential (Table 4.5).

Table 4.4. The redispersion of a 15 wt% aggregated PMMA latex with different methods of agitation in the presence and absence of CO₂.^a

| | | | Method | | | |
|-----------------------------|--------------------------------|---------------------|-------------------------|---------------------------|----------------------|----------------------|
| | | | Sonication ^b | Rotor-stator ^c | Blender ^b | Stirrer ^c |
| No CO ₂ exposure | Immediately after redispersion | Vol.%<1μm | 0 | 0 | 0 | 0 |
| | | Zeta potential (mV) | 18±1 | 16±1 | 21±1 | 19±2 |
| | 7 days after redispersion | Vol.%<1μm | 0 | 0 | 0 | 0 |
| | | Zeta potential (mV) | 20±1 | - | 19±1 | 16±1 |
| CO ₂ exposure | Immediately after redispersion | Vol.%<1μm | 98.2 | - | 0 | 0 |
| | | Zeta potential (mV) | 31±2 | - | 24±2 | 18±1 |
| | 7 days after redispersion | Vol.%<1μm | 98.0 | - | 0 | 0 |
| | | Zeta potential (mV) | 29±1 | - | 29±1 | 20±1 |

^aAll latexes were made with 0.12 mol% C12 and 0.07 mol% VA-061 and destabilized with air at 80 °C.

^bOriginal latex with primary particle size of 107±2 nm and zeta potential of 46±2 mV was aggregated to 8.4 μm with a zeta potential of 24±1 mV.

^cOriginal latex with primary particle size of 139±2 nm and zeta potential of 40±3 mV was aggregated to 8.1 μm with a zeta potential of 17±1 mV.

Table 4.5. Long-term colloidal stability of a 15 wt% aggregated PMMA latex after redispersion with 10 % sonication (probe) and CO₂.

| Time (days) | Vol.% <1 μm | Zeta potential (mV) |
|-------------|-------------|---------------------|
| 0 | 98.2 | 31±2 |
| 7 | 98.0 | 29±1 |
| 14 | 96.4 | 32±1 |
| 21 | 97.4 | 32±2 |

^aOriginal latex was made with 0.12 mol% C12 and 0.07 mol% VA-061. The latex had a primary particle size of 107±2 nm and zeta potential of 46±2 mV and was aggregated to 8.4 μm with a zeta potential of 24±1 mV.

4.4.3 Redispersion with different sized rotor-stators

Redispersion was also carried out with different rotor-stator probes other than the 5.5 cm rotor-stator mentioned above. These rotor-stators were capable of redispersing 40 mL samples whereas the 5.5 cm rotor-stator required approximately 500 mL of sample. A 5 wt% sample with 0.12 mol% C12 and 0.07 mol% VA-061 was redispersed without CO₂ and the volume % below 1 μm was measured over time for 1 cm, 1.9 cm and 2.5 cm rotor-stator probes. Each motor was set at 6000 rpm. The 1 cm rotor-stator, at 6000 rpm, did not produce enough shear to redisperse the sample, whereas the 1.9 cm probe redispersed the sample after 5 min (Figure 4.4). Redispersion was complete after 1 min with the 2.5 cm rotor-stator.

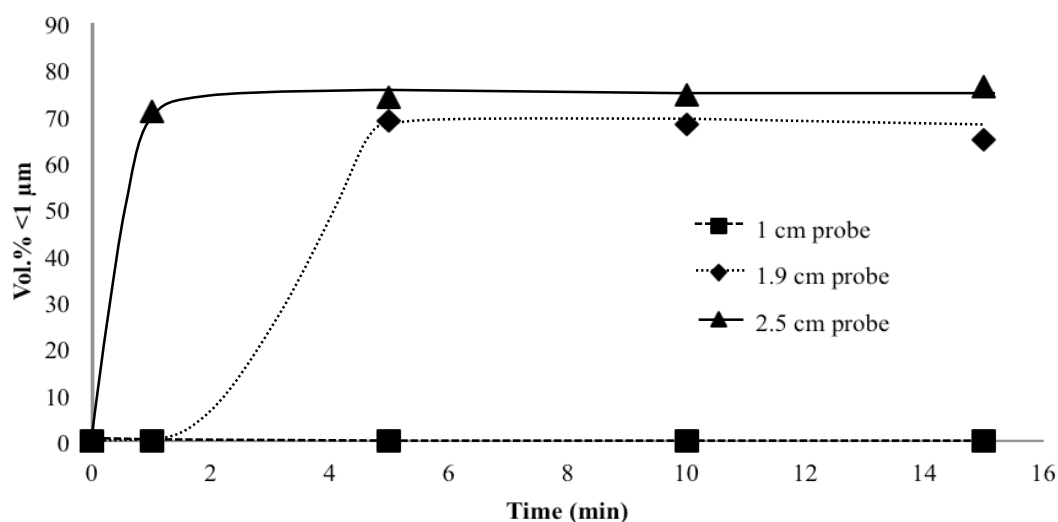


Figure 4.4. Redispersion of a 5 wt% aggregated PMMA latex with 1 cm, 1.9 cm and 2.5 cm rotor-stators at 6000 rpm. The latex was made with 0.12 mol% C12 and 0.07 mol% VA-061 and produced a particle size of 135 ± 2 nm with a zeta potential of 36 ± 1 mV. The latex was aggregated to $10.2 \mu\text{m}$ with air at 80°C .

Redispersion of a 5 wt% sample, from the same batch as above, was carried out with the 1 cm rotor-stator at higher speeds because 6000 rpm was not sufficient. Figure 4.5 shows the volume % below $1 \mu\text{m}$ over time for the 1 cm rotor-stator at various rotations speeds. It was already shown that 6000 rpm was insufficient energy to redisperse the sample, but 10000 rpm was also insufficient. At 14000 rpm, redispersion was successful with a plateau around 65 % by volume below $1 \mu\text{m}$. At 18000 rpm, the plateau was increased to approximately 75 %. Due to the limitations of the Mastersizer 2000, it is likely that there is not much of a true difference between 65 and 75 %. From experience in using this instrument, there is approximately 10 % error associated with volume percentage.

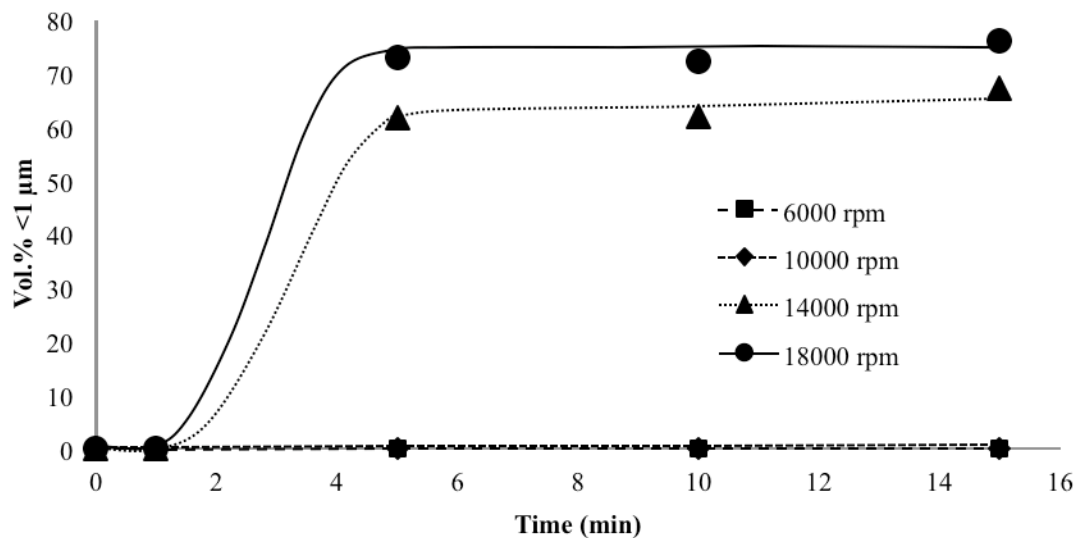


Figure 4.5. Redispersion of a 5 wt% aggregated PMMA latex with a 1 cm rotor-stator at various rotational speeds. The latex was made with 0.12 mol% C12 and 0.07 mol% VA-061 and produced a particle size of 135 ± 2 nm with a zeta potential of 36 ± 1 mV. The latex was aggregated to $10.2 \mu\text{m}$ with air at 80°C .

A similar experiment to the one above was done using a 1.9 cm rotor-stator. Redispersion was successful at 6000 within 5 min and 10000, 14000 and 18000 rpm were successful within 1 min. The plateau reached in this case was between 65 and 75 %. Figure 4.6 shows the volume % below $1 \mu\text{m}$ over time.

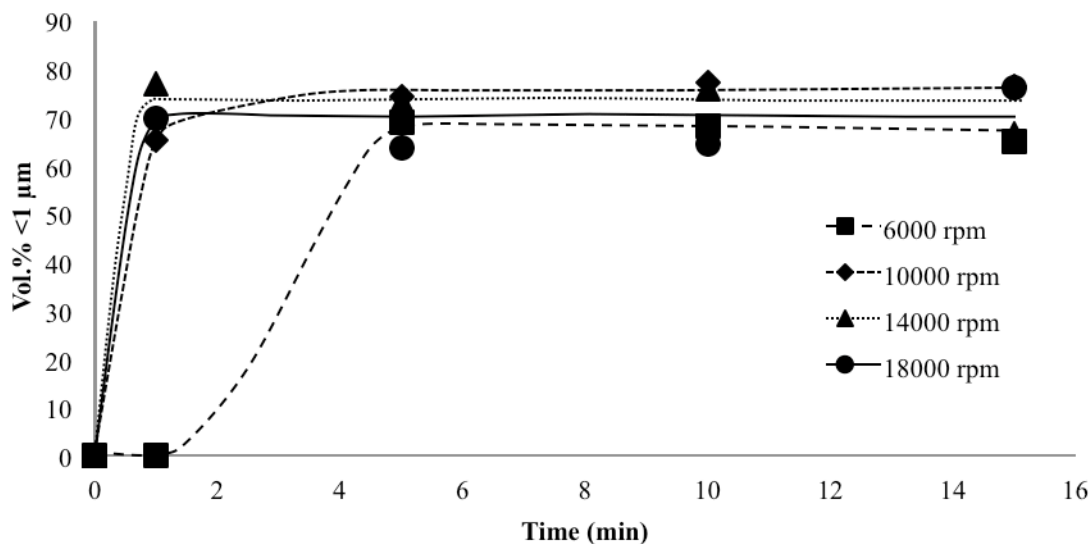


Figure 4.6. Redispersion of a 5 wt% aggregated PMMA latex with a 1.9 cm rotor-stator at various rotational speeds. The latex was made with 0.12 mol% C12 and 0.07 mol% VA-061 and produced a particle size of 135 ± 2 nm with a zeta potential of 36 ± 1 mV. The latex was aggregated to $10.2 \mu\text{m}$ with air at 80°C .

The same experiment was performed with a 2.5 cm rotor-stator, but instead of getting better redispersion, the sample aggregated at higher rotational speeds (Figure 4.7). After 1 min of shear the samples at all speeds were redispersed, but at 10000 and 14000 rpm the percent below $1 \mu\text{m}$ began to decrease, dropping to 0 % at 10 min. At 18000 rpm the sample was aggregated after only 5 min (or possibly sooner). This result is due to shear-induced destabilization. Mechanical agitation increases the frequency of collisions and also provides energy to surpass the energy barrier to reaggregate.¹ During agitation, the samples also increased in temperature, which would only give the particles more energy.

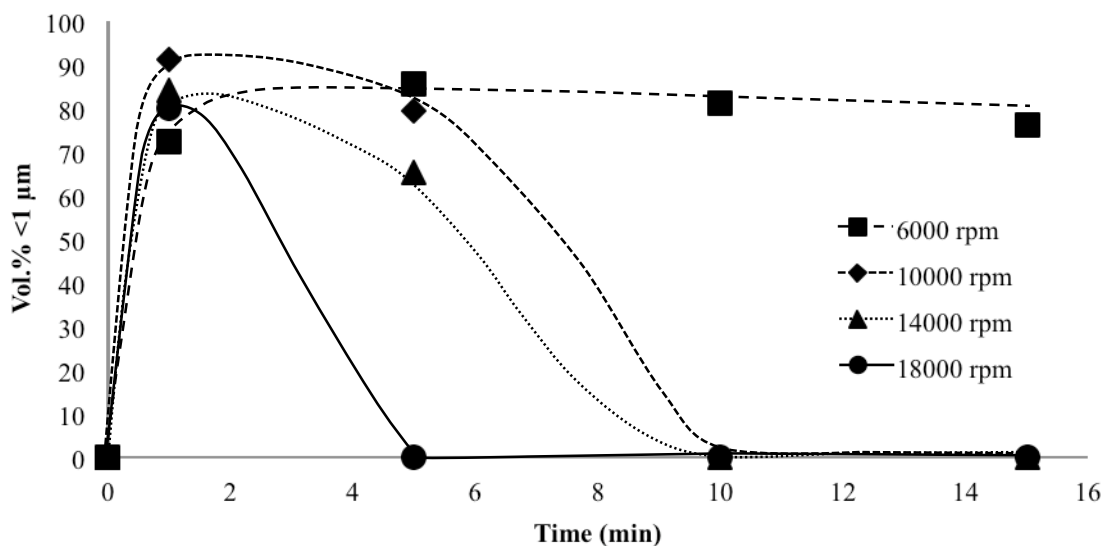


Figure 4.7. Redispersion of a 5 wt% aggregated PMMA latex with a 2.5 cm rotor-stator at various rotational speeds. Original particle size was 135 ± 2 nm with a zeta potential of 36 ± 1 mV and aggregated to 10.2 μm .

4.4.4 Redispersion of polystyrene particles

The redispersion of polystyrene samples was studied qualitatively earlier in this project (Section 4.4.1, Table 4.2). The small polystyrene particles aggregated to very large aggregates and they were very difficult to break up. It was thought that redispersion might be easier if the primary particle size was larger. Another member of the Jessop group devised a method for preparing larger primary particles that provided smaller aggregates upon destabilization, however they were PMMA particles.⁴⁶ The redispersion of these larger PMMA particles seemed to provide more promise. However, to compare, a polystyrene latex with an initial particle size similar to those of PMMA in this project was prepared. A 5 wt% latex prepared with 0.5 mol% C12 and 0.5 mol% VA-061 produced a latex with the particle size 128 ± 1 nm and a zeta potential of 51 ± 1 mV. The latex was aggregated at 80 $^{\circ}\text{C}$ with air to give a particle size of 22 μm with a zeta

potential of 38 ± 1 mV. This is a higher destabilizing zeta potential threshold than PMMA samples, but is consistent with results from other Jessop group members.²⁹ Samples were redispersed with sonication (probe) in the presence and absence of CO₂ and their volume % below 1 μm and zeta potentials are reported (Table 4.6). Although the particle sizes did decrease (~ 5 μm), the samples were not redispersed. This is in contrast to what has been seen by other Jessop group members.²⁹ However, there are some key differences between the two cases. In the other case, the redispersed samples were quite dilute which would help to limit particle collisions. They also used a significant amount of switchable material (5 mol% initiator and 1.5 mol% surfactant, compared to 0.5 mol% and 0.5 mol%, respectively). And finally, they used 15 min of sonication from a sonicator bath, compared to 1 min from a sonicator probe. The aggregates of the polystyrene latex with larger initial particle sizes were smaller than the aggregates from the latex with smaller initial particle sizes (22 μm versus 40 μm), but it appears that they were still too large for adequate redispersion. It is possible that with larger initial particle size the aggregate size will be smaller and redispersion will be possible.

Table 4.6. The redispersion of a 5 wt% aggregated polystyrene^a latex redispersed by 10 % sonication with a sonicator probe in the presence and absence of CO₂.

| | Vol.% <1 μm | Zeta potential (mV) |
|--------------------|------------------------|---------------------|
| No CO ₂ | 0 | 42 \pm 2 |
| CO ₂ | 0 | 46 \pm 2 |

^aLatex prepared with 0.5 mol% C12 and 0.5 mol% VA-061.

4.4.5 Redispersion with extra surfactant added after aggregation

It was mentioned that when using the sonicator, redispersion was not always complete (100 %). Also, it was frequently seen that original zeta potentials were not recovered (Table 4.3). Because it was found that extra surfactant added after aggregation helped with redispersion in polystyrene samples when water was removed (Section 4.4.1), extra surfactant was added to aggregated PMMA samples to improve redispersibility. PMMA latexes were prepared with 0.12 mol% C12 and 0.07 mol% VA-061. Samples were redispersed with sonication, provided by a sonicator bath in the presence and absence of CO₂. Extra surfactant was added (0.06 mol%) after aggregation and prior to redispersion. Either the switchable C12 surfactant was added (in its charged form), or non-switchable CTAB. Table 4.7 shows the particle sizes and zeta potentials of the redispersed latexes measured on the Zetasizer. The zeta potentials increased upon addition of charged surfactant, which led to stability over at least 5 days. In previous experiments the surface charge increased but not to the original zeta potential of the latex (Table 4.3). The addition of extra surfactant may be beneficial to ensure a high zeta potential and provide long-term colloidal stability.

Table 4.7. Redispersion of aggregated PMMA latexes^a with additional surfactant added after aggregation.

| Extra surfactant | Redispersion method | Immediately after redispersion | | 5 days after redispersion | |
|------------------|----------------------------|--------------------------------|----------------|---------------------------|----------------|
| | | Particle size (nm) | Zeta pot. (mV) | Particle size (nm) | Zeta pot. (mV) |
| C12 | Sonication | 140.5±1.3 | 39±1 | 140.0±1.2 | 43±1 |
| C12 | Sonication+CO ₂ | 144.7±0.8 | 42±1 | 144.7±0.9 | 42±1 |
| CTAB | Sonication | 140.6±1.1 | 47±1 | 140.0±1.9 | 46±1 |
| CTAB | Sonication+CO ₂ | 138.6±1.7 | 47±1 | 140.6±1.0 | 47±1 |

^aOriginal latex with primary particle size of 135±1 nm and zeta potential of 45±1 mV was aggregated to 6.3 μm with a zeta potential of 20±1 mV. Latex was prepared with 0.12 mol% C12 and 0.07 mol% VA-061.

4.4.6 Redispersion of an aggregated latex polymerized with a switchable-nonswitchable surfactant mixture

Above, non-switchable surfactant was added to the aggregated latex to help with redispersion. Here it is examined whether the non-switchable surfactant can be added before the polymerization so that there is both switchable and non-switchable surfactant present during the polymerization. To maintain switchability of the latex, a minimal amount of CTAB was added, too much and the latex would not aggregate with air and heat. Table 4.8 shows the trials of polymerization with both switchable and non-switchable surfactant. Polymerizations at 5 wt% monomer content were done with 0.12 mol% C12 and 0.07 mol% VA-061, while varying the amount of CTAB. Samples containing 0.06, 0.03, and 0.015 mol% CTAB could not be aggregated with air and heat because there was enough active CTAB to stabilize the particles even though the switchable surfactant had been switched to its inactive form. At 0.0075 mol% CTAB it was possible to aggregate the latex using air and heat. The zeta potential of the

aggregated particles was 19 ± 1 mV. CO₂ was bubbled through the aggregated sample for 5 min, followed by 1 min of sonication (probe) at 10 % power then bubbled for another 10 min with CO₂. The primary particle size was obtained with 94 % of the particles, by volume, below 1 μm . The zeta potential of the redispersed sample was 21 ± 1 mV. After 7 days the zeta potential increased to 27 ± 1 mV. This increase in zeta potential is most likely due to the C12 surfactant switching to its charged form, but CTAB may also be contributing to the surface charge. When the particles aggregated, some of the surface charge from CTAB would likely have been buried between particles. If so, once the particles were redispersed and broken apart, the surface charge from these molecules would have increased the measurable zeta potential. A sample was also redispersed with only sonication. The zeta potential was found to be 23 ± 1 mV with no exposure to CO₂. It could be that this slight increase was due to the uncovering of CTAB molecules. CTAB does not affect the switchability of the system and likely aids in the redispersion process because it ensures permanently charged surface groups on the particle.

Table 4.8. Polymerization of MMA with C12 (0.12 mol%) and varying amounts of non-switchable surfactant (CTAB).^a

| Mol% CTAB ^b | Wt% | Latex | | Aggregated particles |
|------------------------|-----|--------------------|----------------|---------------------------------|
| | | Particle size (nm) | Zeta pot. (mV) | Particle size (μm) |
| 0.06 | 4.0 | 89 ± 2 | 47 ± 1 | - |
| 0.03 | 3.0 | 80 ± 1 | 49 ± 1 | - |
| 0.015 | 4.0 | 100 ± 1 | 48 ± 1 | - |
| 0.0075 | 4.9 | 105 ± 1 | 45 ± 1 | 11.4 |

^aLatex was prepared with 0.07 mol% VA-061.

^bMol% of CTAB is with respect to total monomers.

4.4.7 Reversibility

Now that redispersion has been demonstrated to be successful it prompts the question of whether the aggregation/redispersion cycle is repeatable. As mentioned in the introduction, redispersible polymers reported in the literature have limited aggregation/redispersion cycles, sometimes because of the buildup of salts formed by the acid and base triggers. Because CO₂ addition and removal is the trigger for the switchable surfactant, there should be no build up of salts and consequently the switch should, in theory, occur several times. It was first examined if a reconstituted latex could be reaggregated by using the switchable surfactant. Figure 4.8 is a plot of the volume % below 1 μm over time for different aggregation methods: 1) air; 2) heat (80 °C); and 3) air and heat (80 °C). Heat was sufficient to cause aggregation on its own after 155 min, but, when combined with the bubbling of air, the aggregation time was decreased. Air, by itself, did not aggregate the reconstituted latex on a reasonable time scale. Because bubbling air through the mixture will remove any dissolved CO₂, there is no reason to believe that bubbling only air should not reaggregate the latex, only that it might take a very long time.

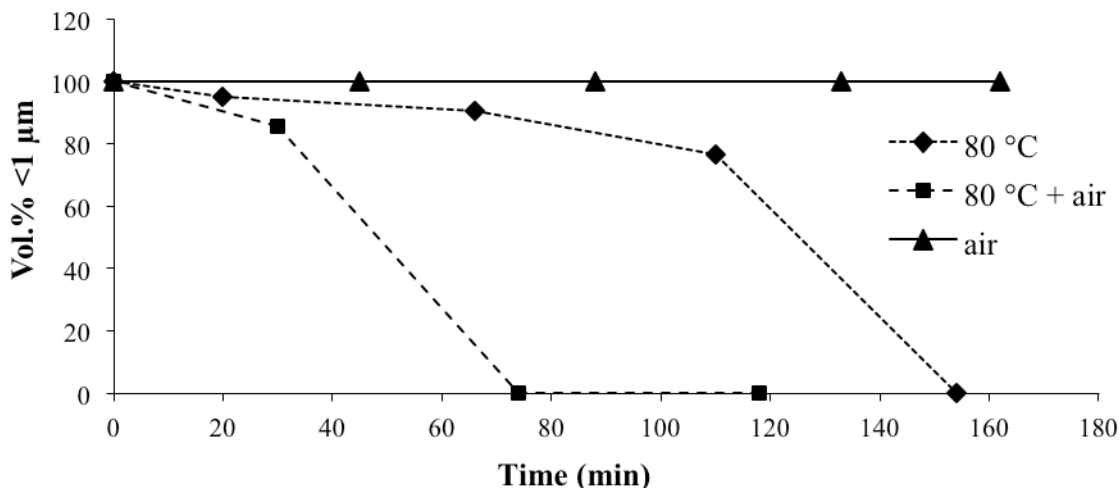


Figure 4.8. The reaggregation of a reconstituted PMMA latex by three different methods. Original latex was made with 0.12 mol% C12 and 0.07 mol% VA-061 to give an initial particle size of 132 ± 1 nm and a zeta potential of 43 ± 1 mV. The latex was initially aggregated with air at 80 °C to a particle size of 8 μ m and a zeta potential of 20 ± 1 mV.

Now that it has been shown that reaggregation is possible, it is necessary to show that a second cycle of redispersion is possible. Three aggregation/redispersion cycles were performed on a 5 wt% latex (Table 4.9). The sample was aggregated with air and heat (80 °C) and redispersed with 10 % sonication (probe) for 1 min followed by 10 min of CO_2 bubbling (the same aggregation and redispersion methods described in Sections 2.6 and 2.6.1). As expected, the first aggregation step with air and heat led to no particles under 1 μ m and a zeta potential of approximately 20 mV. The zeta potential after the first redispersion step was still only approximately 20 mV, but this was expected because previous experiments (Table 4.3) showed that it takes up to 7 days for the zeta potential to increase. The second and third aggregation steps again resulted in complete conversion to particles greater than 1 μ m after heating and bubbling with air. The second and third redispersion steps also successfully converted most or all of the material to under 1 μ m, and increased the zeta potential relative to that after aggregation.

Table 4.9. Multiple cycles of aggregation and redispersion of a 5 wt% PMMA latex.^a

| Treatment | Vol.% <1 μm | Zeta potential (mV) |
|--------------------------------|---------------------------|------------------------|
| None (latex) | 100 | 46 \pm 3 |
| Air and heat | 0 | 20 \pm 1 |
| Sonication and CO ₂ | 100 | 19 \pm 1 |
| Air and heat | 0 | 13 \pm 1 |
| Sonication and CO ₂ | 93.9 | 15 \pm 1 |
| Air and heat | 0 | 13 \pm 1 |
| Sonication and CO ₂ | 100 | 18 \pm 1 |

^aOriginal latex was made with 0.12 mol% C12 and 0.07 mol% VA-061. To aggregate, samples were bubbled with air and heated at 80 °C. To redisperse, samples were sonicated (probe) for 1 min at 10 % power and bubbled with CO₂ for 10 min.

4.4.8 Dewatering

If switchable latexes of this type were to be used for transportation, it would be useful to be able to remove some of the water from the aggregated material to reduce shipping costs. In earlier experiments, water was removed from aggregated polystyrene latexes and redispersion was found to be unsuccessful (Section 4.4.1). Since then, more understanding about the redispersion process had been developed and this experiment was revisited.

A 4.6 wt% aggregated PMMA latex was prepared with 0.12 mol% C12 and 0.07 mol% VA-061 to give a primary particle size of 124 \pm 2 nm and a zeta potential of 49 \pm 3 mV. The latex was aggregated with air at 80 °C to give a particle size of 9 μm with a zeta potential of 20 \pm 1 mV. An aggregated latex (40 mL) was filtered by suction filtration using a fine frit, removing 30 mL of water to give a solids content of 18 %. Fresh deionized water was added to obtain a 4.9 wt% rehydrated aggregated latex. Some of the rehydrated sample was then sonicated (probe) for 1 min at 10 % power without

CO₂. Another portion of the sample was exposed to CO₂ for 5 min, then sonicated for 1 min at 10 % power, followed by further CO₂ bubbling for 10 min. Table 4.10 shows the volume % below 1 μm and the zeta potentials of the redispersed samples immediately after redispersion and one week later. The samples were immediately redispersed after both redispersion methods. This is similar to the results of another latex redispersed under the same conditions except water was never removed (Table 4.3). The zeta potentials were still low in both the CO₂ and no CO₂ exposed samples after one week. The lack of increase in zeta potential is probably due to the low solids concentration and initial low concentration of switchable groups when making the latex or possibly because some of the surfactant was lost when removing the water. The removal of water does not appear to affect the redispersibility of latexes with low solids content.

Table 4.10. Redispersion of a rehydrated 4.9 wt% aggregated PMMA latex with 10 % sonication (probe) for 1 min in the presence and absence of CO₂.^a

| | No CO ₂ exposure | | CO ₂ exposure | |
|--------------------------------|-----------------------------|----------------|--------------------------|----------------|
| | Vol.%<1 μm | Zeta pot. (mV) | Vol.%<1 μm | Zeta pot. (mV) |
| Immediately after redispersion | 99.0 | 18±1 | 97.9 | 18±1 |
| 7 days later | 98.7 | 16±1 | 97.8 | 17±1 |

^aOriginal latex was prepared with 0.12 mol% C12 and 0.07 mol% VA-061.

4.5 DLVO theory

In this section, DLVO theory is applied to a typical PMMA latex prepared in this project. DLVO theory explains why latex particles have colloidal stability when CO₂ is present and why the removal of CO₂ leads to particle aggregation. It also shows why

redispersion is possible and why when CO₂ is not present redispersion is still possible but does not produce thermodynamically stable colloidal suspensions.

As mentioned in Section 1.7, the stability of a system is determined by the interaction energies between surfaces. The interaction between two spheres models the latexes made in this project. When redispersion is successful in producing a single population of particles, this will also be represented by the interaction between two spheres. When redispersion is incomplete and large aggregates exist in the system as well as small particles, then the interaction will effectively be between a sphere and an infinite plate (as mention in Section 4.4.2). Figure 4.9 shows the total interaction energies between spherical PMMA particles⁵⁰ when the switchable surfactant is in its charged (“on”) and uncharged (“off”) forms. The van der Waals interaction energy will be the same in both situations because it is only the electrostatic factors that are changing because of the switching process. It was shown in Section 1.7 that the Debye length depends on the electrolyte concentration in solution, which means that the Debye length will be affected by pH. The pH of the charged system is approximately 3.9¹⁶ and at pH 6 the surfactant will be neutral. The other factor that greatly affects the electrostatic interaction energy is the zeta potential. The surface potential not only depends on the zeta potential, but also the Debye length. Latexes usually had a zeta potential of approximately 40 mV and it was found that 20 mV was the zeta potential where aggregation was induced (in PMMA latexes), these values were used in this calculation (equations from Section 1.7). ΔG is the Gibb’s free energy of coalescence, which means that when it is negative (spontaneous) the particles will coalesce (attraction between particles). If ΔG is positive coalescence is not spontaneous, resulting in a stable

dispersion (repulsion between particles). Stable latex particles will exist to the right of the potential energy barrier of the total interaction energy of the “on” surfactant. The particle dispersion will remain stable ($\Delta G > 0$, repulsion) here unless the particles gain some energy to surpass the potential energy barrier before falling into the primary minimum (an example being shear-induced destabilization). However, if the zeta potential is decreased and the pH is increased in the system by removing CO₂, the total interaction energy curve of the “off” surfactant case is obtained. This has no energy barrier and the particles can easily fall into the primary minimum causing aggregation.

If only a portion of the surfactants were to switch “off” then only the remaining charged surfactants would contribute to the zeta potential. When the zeta potential is decreased the potential energy barrier decreases, making it easier for particles to aggregate. However, a sufficient decrease of surface charge is needed before there is no longer any barrier. The use of non-switchable surfactant, which is permanently charged, will also help to keep the zeta potential from decreasing too much. It could be possible to add enough CTAB so that there is always a small barrier. It could then be possible to aggregate particles when given sufficient energy but the small barrier will also provide stabilization for redispersed particles.

To redisperse, it is necessary to pull the particles apart, but this is not energetically favourable. This is why a sufficient input of energy is required for redispersion to take place. Redispersion was successful with no CO₂ because the interaction curve for the “off” surfactant is positive at some distance, but because there is no energy barrier, the particle dispersion will not be thermodynamically stable. By

increasing the zeta potential of the system, even if only by 5 or 10 mV, a plot more similar to the “on” interaction energy case will be obtained resulting in a higher energy barrier and more thermodynamically stable colloidal particles.^{3,21}

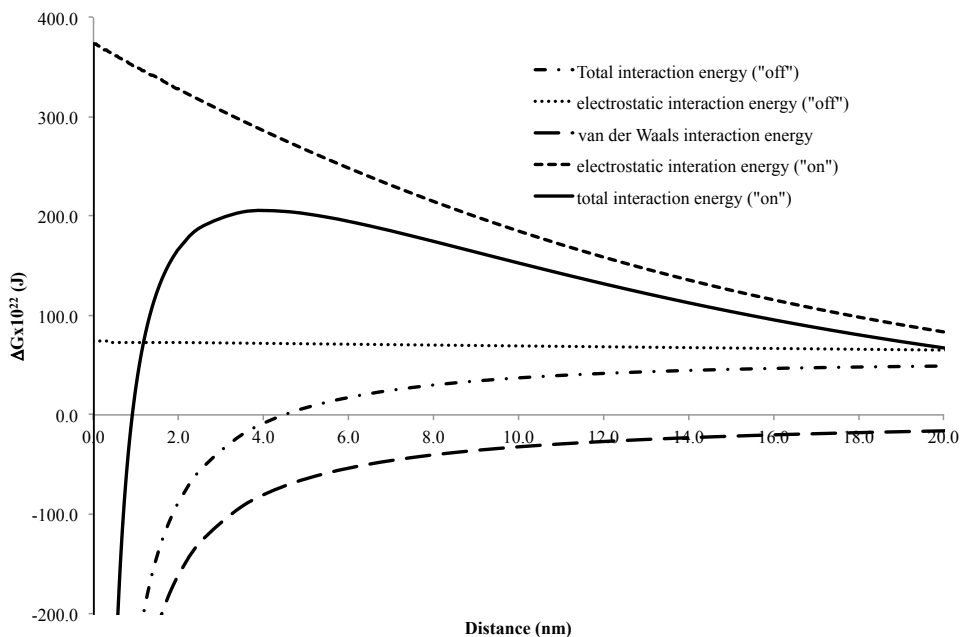


Figure 4.9. The interaction energies between two spherical PMMA particles with diameters of 150 nm in the presence of charged (“on”) and neutral (“off”) switchable surfactant, as a function of distance between the surfaces.

4.6 Conclusions

In this chapter the redispersion of aggregated polymer latexes was discussed. The redispersion of a PMMA latex stabilized only with non-switchable groups maintained long-term colloidal stability if the aggregated latex was washed to remove the salt used to cause destabilization. Aggregates were shown to be non-fused clumps of primary particles, which is necessary for successful redispersion. The destabilization time was also shown to decrease when increasing the temperature of destabilization. Polystyrene

latexes with a small primary particle size aggregated to large particles that were difficult to redisperse, even with the help of sonication and extra surfactant.

A sonicator probe or a blender were used for the redispersion of a 5 wt% latex and successfully redispersed at least 98 % of particles, by volume, in the presence and absence of CO₂. A rotor-stator redispersed at least 60 % of particles, by volume, in the presence and absence of CO₂ (5 wt% latex). A 15 wt% latex was only successfully redispersed with the sonicator probe in the presence of CO₂. This latex maintained colloidal stability for at least 21 days. An overhead stirrer was also used for redispersion, but was unsuccessful at redispersing both 5 and 15 wt% latexes.

Different sized rotor-stator probes were used to redisperse 5 wt% latexes at different speeds. The 1 cm rotor-stator could only induce redispersion if the rotational speed was at least 14000 rpm. The 1.9 cm rotor-stator could redisperse at all speeds but required more than a minute at 6000 rpm. The 2.5 cm rotor-stator provided too much energy at 10000 rpm and caused shear-induced aggregation but redispersion was successful at 6000 rpm.

Extra surfactant (switchable and non-switchable) added after aggregation increased the zeta potential and helped to maintain colloidal stability of redispersed samples. Switchable and non-switchable surfactants were also used at the same time during a polymerization and if a minimal amount of non-switchable surfactant was added, the switchability of the system was maintained.

The reversibility of the system was tested for three aggregation/redispersion cycles and found to be stable for a 5 wt% latex. Aggregation was carried out with air at

80 °C and redispersion was carried out with the sonicator probe (10 % power). Water was also removed from an aggregated latex and fresh water added and then redispersed with sonication and CO₂. The removal of water did not seem to affect the redispersibility of the latex compared to previous samples where water was not removed.

Finally, the colloidal stability of a latex was discussed in relation to DLVO theory. The DLVO-plot of the latex shows a potential energy barrier that maintains colloidal stability. The DLVO-plot of latex with neutral surfactant contains no barrier which is why the particles can easily aggregate to lower the free energy.

5. Results and Discussion: Low T_g polymer for film formation

The polymers used in Chapter 4 were poly(methyl methacrylate) and polystyrene. These have high glass transition temperatures, T_g , of 105 and 100 °C, respectively.⁵¹ When latexes made from these polymers were dried they formed hard brittle pieces. This would of course result in a very poor latex paint. As mentioned in Section 1.9, to form a film the latex needs to be dried above the minimum film formation temperature, and to make a homogeneous film it also needs to be above the T_g . Pure polystyrene and PMMA latexes are not candidates for latex paints because you would need to paint at over 100 °C.

The latexes produced in Chapter 4 were also very low in solids content (5-15 wt%) compared to that of exterior paints (55 wt%).¹ If a latex paint contained only 15 wt% solids, the consumer would need to paint a surface multiple times just to build up a thick enough film to cover the surface. So, is it possible to use the switchable surfactant and switchable initiator to make a more realistic latex formulation?

5.1 Glass transition temperature

The glass transition temperature is affected by the composition of the polymer; so, it can be tuned by mixing two polymers with different T_g 's together. This is accomplished by copolymerization. The T_g 's of poly(butyl acrylate) (BA) and PMMA are -54 °C and 105 °C, respectively.⁵¹ Liu et al.³³ obtained varying T_g values after copolymerizing the monomers in different ratios (Table 5.1). The copolymerization of BA and MMA to give a T_g of 7 °C is representative of a composition that would be used for exterior latex paints.¹⁸ Below the T_g , a polymer is glassy and rigid, but above the T_g the polymer becomes soft and malleable. This is important because the fact that the polymer becomes

soft is why it is possible to form a homogeneous film. Molecular rotations along the polymer backbone become much easier at the T_g which allows the polymer chains between particles to deform and mutually interpenetrate by diffusion.⁵²

Table 5.1. Glass transition temperatures from the copolymerization of BA and MMA in different weight ratios.^{33a}

| Wt% BA | Wt% MMA | T_g (°C) |
|-----------|------------|---------------|
| 60 | 39 | 4 |
| 55 | 44 | 7 |
| 50 | 49 | 7 |
| 40 | 59 | 12 |

^aThe copolymerizations were carried out with 1 wt% methacrylic acid for stabilization purposes.

5.2 Copolymerization

In a binary copolymerization, there is the possibility of four reactions during the propagation of a polymer chain. If the two monomers are M_1 and M_2 , at anytime a polymer chain could end with $\bullet M_1$ or $\bullet M_2$, where \bullet signifies a radical. The four possible reactions are as follows: 1) $\bullet M_1 + M_1$, 2) $\bullet M_1 + M_2$, 3) $\bullet M_2 + M_2$ and 4) $\bullet M_2 + M_1$. Each of these reactions has a corresponding rate constant, k_{11} , k_{12} , k_{22} and k_{21} , respectively. The reactivity ratios, r_1 and r_2 , shown below, are characteristic of the comonomer system.⁵³

$$r_1 = \frac{k_{11}}{k_{12}}, \quad r_2 = \frac{k_{22}}{k_{21}} \quad (5.1)$$

If the reactivity ratios of a comonomer pair are significantly different from each other, then one of the comonomers will preferentially react. When $r > 1$ the comonomer prefers to react with itself, and when $r < 1$ the comonomer prefers to react with the other

comonomer. When r is equal to 1 there is no preference in reactivity and so the polymer is completely random. When r is equal to zero a comonomer will only react with the other comonomer.⁵¹⁻⁵³

Reactivity ratios can also appear to be different when doing emulsion polymerization due to a solubility effect. When copolymerizing a water-soluble monomer and a water-insoluble monomer, the water-soluble monomer will partition between the aqueous and organic phase but a significant portion will reside in the aqueous phase. Because the polymerization takes place in the organic phase, it will appear that the reactivity of the water-soluble monomer is low, but this is only because the concentration of the water-soluble monomer is low in the organic phase. The composition of the copolymer will depend on the partitioning coefficient of the monomer.⁵³

The reactivity ratios of BA and MMA are 0.11 and 2.86, respectively.⁵⁴ This means that MMA will preferentially react with itself, leading to a copolymer rich in MMA and deficient in BA. To solve this issue, the copolymerization of these comonomers is done under starved conditions in a semi-continuous polymerization process.

5.3 Semi-continuous polymerization

The difference between a batch and a semi-continuous, or semi-batch, process is the timing of the addition of the monomer and possibly other reagents. In a batch process, all reactants are added at the beginning of the reaction. In a semi-continuous, process there is an initial batch reaction where seed particles are made, but the majority of the monomer is fed over a period of time at a continuous feed rate. Semi-continuous

processes are typically used in large-scale reactors due to their better temperature control. Free-radical polymerization is an exothermic process and heat transfer is very poor in large reactors.^{18,55}

A semi-continuous process was used in this project to help control copolymer composition, but they do not need to be used for only copolymerizations. Carrying out polymerizations under “starved” monomer conditions helps to control the polymerization rate in emulsion polymerization. In a copolymerization, if two monomers are copolymerized in a batch process this will lead to a chemical compositional distribution, where very different polymers could be created. The more reactive monomer will react preferentially with itself, only occasionally adding a less reactive monomer unit. In the worst case scenario, if there is a lot of compositional drift the copolymer could be heterogeneous, which would have inferior physical properties (if the reactivity ratios are significantly different). This means that there could be so much compositional drift that some polymer chains are different from others made in the same batch (one chain is rich in one of the comonomers and another is rich in the other). In a semi-continuous process, the feed rate of the monomers is approximately equal to the rates of consumption of the monomers. This ensures that both monomers, with high and low reactivity, will be incorporated into the copolymer.⁵⁶

5.4 Chain transfer agent

Another difference in the polymerizations done in this chapter was the use of a chain transfer agent (CTA). CTA's are used to limit the molecular weight of a polymer during a polymerization. They react with a polymer radical to terminate chain

propagation, but do not stop the overall polymerization reaction. A CTA is a molecule that contains an abstractable hydrogen. Thiols are common CTA's; in the present copolymerizations, the CTA used was 1-dodecanethiol. The radical on the end of the polymer chain abstracts the hydrogen from the thiol and terminates the growth of the original chain. The remaining radical then begins to react with monomer and a new chain will begin to propagate. In some cases it is desirable to terminate the polymer chains with CTA to functionalize the polymer.^{51,57} Liu et al.³³ report good control of the molecular weight with dodecanethiol as a CTA during the copolymerization of BA and MMA. They show a linear relationship between the inverse of the molecular weight and the concentration of dodecanethiol.

5.5 Emulsion stability

In the regular batch emulsion polymerizations performed in this project, the emulsions were stable over a reasonable time period (several hours). The emulsions were continuously stirred and not given any time to separate. However, emulsion stability was a concern in the semi-batch process because the preemulsion had to be fed from a syringe pump for 3 h while the reaction proceeded. The preemulsion could not be stirred while in the syringe and during the reaction the emulsion separated within the syringe. This separation occurred when the same amount (0.09 mol%, based on total monomers) of switchable surfactant C12 was used as the surfactant used from literature (Polystep A-16).³³ This is a smaller amount of surfactant than was used in the previous chapter (0.09 vs. 0.12 mol%). Latexes with higher solids content are also generally more difficult to stabilize because the interparticle distance is much smaller and there is more total particle surface area, meaning that a higher mol% of surfactant will most likely be required for

this polymerization. The amount of surfactant was varied in emulsions of BA, MMA and water. All emulsions had a 60/40 BA/MMA weight ratio. The amount of monomer during the tests, 58.6 wt%, reflected that of the preemulsion to be used for the polymerization. CO₂ was bubbled through the emulsions for 15 min before the emulsions were stirred for 1 h and then left to sit. The stability of the emulsions was determined visually. The emulsions were sealed after the CO₂ treatment to prevent CO₂ from escaping. Photos of emulsion separation over time are shown in Figure 5.1. The amount of C12 was varied from 0.24 mol% to 2 mol%. After the stirring was stopped, a photo was taken at 1, 15, 30 and 60 min. After 1 min there was separation at 0.24 and 0.48 mol%, but not a significant amount of separation at 1 and 2 mol%. After 15 min there was a great deal of separation at all surfactant concentrations except 2 mol%. At 30 min the 2 mol% sample began to separate and at 60 min there was very clearly two layers sandwiching the remaining emulsion. At high monomer content, the emulsion required at least 2 mol% to remain stable for at least 30 min. It was decided to load the syringe with preemulsion every 30 min, while the rest remained stirring in a round-bottom flask.

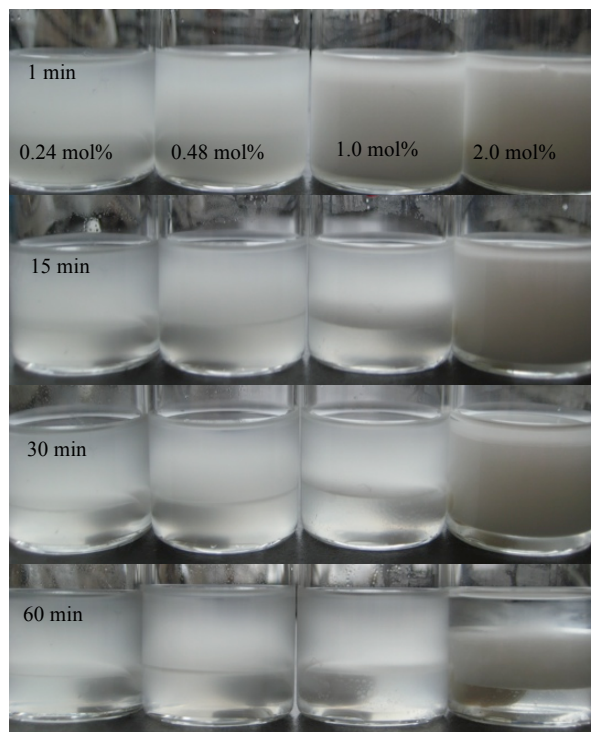


Figure 5.1. Emulsion stability tests of a BA/MMA/H₂O emulsion with a monomer content of 58.6 wt% with different concentrations of C12 relative to the total monomers.

5.6 Latex synthesis

At first it was found that stability in the syringe was poor even with 2 mol% C12. However, if CO₂ was bubbled through the premulsion (which was opened to air every 30 min) 1 min prior to loading the syringe, stability was greatly increased. In fact, the stability was so good after immediate CO₂ treatment that it was decided to lower the surfactant concentration to 1.5 mol%. The emulsions stabilized with 1.5 mol% were stable in the glass syringe for the 30 min intervals. The stability was determined visually.

In the literature procedure,³³ they used an overhead mechanical stirrer, but this equipment, along with the appropriate glassware, was not available during this project. Instead, magnetic stirring was used. A sufficiently large magnetic stir bar (~3 cm) was

required for adequate mixing. When using a small stir bar, it became stuck in the sticky coagulum on the bottom of the round-bottom flask. The larger stir bar did not get stuck.

Frequently, coagulum formed on the needle and caused a partial block in the flow of CO₂. Because of this, the needle was checked often to remove any blockage. However, there was never a complete blockage, so the reaction was always under CO₂.

5.7 Latex characterization

The latex produced from the semi-continuous copolymerization of BA and MMA was stable when kept under CO₂. The copolymerization was carried out twice under the same conditions to examine the reproducibility of the formulation (Table 5.2). The final solids content was 42 wt% for both latexes. This was a lower solids content than the preemulsion due to the dilution from the water present during the batch reaction in the first stage of the copolymerization. The conversion was high in both cases and coagulum only accounted for 7.5-10 % by weight. The wt% of BA and MMA incorporated within the copolymer was determined by NMR and in both trials the ratio of BA to MMA in the copolymer was higher than the ratio of BA to MMA monomer. Because the reactivity ratio of MMA is higher than BA one would think that the copolymer should be richer in MMA. However, it is likely that the MMA reacted with itself and formed a majority of the coagulum in both trials (the actual composition of the coagulum was not measured). This is consistent with the greater deviation from the monomer ratios in trial 2 and the larger amount of coagulum seen in this trial. The particle sizes from the two trials were similar. The particles were smaller than those from Chapter 4 because of the large amount of surfactant used for the copolymerization. The polydispersity of the particle size

distribution was measured by light scattering, where a value below 0.1 indicates a monodispersed latex. In the first trial the PDI was a bit high, but in the second trial the PDI was below 0.1 and can be considered a relatively narrowly dispersed latex. The zeta potentials in both trials were much higher than those seen in the previous chapter; this is due to the large amount of surfactant used. High zeta potentials were also seen in the work by Mihara et al.²⁹ where very large amounts (5 mol% VA-061 and 1.5 mol% C12) of switchable amidine groups were used. This corresponds to the large amounts of switchable surfactant C12 used for the copolymerizations (1.5 mol%). The switchable initiator VA-061 was also used and will contribute to the zeta potential as well. The molecular weight was measured by gel permeation chromatography (GPC) but is not reported because poor results were obtained. The signal appears to be from a very dilute sample but the sample prepared was made to have a high concentration. What is thought to have happened was that a majority of the polymer was lost during the filtration process. Filtration of very high molecular weight samples is very difficult. In future copolymerizations the use of more CTA would probably alleviate this problem. Other than some molecular weight issues, the copolymerization of BA and MMA with the use of switchable surfactant, C12, and switchable initiator, VA-061, was both possible and reproducible.

Table 5.2. The characterization of two latexes prepared by semi-continuous copolymerization under the same conditions to determine reproducibility.^a

| Trial | Conversion (%) | wt% BA | wt% MMA | Particle size (nm) | PdI | Zeta potential (mV) | wt% Coagulum |
|-------|----------------|--------|---------|--------------------|-------|---------------------|--------------|
| 1 | 91 | 56.9 | 43.1 | 94.2±0.4 | 0.14 | 81±3 | 7.5 |
| 2 | 88 | 58.5 | 41.5 | 107±0.8 | 0.082 | 110±1 | 10.4 |

^aCopolymerizations were done with 1.5 mol% C12 and 0.3 mol% VA-061 (based on total monomers). The solids content of the final latexes was 42 wt% in both trials.

5.8 Destabilization

The P(BA-*co*-MMA) latex from trial 1 was destabilized by switching the surfactant to its neutral form by bubbling air through the latex from trial 1 and heating to 80 °C for 2 h. After destabilization, what remained was a large mass of coagulated polymer and some liquid latex. Figure 5.2 is a photograph of the coagulated polymer. The dried polymer had a rubbery texture and appeared to consist of several individual spheres stuck together. Several spheres were measured using calipers and an average of 0.5 mm was found. Because the T_g of the copolymer was approximately 7 °C (see Table 5.1), at room temperature the polymer would be amorphous and have a soft consistency. The latex was aggregated at an even higher temperature so the polymer did not form the brittle glassy aggregates seen in the case of a high T_g polymer but the aggregates were soft and rubber-like. During the destabilization treatment, a majority of the latex became a large mass of copolymer and so, there was no longer any stirring. Some latex remained in pockets of the solid copolymer where the air being bubbled could no longer reach. The remaining latex was collected and the stability was determined to be very poor. With only a small amount of shear (pouring the sample out of one vial and into another) after

dilution, the polymer coagulated. The particles coagulated in the Zetasizer and a particle size could not be measured, the coagulated particles were visible to the naked eye. The zeta potential of the remaining latex was measured before it had time to coagulate. With a zeta potential of 6.1 ± 0.3 mV it is no wonder that the latex was very unstable because it had very little surface charge for stabilization. The latex was also destabilized at room temperature with a 0.1 M KOH solution, resulting in a sticky clump of polymer. This is not unexpected room temperature is above the predicted T_g .



Figure 5.2. Photograph of the coagulated BA/MMA copolymer. The sample was destabilized with air and heat (80 °C).

The SEM image of the aggregated sample shows that the large spheres shown in Figure 5.2 had a rough surface and appeared to be made up of smaller fused particles (Figure 5.3). In the SEM image of the aggregated PMMA particles from Section 4.2.2 (Figure 4.2b) it was seen that the spherical particles retained their shape and there was no fusion between particles. It was therefore possible to break apart the spheres to redisperse

the sample. However, because the copolymer particles fused after destabilization, it is likely that redispersion would not be possible.

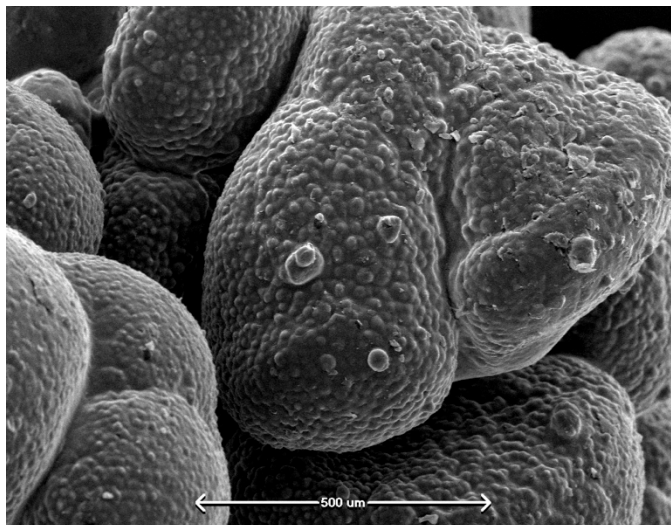


Figure 5.3. An SEM image of the coagulated BA/MMA copolymer. The sample was destabilized with air and heat (80 °C).

5.9 Film formation

As discussed in Section 1.9, for a latex to form a film, the polymer must be above not only the minimum film forming temperature (MFFT), but also the glass transition temperature. The MFFT is generally slightly higher than the T_g .³⁰ Because the T_g of the copolymer should be approximately 7 °C (due to the copolymer composition), it is safe to assume that the copolymer is above the MFFT at room temperature. Figure 5.4 is a picture taken with an optical microscope at 10x magnification comparing films produced by the low T_g copolymer and the high T_g PMMA polymers prepared for redispersion. Approximately 4 drops of latex were deposited on a glass microscope slide and left to dry under a flow of air at room temperature. The resulting films were observed with an optical microscope. Figure 5.4a shows the edge of the copolymer film (where the film

lays to the right of the photo); the film is smooth and transparent. The transparency is expected above the MFFT due to the lack of holes between the particles to reflect light.³⁰ Figure 5.4b shows the edge of the PMMA film (where the film lays to the bottom of the photo). This film contained cracks because the hard polymer particles did not fuse to fill the voids between particles after the water had evaporated. An SEM image of the film produced by the copolymer confirms that there were no spaces between the copolymer particles (Figure 5.5). The particles that are in the image are those due to dust or debris.

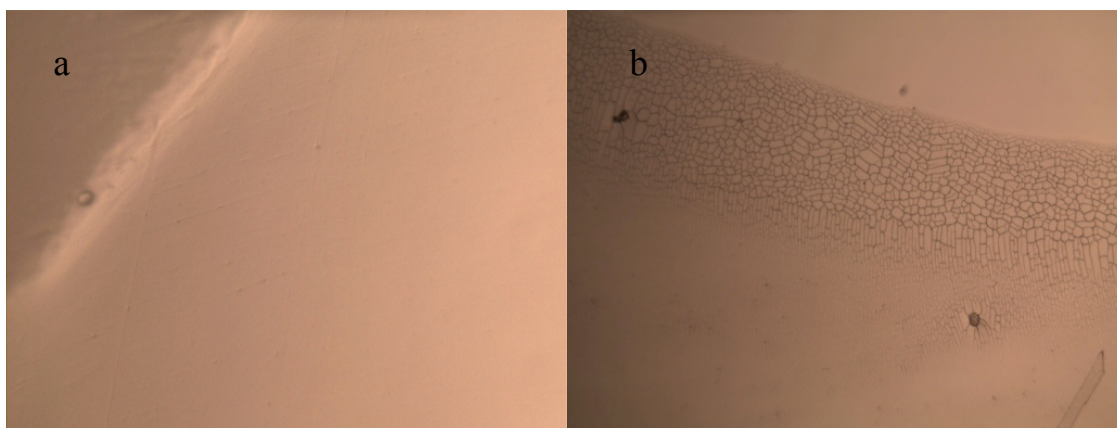


Figure 5.4. Optical microscope images of the films from a) a BA/MMA copolymer and b) a PMMA polymer latexes at 10x magnification.

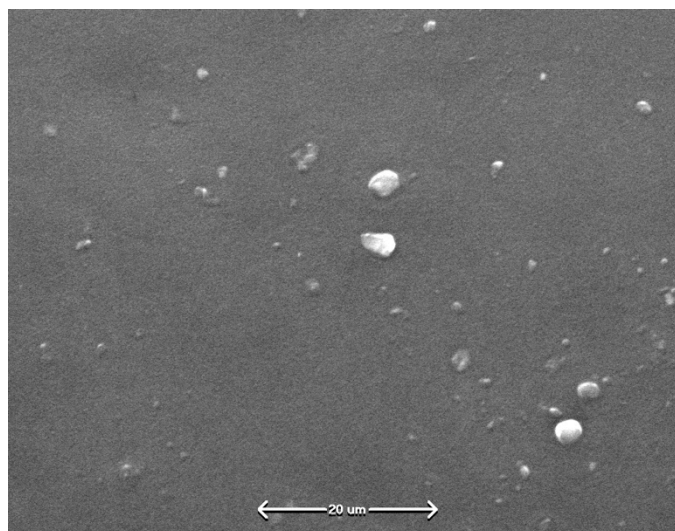


Figure 5.5. An SEM image of the film produced by a BA/MMA copolymer.

5.10 Conclusions

A low T_g copolymer (BA-*co*-MMA) was made by a semi-continuous emulsion polymerization reaction stabilized with the amidine switchable surfactant and initiated with the switchable initiator. Emulsion stability was poor in the syringe but was improved by using 1.5 mol% C12 (based on total monomers) and bubbling CO₂ through the emulsion prior to loading the syringe for 1 min.

The destabilization of this latex by the general method in the previous chapter, air and heat, resulted in a coagulated mass. The particles, once destabilized, fused together. The particles fused because destabilization was carried out above the copolymer's T_g .

A film was produced when allowing the latex to dry under a flow of air at room temperature. The microscope images confirm the deformation of particles (step 2 of film formation), but conclusions cannot be made about molecular diffusion (step 3 of film

formation). It is thought that when the film is cast, the CO₂ will leave and the diffusion of molecular chains will be faster due to absence of a charged surfactant. The interdiffusion of molecular chains needs to be monitored using fluorescent-dye labeled latexes. This will be discussed further in future work (Section 6.2).

6. Conclusions and Future Work

6.1 Conclusions

In this project, redispersible particles were prepared by emulsion polymerization using switchable surfactants. The SEM images in Section 4.2.2 showed that the particles of the aggregated latexes were clumps of individual primary particles. This was a promising result for the ability to redisperse these aggregated particles. If the particles had fused together, it is likely that they would not have been able to be pulled apart.

A minimum amount of energy was necessary for successful redispersion as was shown from DLVO theory (Figure 4.9). Energy was supplied by a sonicator, a rotor-stator, a blender or an overhead stirrer. The stirrer was not able to induce redispersion. Different sized rotor-stator heads and different rotational speeds provided different amounts of energy input into the system for the redispersion step. Again, a minimum amount of energy was required for successful redispersion. If too much energy was provided there was shear-induced destabilization. Rotor-stators are more likely to be used on an industrial scale and it is promising that they promoted redispersion. The geometry of the rotor-stator head and the vessel will affect the efficiency of mixing and will provide more or less energy at a certain rotation speed. Lower energy methods of redispersion are desirable to make redispersible polymers more environmentally friendly and economically viable.

Solids concentration also affected redispersion, with higher solids content aggregated latexes being more difficult to redisperse. CO₂ addition during redispersion was found to be not necessary for long-term colloidal stability of redispersed samples at

low solids content (5 wt%) due to the limited frequency of particle collisions. At high solids content (15 wt%), CO₂ was necessary to provide stabilization. The difficulty associated with redispersing higher solids content is problematic for applying these redispersible polymers to real world latexes. The “high” solids containing latexes (15 wt%) redispersed in this project are quite low compared to the latexes produced industrially (typically 50-60 wt%).

Additional surfactant, CTAB or C12, was added immediately before redispersion to provide added stabilization by increasing the zeta potential. The non-switchable surfactant CTAB was also added before the polymerization to help with stabilization during the redispersion later. The latex was still able to be destabilized with air and heat if a minimal amount of CTAB was added. It is common practice that mixtures of surfactants are used to stabilize systems.

A latex prepared with switchable surfactant and switchable initiator was also found to have reversible colloidal stability for multiple cycles. Air and heat were used to aggregate and CO₂ and sonication were used to redisperse for at least three cycles.

When water was removed from the aggregated latex, resulting in an 18 wt% polymer, and fresh water was added, the redispersibility of the system was retained. This is a similar situation to the application of shipping dehydrated latexes to be redispersed once reaching their destination. Although the latex was redispersed with sonication, it is probable that a high-speed mixer would provide enough energy (similar to a rotor-stator). High-speed mixers are likely to be found at a construction site (as well as water) and it

would not be very labour intensive to redisperse an aggregated latex with minimal water content.

The switchable surfactants were also used to stabilize an emulsion copolymerization of BA and MMA. The solids content, 42 wt%, also reflected that of a latex more commonly produced in industry. The copolymerization was done using a semi-continuous process. The latex was destabilized with air and heat, however, due to the predicted low polymer T_g , the copolymer coagulated into a sticky solid mass. The copolymer was able to form a film at room temperature because of its low T_g , unlike the high T_g PMMA latex that formed a cracked, broken film. The use of the switchable surfactant to stabilize a high solids content latex, 42 wt%, had not previously been done with either high or low T_g polymer. These latexes would not be able to be aggregated and redispersed at room temperature as those from Chapter 4. However, because the latex dries as a film at room temperature this shows that there is the possibility of using switchable surfactants in latex paint formulations.

6.2 Future Work

The investigation into the use of switchable surfactants to make particles with switchable colloidal stability is still very new and further research must be carried out before use on an industrial scale. There is also a need for a deeper fundamental understanding of the system.

In Section 4.4.2 it was mentioned that the increase in zeta potential was very slow. This may be due to the slow dissociation of the amidine headgroup from the hydrophobic particle surface to allow for the conversion to the bicarbonate salt. It may help to add a

hydrophilic group, such as poly(ethylene glycol), between the hydrophobic tail and the head group. The hydrophilic group would help to keep the neutral amidine headgroup from lying along the hydrophobic surface of the particle.

The largest unknown in the project currently is the location of the surfactant after aggregation and redispersion. It is unknown whether the surfactant remains on the outside of the large aggregates or if it migrates to the hydrophobic region between the primary particles of the aggregate. This will of course affect the ability to switch the surfactant to its “on” form during redispersion. It is also unknown where the surfactant is located after redispersion. It is possible that some surfactant remains trapped within large aggregates, or has been released into the water phase, and of course there should still be some on the particle surface providing stabilization. It was seen that the original zeta potentials of the latexes were not recovered after redispersion with CO₂, which may be indicative of surfactant being trapped between particles or lost in the water phase. The use of a hydrophilic group between the tail and headgroup may also help to prevent trapping of surfactants within aggregates. If the headgroup sticks out farther away from the particle surface, this may prevent the particles from coming so close together. This would result in looser flocs and because redispersion would be easier it would be less likely that surfactant molecules would get trapped within aggregates. To prevent the surfactant from leaving the particle surface and going into the water phase a reactive surfactant could be used. Currently, the surfactants are only adsorbed onto the surface, which is why the surfactant can leave the surface. By adding a reactive group, such as an olefin, to the tail of the surfactant it could be possible to chemically bind the surfactant to the surface of

the particle. However, it would be necessary to match the reactivities of the monomer and surfactant to ensure surfactant incorporation.

Another method to chemically bind switchable groups to the surface of the particle is to do a copolymerization with a small (switchable) molecule and the monomer. The biggest issue with this method is matching the reactivities of the comonomers. This was a route that was started but not pursued during this project. This method has just very recently been published from another research group.⁵⁸ To match the reactivities of styrene and their switchable comonomer they functionalized the phenyl ring in styrene with the switchable group to form the comonomer. They performed the emulsion polymerization surfactant-free and obtained particles with switchable colloidal stability. However, their system did not undergo aggregation with the application of air and heat, most likely due to their poor choice of initiator, which contained acid that would permanently protonate their switchable groups.

Film formation studies are also required to examine the interdiffusion of the BA/MMA copolymer chains. Fluorescence resonance energy transfer (FRET) is used to measure the interdiffusion of polymer molecules during film formation. One latex is labeled with a donor dye and another is labeled with an acceptor dye. The donor dye will fluoresce and the energy will be transferred to the acceptor dye. As the labeled molecules approach each other the energy transfer will become more efficient.^{59, 60} These experiments will be done at the University of Toronto in Prof. Mitchell Winnik's research group using samples prepared during the study described in Chapter 5.

References

- [1] Blackley, D. C., *Polymer Latices: Science and Technology*, 2nd ed.; Chapman & Hall: London, 1997.
- [2] *Polymer Dispersion and Their Industrial Applications*; Urban, D., Takamura, K., Eds.; Wiley-VCH: Weinheim, Germany, 2002.
- [3] Meyers, D. *Surfaces, Interfaces, and Colloids: Principles and Applications*, 2nd ed.; Wiley-VCH: New York, 1999.
- [4] Schramm, L. L.; Marangoni, D. G. Surfactants and Their Solutions: Basic Principles. In *Surfactants: Fundamentals and Applications in the Petroleum Industry*; Schramm, L. L., Ed.; Cambridge University Press: Cambridge, U.K., 2000; pp 3-50.
- [5] Meyers, D. *Surfactant Science and Technology*, 3rd ed.; Wiley: Hoboken, NJ, 2006.
- [6] Anton, P.; Koeberle, P.; Laschewsky, A. *Prog. Colloid Polym. Sci.* **1992**, *89*, 56-59.
- [7] Saji, T.; Hoshino, K.; Aoyagui, S. *J. Am. Chem. Soc.* **1985**, *107*, 6865-6868.
- [8] Schmittl, M.; Lal, M.; Graf, K.; Jeschke, G.; Suske, I.; Salbeck, J. *Chem. Commun.* **2005**, 5650-5652.
- [9] Sakai, H.; Matsumura, A.; Yokoyama, S.; Saji, T.; Abe, M. *J. Polym. Chem. B.* **1999**, *103*, 10737-10740.
- [10] Wang, K.; Guo, D.; Zhang, H.; Li, D.; Zheng, X.; Liu, Y. *J. Med. Chem.* **2009**, *52*, 6402-6412.
- [11] Liu, Y.; Jessop, P. G.; Cunningham, M.; Eckert, C. A.; Liotta, C. L. *Science.* **2006**, *313*, 958-960.
- [12] Jessop, P. G.; Guang, C. L.; Harjani, J. R. Switchable Anionic Surfactants and Methods of Making and Using Same. U.S. Patent Appl. 20110124745, May 26, 2011.
- [13] Ceschia, E. Switchable Surfactants for Soil Remediation. M.Sc. Thesis, Queen's University, February 2011.
- [14] Kerton, F. M. *Alternative Solvents for Green Chemistry*, RSC Green Chemistry Book Series; RSC Publishing: Cambridge, U.K., 2009.
- [15] Sharavanan, K.; Komber, H.; Fischer, D.; Bohme, F. *Polymer.* **2004**, *45*, 2127-2132.
- [16] Arthur, T.; Harjani, J. R.; Phan, L.; Scott, L. M.; Jessop, P. G.; Hodson, P. V. The Acute Toxicity of Switchable Surfactants to Rainbow Trout can be Predicted from Octanol-Water Partition Coefficients. *Environ. Sci. Technol.*, submitted for publication.
- [17] Schramm, L. L. *Emulsions, Foams and Suspensions: Fundamentals and Applications*; Wiley-VCH: Weinheim, Germany, 2005.
- [18] Chern, C. *Principles and Applications of Emulsion Polymerization*; Wiley: Hoboken, NJ, 2008.
- [19] Liu, Y. Switchable Surfactants. M. Sc. Thesis, Queen's University, October 2006.

- [20] Dunn, A. S. Harkins, Smith-Ewart and Related Theories. In *Emulsion Polymerization and Emulsion Polymers*; El-Aasser, M., Lovell, P., Eds.; John Wiley & Sons, Inc.: Chichester, NY; 1997, 125-163.
- [21] Van Oss, C. J. *Interfacial Forces in Aqueous Media*, 2nd ed.; Taylor & Francis: Boca Raton, FL, 2006.
- [22] Xu, R. *Particle Characterization: Light Scattering Methods*; Particle Technology Series; Kluwer Academic Publishers: Dordrecht, Netherlands, 2000.
- [23] Hyman, M. P.; Medlin, J. W. Mechanistic studies of electrocatalytic reactions. In *Catalysis*, Spivey, J. J., Dooley, K. M., Eds.; Specialist Periodical Reports 20; The Royal Society of Chemistry: Cambridge, UK, 2007; pp 309-337.
- [24] Guziak, L. F.; Maclay, W.N. *J. Appl. Polym. Sci.* **1963**, *7*, 2249-2258.
- [25] Saija, L. M.; Uminski, M. *J. Appl. Polym. Sci.* **1999**, *71*, 1781-1787.
- [26] Fujii, S.; Kakigi, Y.; Suzaki, M.; Yusa, S.; Muraoka, M.; Nakamura, Y. *J. Polym. Sci. A1.* **2009**, *47*, 3431-3443.
- [27] Greene, B. W.; Nelson, A. R.; Keskey, W. H. *J. Phys. Chem.* **1980**, *84*, 1615-1620.
- [28] Duchesne, A.; Bojkova, A.; Gapinski, J.; Seip, D.; Fischer, P. *J. Colloid. Interf. Sci.* **2000**, *224*, 91-98.
- [29] Mihara, M.; Jessop, P. G.; Cunningham, M. F. *Macromolecules.* **2011**, *44*, 3688-3693.
- [30] Keddie, L.J., Routh, A.F., *Fundamentals of Latex Film Formation: Processes and Properties*. Springer: Dordrecht, 2010.
- [31] Brander, J., Thorn, I., *Surface Applications of Paper Chemicals*. Blackie Academic & Professional: London, 1997.
- [32] Eckersley, S. T.; Rudin, A. Film Formation of Acrylic Copolymer Latices: A Model of Stage II Film Formation. In *Film Formation in Waterborne Coatings*, Provdor, T., Winnik, M. A., Urban, M. W., Eds.; ACS Symposium Series 648; American Chemical Society: Washington, DC, 1996; pp 2-21.
- [33] Liu, Y.; Haley, J. C.; Deng, K.; Lau, W.; Winnik, M. A. *Macromolecules.* **2007**, *40*, 6422-6431.
- [34] Elizalde, O.; Leal, G. P.; Leiza, J. R. *Part. Part. Syst. Charact.* **2000**, *17*, 236-243.
- [35] Scheider, M.; McKenna, T. F. *Part. Part. Syst. Charact.* **2002**, *19*, 28-37.
- [36] *Zetasizer Nano Series User Manual*; MAN0317 5.0; Malvern Instruments Ltd.: Malvern, U.K., August 2009.
- [37] Burlak, G. *The Classical and Quantum Dynamics of the Multispherical Nanostructures*; Imperial College Press: London, 2004.
- [38] Merkus, G. H. *Particle Size Measurements: Fundamentals, Practice, Quality*. Springer: New York, 2009.

- [39] Podzimek, S. Light Scattering. *Light Scattering, Size Exclusion Chromatography and Asymmetric Flow Field Flow Fractionation: Powerful Tools for the Characterization of Polymers, Proteins and Nanoparticles*; Wiley: Hoboken, NJ, 2011; pp 37-98.
- [40] *Mastersizer 2000 Application Note*; MRK561-01; Malvern Instruments Ltd.: Malvern, U.K.
- [41] Ward-Smith, S. Mastersizer 2000 Software Assistance Data Interpretation. Presented at the Malvern Particle Summit, Boston, MA, October 19-21, 2010.
- [42] Ward-Smith, S. Best Practices in Laser Diffraction. Presented at the Malvern Particle Summit, Boston, MA, October 19-21, 2010.
- [43] Kippax, P. Particle Sizing Basics. Presented at the Malvern Particle Summit, Boston, MA, October 19-21, 2010.
- [44] Kopesky, W. Tales from the service lab trenches. Presented at the Malvern Particle Summit, Boston, MA, October 19-21, 2010.
- [45] Everette, D. H. *Basic Principles of Colloid Science*; Royal Society of Chemistry: London, 1988.
- [46] Fowler, C. I.; Muchemu, C. M.; Miller, R. E.; Phan, L.; O'Neill, C.; Jessop, P. G.; Cunningham, M. F. *Macromolecules*, **2011**, *44*, 2501-2509.
- [47] Suslick, K. S. *Science*. **1990**, *247*, 1439.
- [48] Berg, J. C. *An Introduction to Interfaces and Colloids: The Bridge to Nanoscience*; World Scientific Publishing Co. Pte. Ltd.: Singapore, 2010.
- [49] Grulke, E. A. Solubility Parameter Values. In *Polymer Handbook*, 4th ed., Brandrup, J.; Immergut, E. H.; Grulke, E. A., Eds.; John Wiley & Sons: Toronto, 1999; pp 675-714.
- [50] Volpe, C. D.; Maniglio, D.; Siboni, S. The Evaluation of Surface Free Energy of Polymer: The Role of Water Acid-Base Properties and the Measurement of an "Equilibrium" Contact Angle. In *Contact Angle*; Mittal, K. L., Ed.; VSP BV: Zeist, Netherlands, Vol. 2, 2002, 45-71.
- [51] Fried, J. R. *Polymer Science and Technology*, 2nd ed.; Prentice Hall PTR: Upper Saddle River, NJ, 2003.
- [52] Nicholson, J. W. *The Chemistry of Polymers*, 3rd ed.; RSC Publishing: Cambridge, U.K., 2006.
- [53] Hagiopol, C. *Copolymerization: Toward a Systematic Approach*; Kluwer Academic/Plenum Publishers: New York, 1999.
- [54] Greenley, R. Z. Free radical Copolymerization Reactivity Ratios. In *Polymer Handbook*, 4th ed.; Brandrup, J.; Immergut, E. H.; Grulke, E. A.; Abe, A.; Bloch, D. R., Eds.; Wiley: New York, 1999, pp 188.
- [55] Chern, C. Polymerization of Monomer Emulsions. In *Encyclopedia of Surface and Colloid Science*, 2nd ed.; Somasundaran, P; Hubbard, A. T., Eds.; Vol. 3; Taylor & Francis: New York, 2006, 4990-5011.

- [56] Hutchinson, R.; Penlidis, A. Free-Radical Polymerization: Homogeneous Systems. In *Polymer Reaction Engineering*; Asua, J. M., Ed.; Blackwell Publishing: Oxford, U.K., 2007, pp 118-178.
- [57] Chiefari, J.; Rizzardo, E. Control of Free-Radical Polymerization by Chain Transfer Methods. In *Handbook of Radical Polymerization*; Matyjaszewski, K.; Davis, T. P., Eds.; Wiley: New York, 2002, pp 629-690.
- [58] Zhang, Q.; Wang, W.; Lu, Y.; Li, B.; Zhu, S. *Macromolecules*, **2011**, *44*, 6539-6545.
- [59] Keddie, L.J.; Routh, A.F. *Fundamentals of Latex Film Formation: Processes and Properties*; Springer: Dordrecht, 2010.
- [60] Geddes, C. D. *Reviews in Fluorescence 2007, Vol. 4*; Springer: New York, 2007.
- [61] Bakhshi, H.; Zohuriaan-Mehr, M. J.; Bouhendi, H.; Kabiri, K. *J. Mater. Sci.*, **2011**, *46*, 2771-2777.

Appendix A: Important spectra and data sheets

Zetasizer Nano ZS and Mastersizer 2000 data sheets:

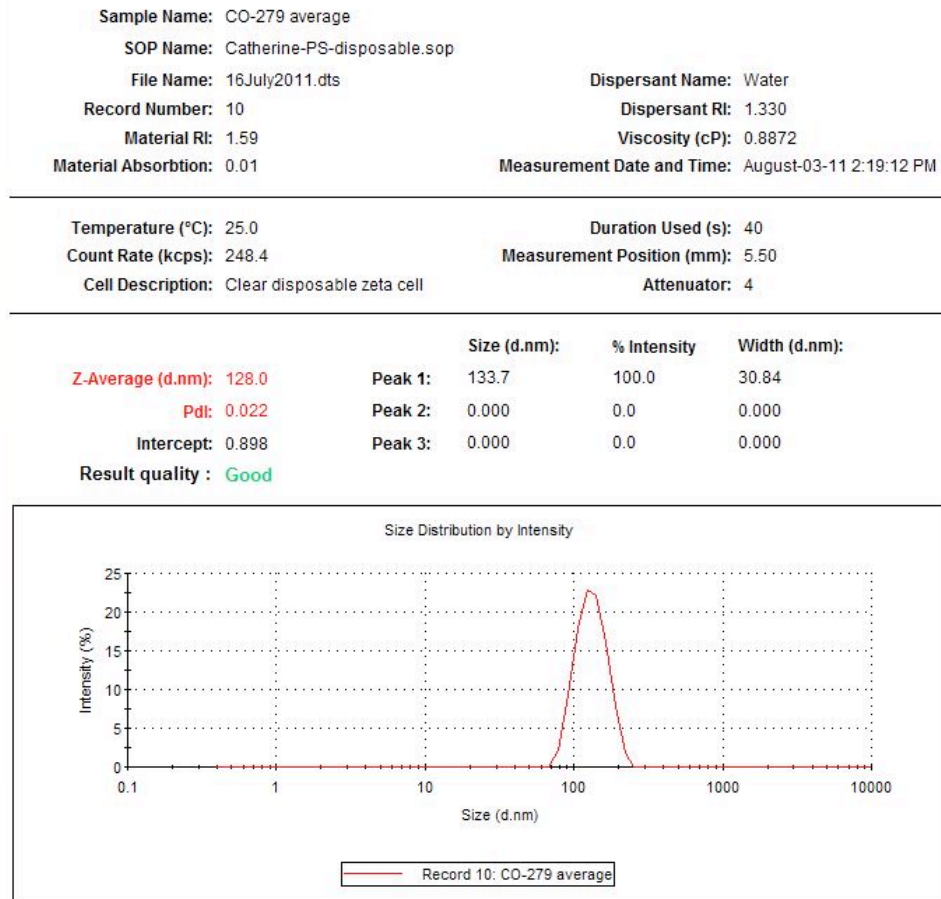


Figure A.1. The datasheet from the Zetasizer Nano ZS after the particle size measurement of a polystyrene latex.

Sample Name: CO-238 10%son.+CO2 average
SOP Name: Zeta pot-Candace-PMMA-disposable.sop
File Name: 16Apr2011.dts
Record Number: 35
Date and Time: August-03-11 2:29:30 PM
Dispersant Name: Water
Dispersant RI: 1.330
Viscosity (cP): 0.8872
Dispersant Dielectric Constant: 78.5

Temperature (°C): 25.0
Count Rate (kcps): 0.0
Cell Description: Clear disposable zeta cell
Zeta Runs: 14
Measurement Position (mm): 2.00
Attenuator: 7

| | Mean (mV) | Area (%) | Width (mV) |
|-------------------------------------|---------------------|----------|------------|
| Zeta Potential (mV): 15.6 | Peak 1: 15.6 | 100.0 | 8.61 |
| Zeta Deviation (mV): 8.53 | Peak 2: 0.00 | 0.0 | 0.00 |
| Conductivity (mS/cm): 0.0598 | Peak 3: 0.00 | 0.0 | 0.00 |

Result quality : Good

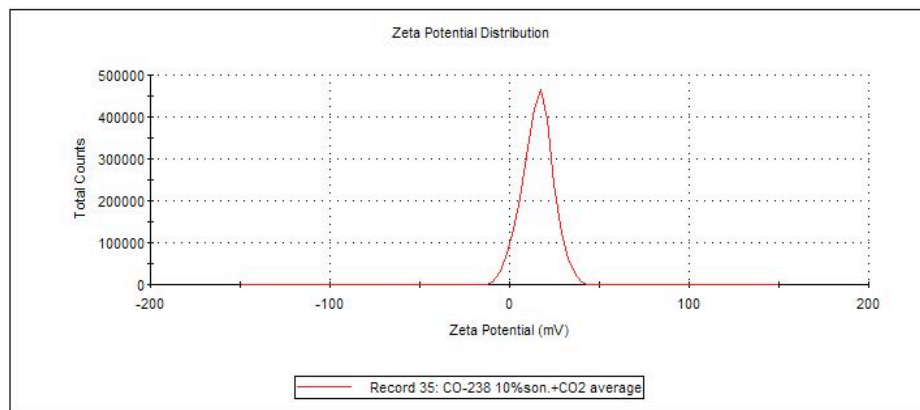


Figure A.2. The datasheet from the Zetasizer Nano ZS after the zeta potential measurement of a redispersed PMMA latex.

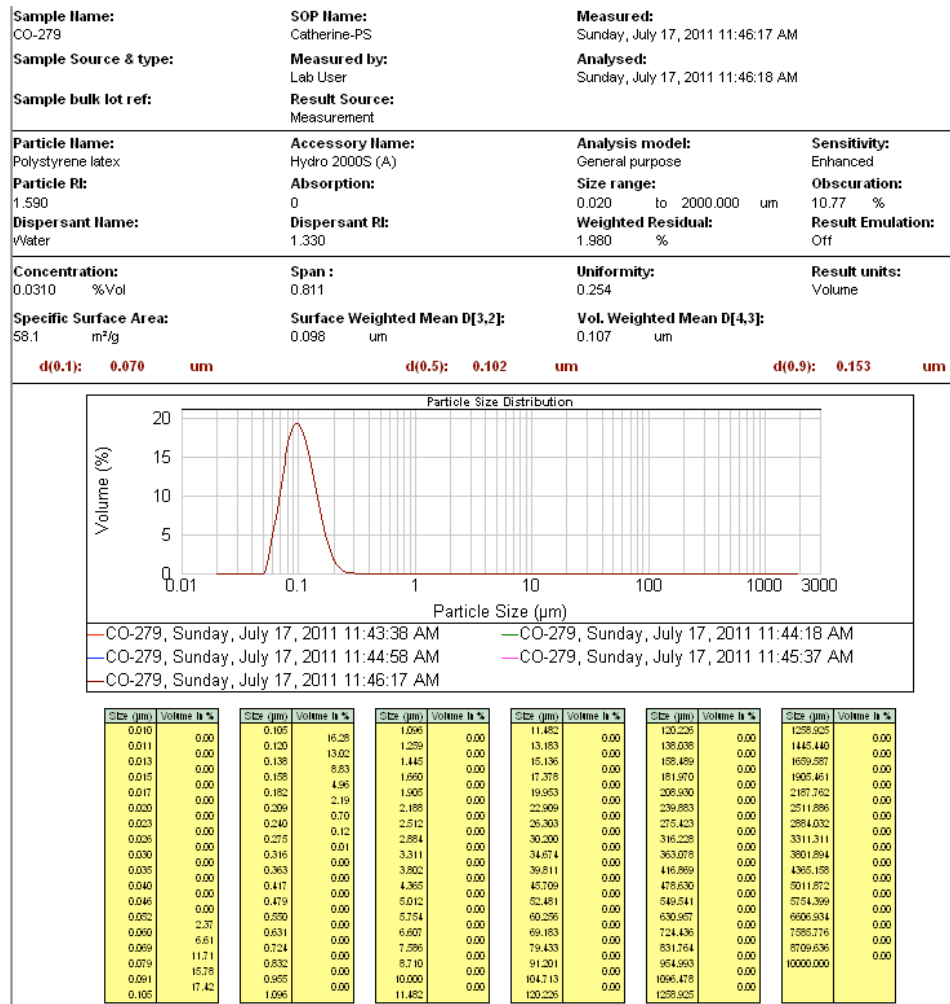


Figure A.3. The datasheet from the Mastersizer 2000 after the particle size measurement of a polystyrene latex.

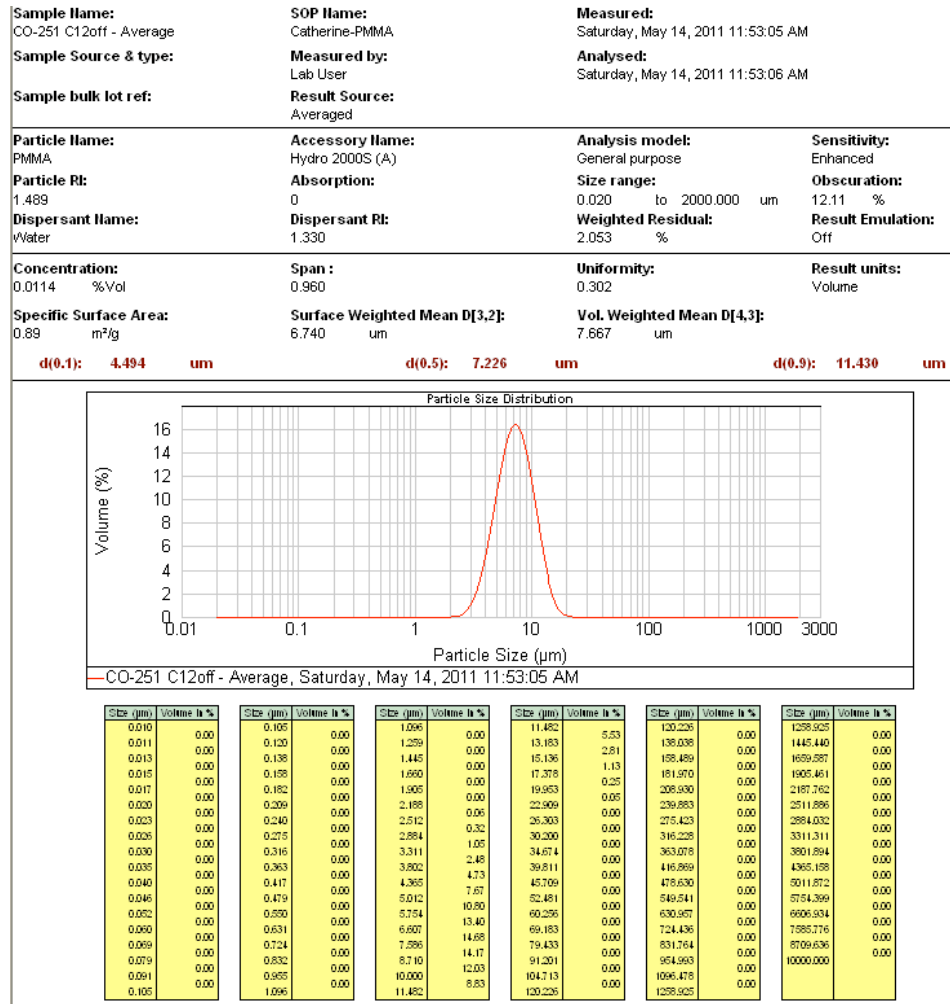


Figure A.4. The datasheet from the Mastersizer 2000 after the particle size measurement of an aggregated PMMA latex.

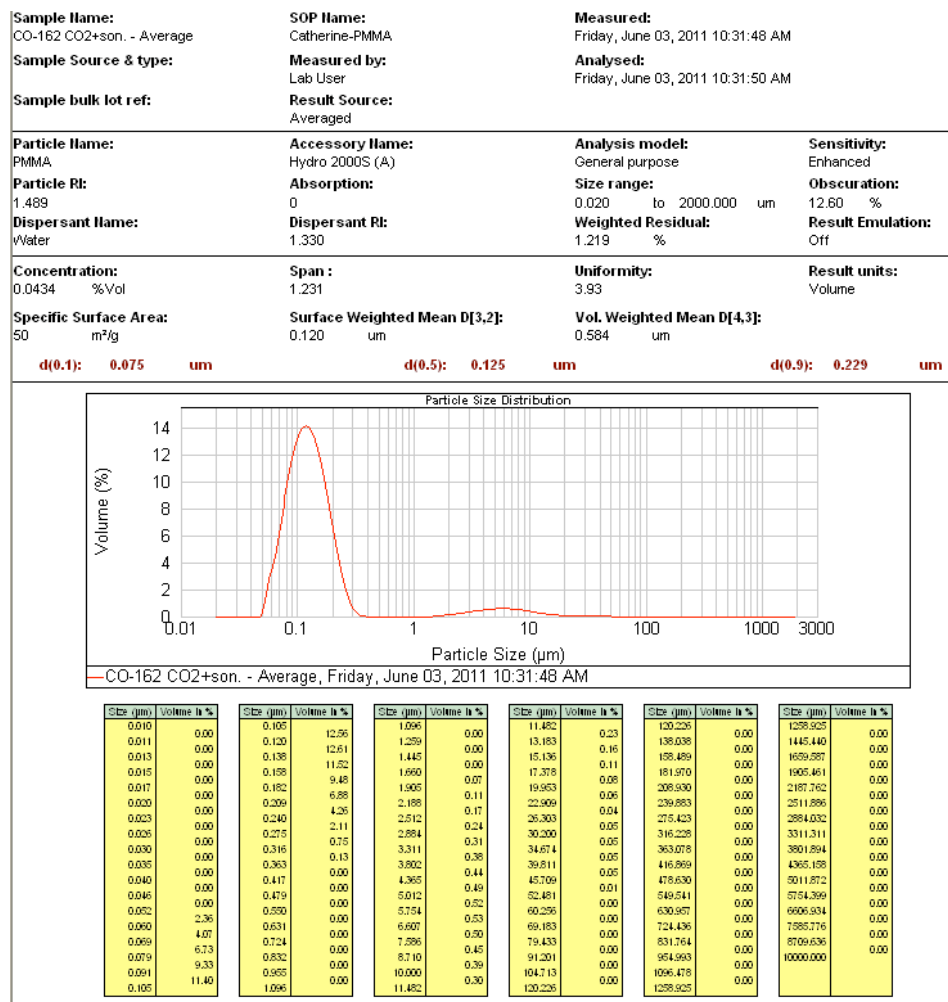


Figure A.5. The datasheet from the Mastersizer 2000 after the particle size measurement of a redispersed PMMA latex.

¹H NMR spectrum of the BA-MMA copolymer to measure the relative amounts of comonomers incorporated in the polymer chain. The peak at ~3.9 ppm represents the 2 methylene protons next to the acrylate group of BA and was calibrated to have an integration of 2. The peak at ~3.5 ppm represents the 3 protons on the methyl group (OCH₃) of the MMA. These peaks were used to determine the relative amounts of BA and MMA in the copolymer.

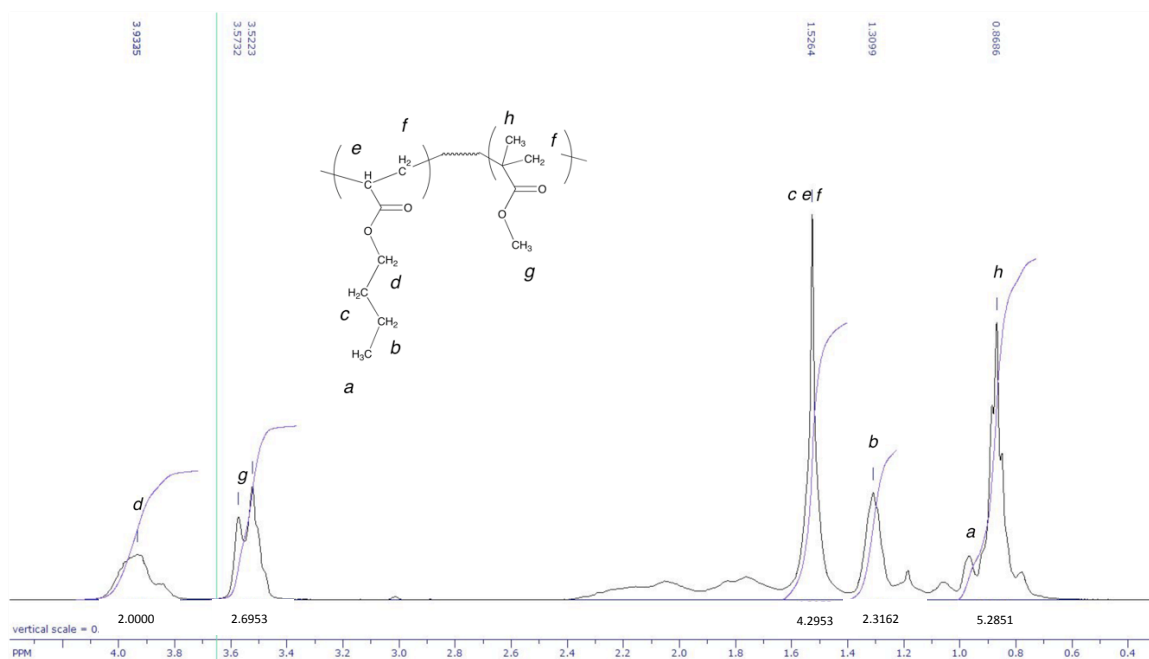


Figure A.6. The proton NMR of the BA-MMA copolymer made by a semi-continuous process with peak assignments.⁶¹

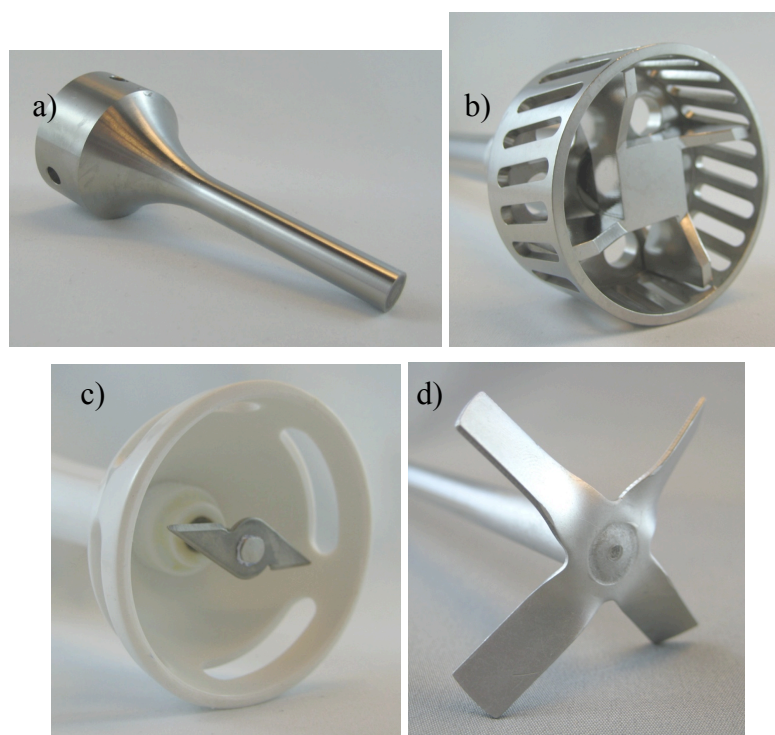


Figure A.7. Photographs of the a) sonicator probe, b) the 5.5 cm rotor-stator, c) the blender and d) the stirrer propeller.